NASA CR-112143
MARCH 31, 1973

65-194

SPACE DIVISION

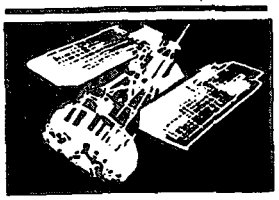

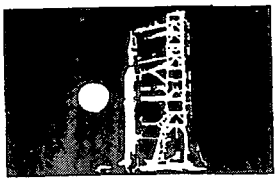

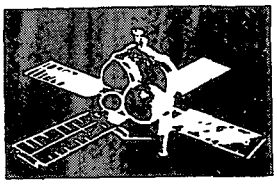

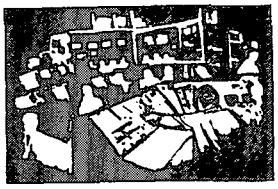

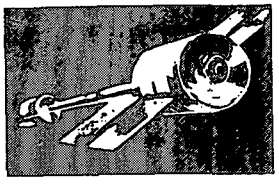

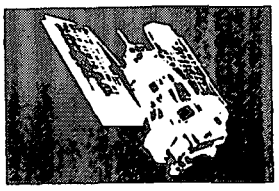

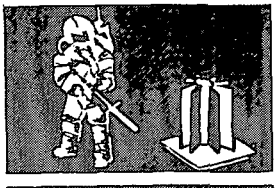

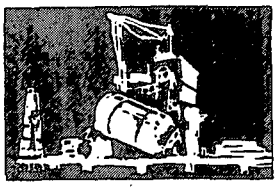

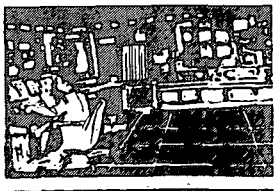

AN INVESTIGATION AND CONCEPTUAL DESIGN OF A "HOLOGRAPHIC" STARFIELD AND LANDMARK TRACKER

GENERAL ELECTRIC

NASA CR-112143

AN INVESTIGATION AND CONCEPTUAL DESIGN OF A "HOLOGRAPHIC" STARFIELD AND LANDMARK TRACKER

By Joseph D. Welch

Prepared under Contract No. NAS 1-10739 by
GENERAL ELECTRIC COMPANY
Space Division
Valley Forge, Pa. 19481

for

NATIONAL AERONAUTICS AND SPACE ADMINISTRATION
Langley Research Center
Hampton, Virginia 23365

TABLE OF CONTENTS

TABLE OF CONTENTS - Continued

TABLE OF CONTENTS - Continued

LIST OF ILLUSTRATIONS

LIST OF TABLES

FOREWARD

This report summarizes the results of an investigation and conceptual design of a "holographic" starfield and landmark tracker. This program was performed under the technical leadership of Mr. J. D. Welch who was also a primary technical contributor and who also prepared the final report. The laboratory and observatory experimental evaluation of the imaging media was conducted primarily by Mr. John Holeman with assistance by J. D. Welch. Mr. J. Bamberg contributed in the area of photometric analysis and investigation of alternative electro-optical readout techniques. The work was performed on Contract No. NAS1-10739 under the technical direction of Dwayne E. Hinton of the NASA Langley Research Center.

1.0 INTRODUCTION, SUMMARY, BACKGROUND AND APPROACH

By Joseph D. Welch

1.1 Introduction.- The objective of this investigation was to further evaluate the key components and projected performance of a "holographic" starfield and landmark tracker and perform a conceptual design of such a device.

The function of the "holographic" tracker, as it is defined in this program is to automatically recognize and track starfields and/or landmarks which are detected on-board the spacecraft by passive optical means. These starfields and/or landmarks are recognized and tracked by means of an on-board coherent optical data correlator. The system incorporates a file of matched spatial frequency filters which have been previously made in an Earth-based laboratory based on imagery of preselected (i.e., "known") starfields and landmarks.

Automatic recognition and tracking of landmarks and starfields from a spacecraft has several potentially useful applications including:

- Providing vehicle attitude determination and reference by relative vector direction to known starfields.
- Providing a sequence of positional constraints as part of an autonomous space navigation system. A continuing sequence of such constraints would be processed by recursive statistical means to provide a continually updated best estimate of the vehicle ephemeris. (This is discussed more at length in Appendix A.)
- Providing precise reference pointing for various scientific and observational payloads.
- Updating gyro references.
- Verification of specific stellar references.

The technology of automated on-board parallel optical data processing has broad future potential for several other advanced aero/space mission requirements. Among the interrelated data processing applications having such potential applicability are:

- On-board automatic classification and/or spatial frequency analysis of patterns which are interpretable in terms of Earth Resources investigations.
- On-board automatic recognition and classification of generic cloud patterns and their associated weather systems.
- On-board compression of imagery data in order to conserve bandwidth of ground link transmission.

It is expected that the further pursuit of the objectives of the contract reported here, which thus far has emphasized the attitude reference and autonomous navigation problems, will also provide a key to component selection and system design to solve these other problems of practical interest to future aero/space missions.

The results of this contract have been sufficiently encouraging as to recommend, as a next phase the detailed design, fabrication and test of an automatic coherent optical data processor having a design which would ultimately be applicable to operation in a space vehicle.

1.2 Summary.- Some of the principal results of this investigation may be summarized as follows:

1) The analysis, experiments and design effort of this investigation have supported the feasibility of the basic "holographic tracker" concept.

2) Analysis and experiments were performed in the area of image intensifiers. It is concluded that applications of some of the more advanced types of intensifiers, such as the low distortion wafer types of intensifiers, will permit the application of some of the more advanced input imaging media which would otherwise have inadequate sensitivity.

3) Experimental evaluations of photoplastic recording material (PPR) demonstrated somewhat less sensitivity when imaging stars than had been previously predicted. However when exposing simulated star images on PPR with an image intensifier a large effective gain was experienced. It is predicted that, in effect, the use of an intensifier in this way will provide a usable gain in the range of 10^4.

4) A Polaroid rapid process silver halide material was evaluated as an input medium for landmark and starfield tracking. Adequate image correlation was demonstrated with optical energy densities as low 10^{-8} watt sec/cm^2. In some cases, however, "star like" noise appeared unpredictably on the image in some of the experiments. This noise was judged to be sometimes so extensive as to raise considerable doubt as to the utility of this material for a practical starfield tracker. Furthermore the complexities of developing this material continued to make it look unattractive for space applications.

5) The two reference beam coherent optical matched filter technique developed by J. Hallock (reference 8) is recommended as the best means for multiplexing spatial frequency filters for starfields. It is expected that up to 30 starfields can be multiplexed on a single frame. For a tracking system requiring a very large number of stored matched landmark spatial filters, a pin registration film loop system has been shown to provide the required registration positioning accuracy (reference 9).

6) Although a 1 mwatt HeNe laser is recommended for the conceptual design it is expected that solid state laser diodes will ultimately be a practical source of coherent illumination after it has been more fully evaluated for this function. Such laser diodes have been demonstrated to have practical potential in a coherent correlator (reference 10).

7) An electro-optical readout based on the application of an image dissector is shown to be the best approach to correlation readout for the conceptual design. Ultimately, however, when evaluated for this function, solid state linear arrays are expected to provide a more compact completely parallel non-scanning readout system.

8) One of the promising alternative types of real time input imaging devices is an optically addressable liquid crystal device. One approach to such a use of liquid crystals has been developed for NASA-GSFC (reference 11). Encouraging results have been obtained to recommend further evaluation of this type of device for applicability to the present conceptual design.

9) A conceptual design of a holographic tracker has been made which fits in a volume 132 cm x 48 cm x 24 cm.

   Its principle components are

   - A 20 cm clear aperture Schmidt-Cassegrain telescope having an 8^{o} field of view.
   - A 1 mwatt HeNe laser.
   - A 40 mm wafer type image intensifier.
   - Paraboloidal mirror segments for performing the Fourier transform.
   - A fixed multiplexed starfield matched spatial filter.
   - An image dissector electro-optical read-out system.
   - An optically excited liquid crystal type of real time input imaging device.

10) The predicted tracking accuracy of the above conceptual design is in the range of 1 min. of arc. Ultimate landmark and starfield tracking accuracies in the range of 15 sec. of arc are predicted for this type of correlation tracker.

1.3 Background of the Concept.- The work of this contract was based on previously developed technology application concepts originated by General Electric on earlier Company-sponsored investigations (cf. references 1 to 6) and further explored by GE under a previous NASA/ERC contract (NAS 12-2148) (cf. reference 7). Specifically the original concept related to the application of near real time coherent optical matched filter techniques for recognizing and tracking landmarks as part of a navigation and/or attitude reference system.

1.4 Approach.- The specific task areas covered under this contract have included:

- An investigation of two candidate near "real time" input imaging media: a photodeformable and a rapid process silver halide. These media were investigated with both the starfield and landmark applications in mind.

- An investigation of alternative electro-optical devices for precision readout of the correlation function.

- An analysis of the overall recognition and tracking system for the purposes of providing a guide to system design and performance prediction. This included a simplified simulation of the starfield recognition and tracking problem.

- An overall conceptual design of the system. This includes selection of the basic size and scale factors of the system as well as selection of the key components. Layout drawing and dimensions of the system as it is presently conceived are provided.

In addition to the above effort an investigation and limited experimental evaluation of image intensifiers was performed. It was concluded that these intensifiers may provide a key to the practicality of using some of the advanced "real time" imaging media for recording input images.

2.0 SYSTEM ANALYSIS

2.1 Application Considerations.- Application considerations in the design of the holographic tracker have been discussed in some detail in previous reports (references 1-7). System performance requirements desired for specific applications and certain problems associated with achieving this performance were considered. The problems considered in this section are those which are primarily extrinsic to the mechanization of the tracker system hardware. Problems and design alternatives more specifically associated with the tracker mechanization itself are discussed in Section 2.2. Among the problems to be discussed are:

- Effect of image motion induced by vehicle path and attitude dynamics.
- Obscuration or truncation of the observed scene.
- Other types of image degradation.
- "False alarm" problems in recognition.

In considering the performance specifications and associated problems, a variety of spacecraft and applications could be considered. However, attention will be limited to three types of vehicles and missions which are believed to be representative of most of NASA Space Missions:

- Spacecraft Type A: A non-spinning Earth Observation type of satellite nominally stabilized relative to the local vertical.
- Spacecraft Type B: A non-spinning spacecraft nominally stabilized relative to inertial space.
- Spacecraft Type C: A spin stabilized spacecraft nominally stabilized relative to inertial space.

In the case of Type C it will be assumed that the starfield holographic tracker will be pointed along the vehicle spin axis.

We will make the assumption that starfield recognition and tracking will be desired for all three types of vehicles listed above. However we will also make the realistic assumption that landmark tracking will be applicable only for the Type A vehicles.

Since we are considering a fully automated system no distinction will be given to manned or unmanned spacecraft.

2.1.1 Performance Goals.- In order to provide performance guidelines for the conceptual design considered in this program the performance goals as listed in Table 2-1 were selected. These are based on an engineering judgment of requirements for future space missions. These goals include both performance goals for an initial feasibility model as well as for an ultimate operational vehicle. The performance goals for the operational vehicle are believed to be realistic in relation to anticipated future NASA missions.

TABLE 2-1

PERFORMANCE GOALS

	INITIAL FEASIBILITY MODEL			TYPICAL OPERATIONAL MODEL		
	SPACECRAFT TYPE			SPACECRAFT TYPE		
	A	B	C	A	B	C
Tracking Accuracy (Starfields) (3σ)	60 arc sec	60 arc sec	60 arc sec	15 arc sec	15 arc sec	15 arc sec
Tracking Accuracy (Landmarks) (3σ)	60 arc sec	Not Applicable	Not Applicable	15 arc sec	Not Applicable	Not Applicable
Probability of False Recognition	$< 10^{-2}$	$< 10^{-2}$	$< 10^{-2}$	$< 10^{-3}$	$< 10^{-3}$	$< 10^{-3}$
Unattended Operational Life	3 Mo.	3 Mo.	3 Mo.	2 Yrs.	2 Yrs.	2 Yrs.
Min. Number of Operational Cycles	$(0.5)10^4$	$(0.5)10^4$	$(0.5)10^4$	10^5	10^5	10^5

2.1.2 Vehicle Dynamics Considerations.- The typical angular viewing rates which can be anticipated for realistic space missions are listed in Table 2-2. The viewing rates due to orbit motion are directly obtainable from considerations of orbit mechanics. Rates related to attitude control are based on engineering judgment of present and future anticipated state of the art of attitude control systems. The minimum attitude rate shown as 10^{-5} rad/sec due to attitude control system dynamics, for example, would be expected with the application of a high quality Control Moment Gyro system.

The effective angular rates listed in Table 2-2 could be reduced on-board the vehicle by appropriate use of an image motion compensation (IMC) device incorporated in the system. However, IMC is not considered in this analysis because it is desired that its complexities be avoided if system performance can be obtained without its use.

These image rates are important in that they provide a measure of the maximum exposure time and/or relaxation time constant of the optical-to-optical interface input image device (relaxation time being the more significant parameter for the self-erasing input imaging devices such as certain types of optically excited liquid crystal devices).

In general, it appears desirable that the image smear due to vehicle dynamics should be "small" relative to the size of the resolution element of the input imaging system. Just how "small" the smear should be is a matter of some judgment for the specifically intended mission. As pointed out in reference 12, a smeared input image of a star function can, as expected, result in an improved (i.e., higher intensity) correlation signal level. It does this, however, at some cost in the increase in the width of the correlation function. Thus, the rather modest improvement in correlation signal level intensity is bought at the price of more complexity in the operation of the electro-optical readout of the correlation signal. A significant degree of smear can necessitate a somewhat more complex pulse-center detection and interpolation scheme for the correlation function readout in order to obtain low tracking uncertainty.

For the above reasons, a recommended guide is established which would limit the smear due to exposure time or input imaging relaxation time constant to about 1/3 to 1/2 of an effective input imaging system point spread function.

2.1.3 Field of View Selection and Considerations of Minimum Stellar Magnitude, System Sensitivity and False Alarm Probability.- To some extent, a model, based on the statistical distribution of stars as a function of stellar magnitude, can be established to provide a predictive guide to the probability of false detection of starfields. This is useful because it can provide a design guide for selecting the number of stars in a nominal starfield and the desired resolution of the input imaging part of the system and the desired telescope field of view.

Clearly a similar model cannot be as readily established for predicting performance of landmarks. There we must depend on experimental results with a variety of landmark types. Laboratory simulation results to date have

TABLE 2-2

TYPICAL LINE-OF-SIGHT ANGULAR RATES

VEHICLE TYPE	ANGULAR RATES (rad/sec)
. TYPE A	
. Relative to Landmarks	
. Due to Orbit Rate	
Min. Altitude	$3(10^{-2})$
Inter. Altitude	$1.5(10^{-2})$
Synchronous Equatorial Altitude	0
. Due to Residual Attitude Control System Dynamics	10^{-2} to 10^{-5}
. Relative to Starfields	
. Due to Orbit Rate	
Min. Altitude	10^{-3}
Inter. Altitude	$0.5(10^{-3})$
Synchronous Altitude	10^{-4}
. Due to Residual ACS Dynamics	10^{-2} to 10^{-5}
. TYPE B	
Relative to Star Fields (Due to Residual ACS Dynamics)	10^{-2} to 10^{-5}
. TYPE C	
Relative to Starfields	
Spin Rate About Tracking Axis	10^{-1} to 10

indicated that, for well-selected landmarks, the false alarm problem can be made negligible. This is due to the unique pattern characteristics of well-selected landmarks.

The required minimum number of stars needed in each recognition starfield will be determined largely by considerations of signal to false alarm ratio. Acceptable false alarm rejection will be determined not only by the response of the coherent optical system but also by the discrimination capability of the electro-optical detector of the "correlation spot".

The problem of three star patterns has been evaluated in reference 13. This reference shows computed results of the total number of three star patterns as a function of the field of view, and the stellar magnitude. It also shows the number of "equivalent" three star patterns as a function of input image sensing resolution. By "equivalent" we refer to three star patterns which cannot be distinguished from each other in view of the finite resolution of the system. These represent potential "false detections" or "false alarms" in starfield correlation.

An examination of the results obtained in reference 13 indicates that for a 500 x 500 element resolution system the false alarm ratio is approximately 10^{-2}. For a 1200 x 1200 element resolution system, the false alarm ratio is about $0.3(10^{-2})$. Thus the false alarm probability is acceptable from the standpoint of performance goals established for the initial feasibility model even with a 500 x 500 element resolution system. (Note that based on a 60 arc sec tracking accuracy that 500 x 500 element system would correspond to about a 8^{o} x 8^{o} field of view for the initial feasibility model. This is not an unreasonable field of view for the initial model.)

The above false alarm ratios are based on a system with the sensitivity to three stars within the field of view. It is evident that with a more sensitive system (one which can detect stars of higher visual magnitude) it is possible to obtain starfields containing more than three stars within a given field of view which would result in a lower false alarm ratio. An initial evaluation indicates that the probability of false alarms for a five star pattern is less than 10^{-4} for an input imaging system having a resolution of 1200 x 1200 elements. This represents a performance in terms of rejection of false alarms which exceeds the requirements for the operational model.

Based on the above, the system sensitivity and field of view should be selected so as to provide a minimum of 3 to 5 stars in a defined star pattern. Since the telescope field of view is specified largely by system tracking accuracy, the nominal number of stars in a given field will be determined by system sensitivity.

Assuming a realistic tracking accuracy of a $2(10^{-3})$ and $0.5(10^{-3})$ fraction of the field of view for the initial feasibility model and the operational model respectively and for false alarm rejection purposes, a minimum of three stars and four stars (near the galactic pole) respectively for the initial feasibility and the operational model, the performance requirements for the two systems are obtained as listed in Table 2-3.

TABLE 2-3

NOMINAL SYSTEM PARAMETERS
(Assuming Operational Requirements Throughout the Stellar Sphere)

	INITIAL FEASIBILITY MODEL	TYPICAL OPERATIONAL MODEL
Field of View	8^{o}	8^{o}
Minimum Required Detectable Stellar Magnitude	+6	+6.5
Number of Stars in Nominal Field		
. At Galactic Pole	3	4
. Visual Mean	6	9
. At Milky Way	8	18

Note from Table 2-3 that 6^{th} magnitude stars will have to be sensed for the initial feasibility model and 6.5^{th} magnitude stars for the operational model. This requirement for sensing rather faint stars is clearly imposed by the requirement for operation at the regions of sparse stellar density (i.e., near the galactic poles). If the requirements are relaxed so that operation is required only in the region having visual mean stellar density or greater, then the stellar magnitude which must be sensed is significantly relaxed as shown in Table 2-4. Note that this still permits operation over 60% of the celestial sphere which is probably acceptable for most operational applications of the system.

Note that the data in Tables 2-3 and 2-4 is based on the performance goals listed in Table 2-1. It is recommended that these performance goals as well as the nominal system parameters of Table 2-4 serve as realistic guides to the design of both the initial feasibility model and the operational model.

2.1.4 Landmark Selection and Image Degradation.- Extensive analytical and experimental efforts in the area of landmark selection and image degradation have been pursued and are described in several references (reference Nos. 2, 3, 4, and 5). The results of these investigations have provided encouragement for the mechanization of a holographic landmark tracking approach. The highlights of the results of these earlier investigations are listed below.

TABLE 2-4

NOMINAL STARFIELD TRACKER SYSTEM PARAMETERS
(Assuming Operation Restricted to Celestial
Sphere Exclusive of Region near Galactic Poles)

	INITIAL FEASIBILITY MODEL	TYPICAL OPERATIONAL MODEL
Field of View	8^{o}	8^{o}
Minimum Required Detectable Stellar Magnitude	+4.5	+5.5
Number of Stars in Nominal Field		
. Visual Mean	3	4
. At Milky Way	4	6

- "Very good landmarks" are those which contain high contrast boundaries such as land-water boundaries. With such landmark areas considerable image degradation can be tolerated including obscuration of over 90% of the landmark area and large changes in solar aspect angle (e.g., recognizing a landmark in the morning using a filter made from an evening photograph).

- Poorer quality landmarks such as desert areas were also shown to have surprisingly good utility but could tolerate a significantly lesser amount of image degradation of the types described above.

- Tolerable rotation "errors" (i.e., observed scene rotation about the optical axis relative to scene used for reference filter) for landmarks were typically in the range of a small fraction of a degree (for relatively very large landmarks) to as much as 20^{o} (for smaller landmark areas).

- Tolerable magnification "errors" (i.e., observed scene image size relative to scene used for reference filter) for landmarks were typically in the range of a fraction of a percent to as much as 20 or more percent depending primarily on the relative size of the landmark.

In general the conclusion was made that landmarks can be recognized and tracked under conditions of degradation much greater than a typical human can tolerate. By preselecting a sufficient number of relatively "good" landmarks, the coherent optical recognition and tracking approach appears as an attractive one.

Because of the more critical problem of star field recognition from a photometric point of view much of the conceptual design will be based largely on the starfield tracking problem.

2.2 Tracking System Configuration Trade-Offs and Alternatives.- As discussed in Section 1.0, the application of the "holographic tracker" is to provide a rapid process recognition and tracking of starfields and landmarks for autonomous navigation and/or vehicle attitude reference. As will be noted below, the tracking requirements for an autonomous navigator are quite different than those of a vehicle attitude reference.

The purpose of this section is to discuss some of the key system trade-offs and alternatives. As such it will serve as an introduction to the material to follow on the key components (Section 3) and to the discussion of the overall conceptual design (Section 4).

2.2.1 Comparison of Operational Requirements for an Autonomous Navigation System and for an Attitude Reference.- The function of an autonomous navigator is to determine the ephemeris of the spacecraft by completely self-contained means (see Appendix A). Typically it functions from a sequence of discrete angular measurements between nearby points (e.g., landmarks) and distant points (e.g., stars or starfields).

By contrast, the vehicle attitude reference system is concerned only with the attitude dynamics. It typically needs to measure angles between vehicle axes and some external reference "targets" (typically stars).

In both cases the tracking operations can be considered as sampled data operations where the sampling period must be short relative to the time constant of the ephemeris uncertainty (in the case of autonomous navigation) and relative to the space vehicle attitude dynamics and control response (in the case of the attitude determination). Herein lies a major difference. Ephemeris uncertainty time constants are typically very long (i.e., measured in terms of hours) whereas vehicle attitude dynamics time constants are usually relatively so short (i.e., measured in fractions of seconds) as to frequently require nearly "continuous" reference data. An exception to this exists in the case of the attitude of a spin stabilized spacecraft. The prime purpose of the spinning is to increase the time constant of the attitude drift and uncertainty in two axes.

The vehicle system time constant is determined by the ratio of uncertainty in the forcing functions relative to the inertia of the state system being determined.

Typical minimum required data sampling rates for various applications are expected to be in this range:

	TYPICAL SAMPLING PERIOD
Autonomous Navigation (Most Phases)	10 Min. to Many hours
Autonomous Navigation (Terminal and other critical phases)	1 to 30 secs.
Attitude Reference (Spinning Vehicle)	1 Min. to 1 Hr. or more
Attitude Reference (Non-Spinning)	5 msec to 1 sec

Thus, depending on the problem, the sampling rate may range over a factor 10^6 or more. If the sampling period is relatively short compared to the finite operational time constant of the holographic tracker (as in some non-spinning attitude determination problems) then it may be necessary to complement the long period tracker reference with a short period inertial reference unit. The concept of updating inertial systems with "external" sensors is well-known. However inertial references and their updating procedures are beyond the scope of the present investigation.

From the above it is evident that, for some attitude reference applications, a system capable of a short sampling period and many recycles is desired. As we will see this imposes demands on the entire correlator tracker but especially on the "optical-to-optical" input device, the spatial filter selection system and the electro-optical readout system.

A further, but related, distinction typically exists in the attitude determination problem and the autonomous navigation problem. The former frequently requires a detected tracking error to be nulled whereas the navigation tracking function can operate very satisfactorily in an off-axis mode.

2.2.2 Interface Between Holographic Tracker and Spacecraft.- Several alternatives exist for integrating the holographic tracker to the spacecraft. The design configuration to be selected is, to a large extent, application and vehicle oriented. Some of the possible alternatives which can accomplish both the landmark and starfield function are:

a) Separate Fixed "Holographic" Trackers.- Simultaneous starfield and landmark recognition and tracking using a separate starfield coherent correlator. In this option, the optical axes of the telescopes associated with each correlator would be maintained at some very precise relative angular orientation relative to each other. Although this approach may have merit for certain missions it would be judged as being less flexible than desired in the selection of landmarks and starfields for other vehicles and missions. Furthermore a total duplication of the entire coherent optical processor may not be attractive from a weight, size, power standpoint nor may it represent the optimum mode of redundancy from a reliability point of view.

b) Separate Holographic Trackers Relatively Articulatable with Respect to Each Other.- This approach overcomes much of the operational inflexibility of system (a) in that it permits a wider choice of landmarks and starfields which can be tracked simultaneously.

However it has the distinct disadvantage that one or more precision angle readout transducers must be added in order to provide the relative angular orientation between the two trackers.

Because of the added complexity and possible long life reliability problems associated with such angle readout transducers, this approach is probably not attractive for most applications.

c) Separate Starfield and Landmark Telescopes Fixed Relative to Each Other but Operating on a Time-Shared Basis with the Same Coherent Optical Data Processor.- Since this approach utilizes a time shared operation, a short period vehicle attitude reference is required. This short period attitude reference may typically be an inertial reference unit which may already be available for other phases of the mission.

d) Separate Starfield and Landmark Telescopes Articulated Relative to Each Other but Operating on a Time-Shared Basis with the Same Coherent Optical Data Processor.- This approach also needs a short period vehicle attitude reference such as an inertial reference unit. Although the relatively articulated telescopes have advantages relative to operational flexibility, the need for one or more precision angle transducers is considered to be a significant disadvantage for most applications.

e) A Time-Shared Common Telescope for Both Landmark and Starfield Tracking.- This telescope would couple (usually through an image intensifier) to the coherent optical processor which is also time-shared. Since it is a time-shared system, a short period vehicle attitude reference such as an inertial reference unit is required for an autonomous navigation system.

Whether a short period inertial reference is required for an attitude reference would depend on the relative time constants of the vehicle attitude dynamics and the time constants of the holographic tracker. Thus, a spin stabilized vehicle would not ordinarily require any further short period inertial reference. Likewise a non-spin stabilized vehicle would not require such a short period inertial reference for an attitude determination system if the holographic tracker itself had a very rapid reaction time as might be possible with an optical-to-optical input image interface having a very short relaxation time constant.

In its simplest form this configuration would be fixed relative to the spacecraft. This would normally mean that the entire vehicle would have to be rotated in order to first look at landmarks and then at starfields.

However, this vehicle rotation is clearly not always attractive - particularly for rather large spacecraft. A variation of this approach would place the telescope together with the coherent correlation tracker and the inertial reference unit in an encapsuled assembly which is rotatable relative to the main part of the vehicle.

Note that, since the short period reference unit would be in the same assembly with the tracker, no precision angular measurements are required (for navigation purposes) to determine the relative orientation of the spacecraft and the tracker assembly. Indeed, for autonomous navigation purposes, configurations mounted on a boom or a tethered sub-vehicle are possible approaches especially for autonomous navigation of large vehicles.

The above list of alternative approaches is representative of possible configurations for autonomous navigation based on tracking landmarks relative to starfields with coherent optical techniques. It is not an exhaustive list, however, as still other variations can be conceived. One other approach, for example, might use separate landmark and starfield telescopes to produce a superimposed starfield image on the landmark image. By using multiplexed landmark and starfield matched spatial frequency filters two simultaneous correlation functions could be obtained. The measured linear displacement between the two correlation functions would provide a straightforward measurement of the desired navigation constant.

The exact selected configurations of the "holographic" tracker for an autonomous navigation system will depend on the mission requirements, vehicle size, required vehicle attitude and other factors.

Consider next the integration of a holographic tracker which has the sole function of providing a vehicle attitude reference by recognizing starfields. This is a simpler problem and generally a vehicle mounted system is preferred. Presuming a sufficiently large file of matched filters are made available then three axis vehicle attitude determination is always possible except when the stars are obscured by the Earth or other planet or when the Sun protective system deactivates the tracker.

In the case of a spin stabilized vehicle, mounting the holographic tracker along the spin axis is an attractive approach.

For the present investigation we will assume a "base line" configuration having a single telescope used on a time-shared basis for landmark and starfield tracking and coupled to a single coherent optical parallel image correlator. Note this is type (e) described above. This is an attractive approach for many autonomous navigation problems as well as attitude determination applications.

2.2.3 Primary Components and Interfaces of the Holographic Tracker System.- In order to facilitate the discussion of the "holographic" tracker, the primary components and interfaces of the holographic system are presented in the block diagram of Figure 2-1.

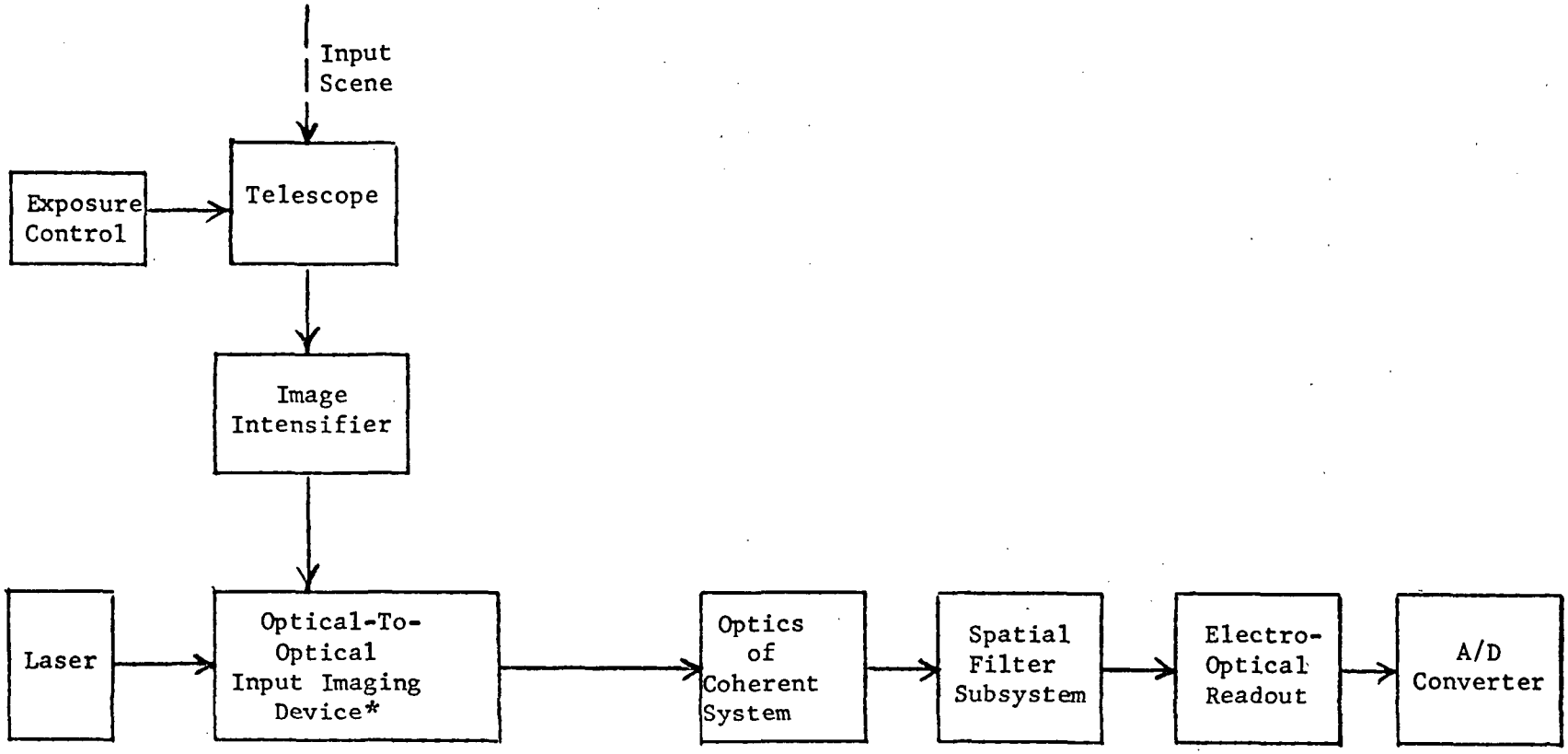

A SIMPLIFIED SCHEMATIC DIAGRAM OF "HOLOGRAPHIC" STARFIELD/LANDMARK TRACKER

FIGURE 2-1

*Also referred to as an
Optical-to-Optical Interface Device

An image intensifier is included in the system because investigations to date have indicated that such a device has significant potential for improving system performance (see Section 3.3).

2.3 Digital Simulation of a Starfield Mapper.- The objective of this simplified digital computer simulation is to determine the characteristics of the correlation function resulting from the recognition and tracking of a starfield by coherent optical means in order to provide a guide for the performance prediction of the overall recognition and tracking operation. This guide is made by computing the nature of the correlation function for a given starfield input, for a spatial filter of given characteristics and by an evaluation of the capability of the optical-electrical readout device when detecting the location of the correlation function.

A key parameter in predicting this operation is the spatial frequency response of all of the elements in the system, especially that of the matched filter. In this simulation we are concerned primarily with the effect of spatial frequency band-limiting by the matched spatial frequency filter in causing a peaking of the correlation function.

In the pursuit of this analysis we will assume that the candidate starfield as well as the matched filter is recorded on an amplitude storage medium (i.e., a variable transmission medium). It can be shown that similar conclusions will result when using a phase medium (intermodulation errors arising from the phase medium can be made negligible).

The candidate input image on the input medium will be several focused stars. In order to simplify the analysis we will initially assume that these stars are nearly the same magnitude. In the most ideal of situations each star image will be recorded as an Airy pattern. As practically observed however these recorded star images can frequently be better described as binary near-circular apertures or, in some cases, by images whose density approximates a circularly symmetric Gaussian function. These departures from an Airy function are due to transfer characteristics of both the optics and the imaging medium. An analysis which assumes that each star is represented by a binary disk is a realistic simplified approach which can provide insight into the response of the starfield correlation operation.

By a binary disk image we mean one which is described by the function:

$$f(r) = 1 \qquad 0 < r < a$$

$$f(r) = 0 \qquad r > a$$

where "a" is the radius of a star image on the input image plane having typically a value of (10^{-3}) cm, as determined primarily by the characteristics of the telescope, the sensor and the imaging medium. In our analysis below we will initially consider the disk radius, a, to be normalized to unity.

2.3.1 Correlation with a Single Star Image.- Consider initially the case of a single star image. The two dimensional Fourier transform of the amplitude function of a single binary disk which will be formed at the first Fourier transform plane can be shown to be described by a circular symmetric function:

$$\frac{a\, J_1\,(a\omega)}{\omega}$$

where the J_1 indicates the first order Bessel function and ω is the independent radial parameter of the transform plane.

This is the amplitude of the Fourier transform of the live image of a single star image as would transit the Fourier plane of the correlator. At this point in a matched filter system a recorded spatial frequency filter of the starfield to be recognized will be located.

Let us consider first the effect of spatial frequency band limiting on the recognition of a single star. We would expect the most significant type of band limiting to be low spatial frequency rejection which is almost inevitable due to the limitation on the dynamic response of the spatial filter media.

For a real symmetric image such as a single star image the correlation function will be identical to the convolution in evaluating the correlation response. The band limited convolution can best be computed in the frequency domain by the convolution theorem and then inverse transforming it to the spatial domain. In the case of circularly symmetric images, such as our assumed star model, the inverse transform takes the form of a Hankel transformation.

Before computing the convolution, however, it is instructive to simply look at the equivalent band-limited amplitude of the binary disk function itself. This has been found by computing with a digital computer the inverse Hankel transformation of the Fourier transform of the unit radius binary disk. This inverse Hankel transformation is computed by:

$$f(r) = \int_{\omega_1}^{\infty} \omega \frac{J_1\,(\omega)}{\omega}\, J_o\,(r\omega)\, d$$

where ω_1 represents the upper bound of the low frequency rejection filter.

This amplitude function was computed and is shown in Figure 2-2 for several values of ω_1. The form of the function with varying degrees of low frequency suppression conforms to a physical interpretation. As ω_1 increases, the extent of r over which a low frequency (i.e., "DC") signal can be supported

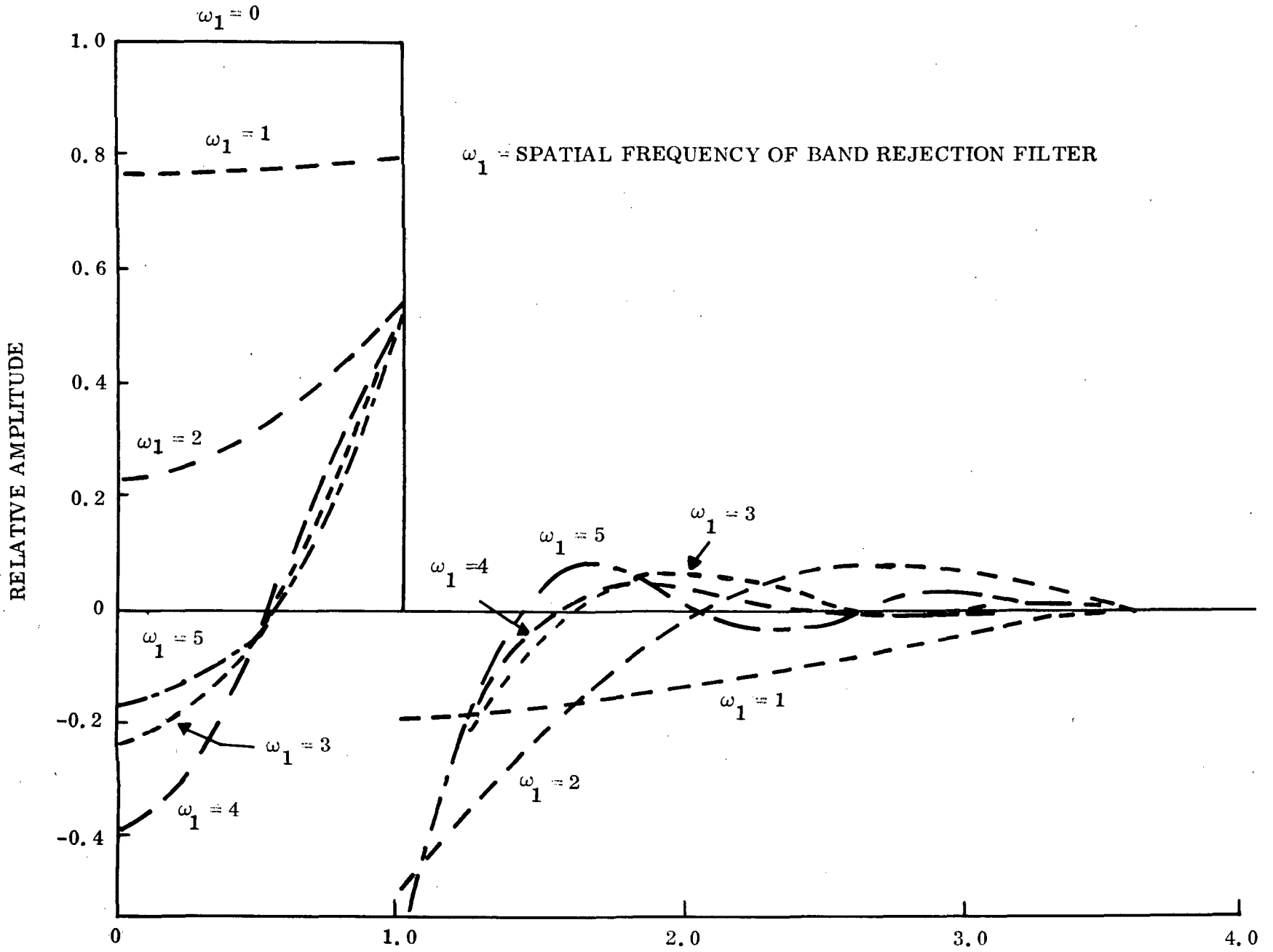

Figure 2-2. Equivalent Amplitude in the Spatial Domain of a Spatial Frequency Band Limited Star Image for the Case of a Single Star Represented as a Binary Disk

is reduced. This is shown to be the case. An examination of this band limited reconstruction leads intuitively to an understanding of band limiting as a means for sharpening the correlation function. This is derived next.

If the band limited convolution of the input image and the spatial frequency image is designated as

$$\left[f(r)**f(r)\right]_{BL}$$

then:

$$\left[f(r)**f(r)\right]_{BL} = \int_{\omega_1}^{\infty} \omega \left(\frac{J_1(\omega)}{\omega}\right)^2 J_o(r\omega)\, d\omega$$

This function describes the amplitude characteristics of the correlation function (or "recognition spot") appearing in the output plane when a single star is the input image and when the spatial frequency filter is designed to model the amplitude of the band limited spatial frequency representation of the star. This is the function whose center is to be detected in order to determine the vector direction to the "starfield" relative to the telescope axes system.

Note that since we have normalized the star image radius to unity, that a value of $\omega_1 = 1$ refers to a spatial frequency of 1 spatial radian per radius of the star image. Recall that the scale factor relating the displacement in the spatial frequency domain to the spatial frequency in the spatial domain is $\frac{\lambda F}{2\pi}$. For a typical system in the present application, this scale factor will be in the neighborhood of 0.05 mm per line pair per mm. Therefore for a star image of diameter 10^{-3} cm, a normalized value of $\omega_1 = 1$ would correspond, in the spatial frequency plane to a displacement of 2.5 mm. Hence, for the example cited, a value of ω_1 would correspond to a low frequency rejection filter in the form of an opaque disk in the filter domain of radius 2.5 mm. Likewise $\omega_1 = 2$ would correspond to an opaque disk 5 mm in radius, etc. Since we are considering 40 mm image format, a maximum realistic value, for the present case, of ω_1 would likely be in the range of 7 or 8. Note that these central opaque disks, as expected, sharpen the correlation peak but at some reduction in overall output power. This is not considered to be necessarily a limiting problem since laser power itself has been shown not to be a critically limiting factor except for a relatively high dynamic attitude determination system (see Section 3.4).

This result has been computed and is plotted for "Binary" input star images for several values of ω_1 in Figure 2-3. Figure 2-4 shows similar results for input star images which are assumed to be more properly represented

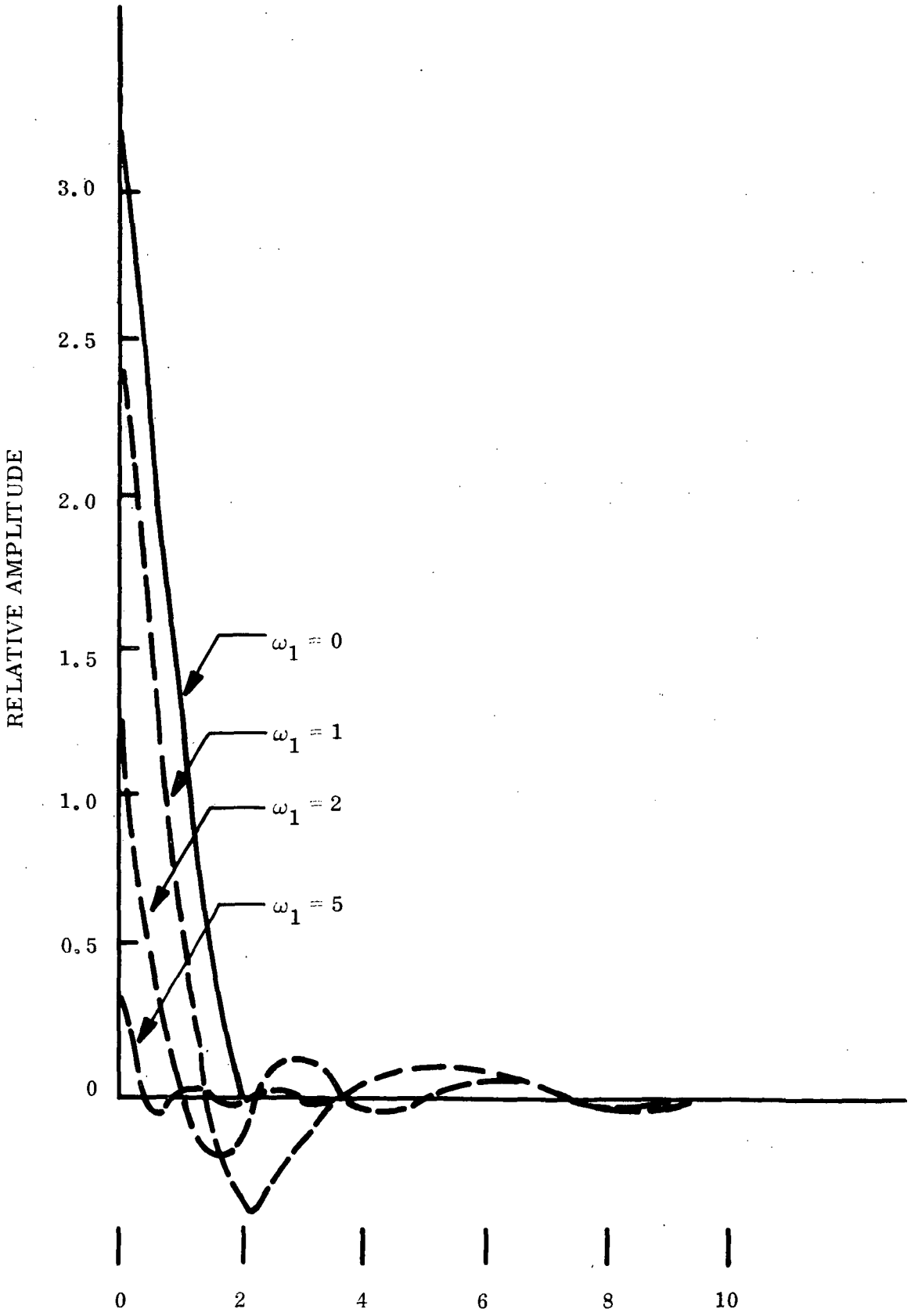

Figure 2-3. Central Cross Section of Cross-Correlation Function of Frequency Band Limited Binary Star Images

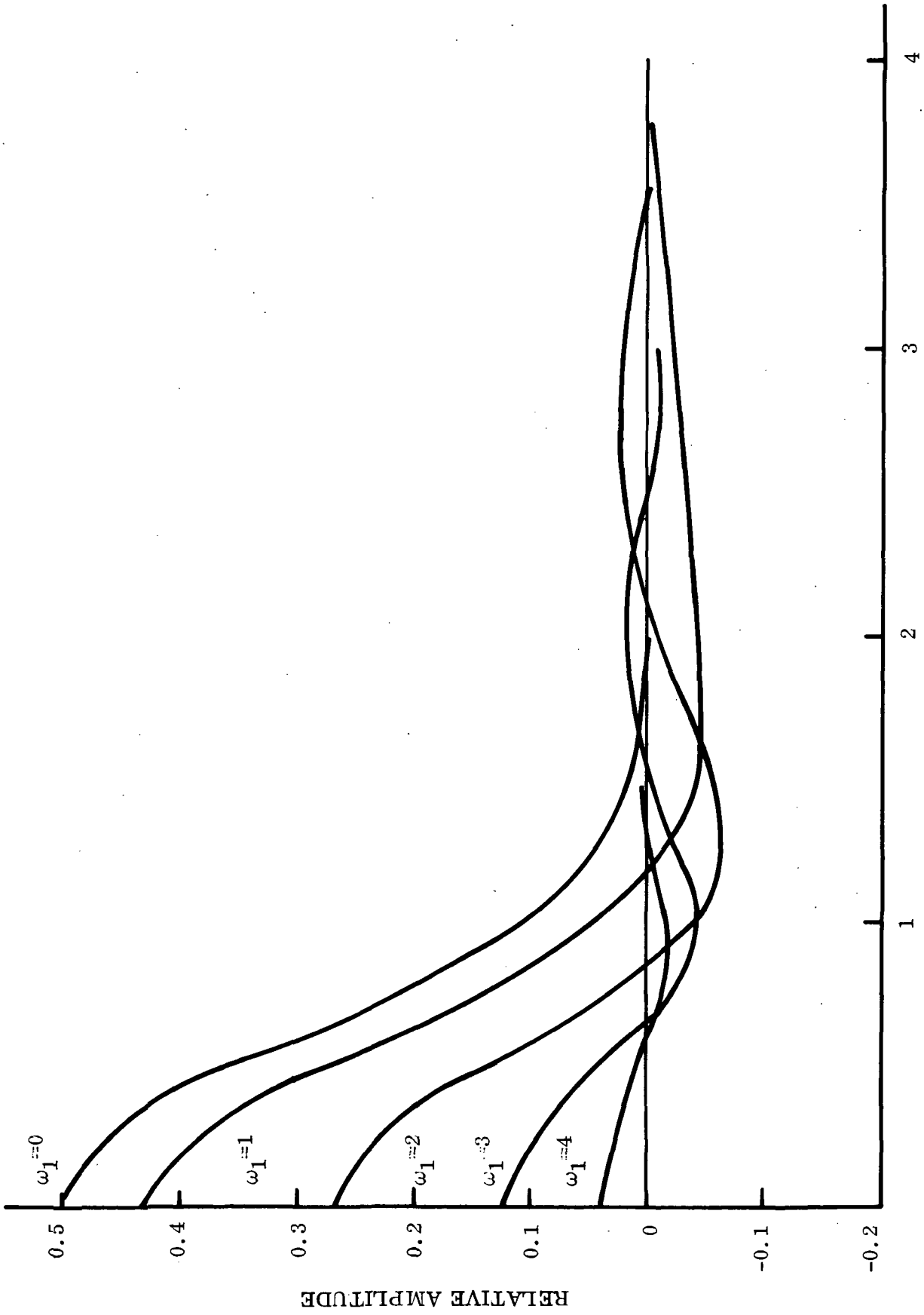

Figure 2-4. Cross Section of Cross-Correlation Function of Frequency Band Limited Gaussian Star Images

by Gaussian functions. As expected, we note from these figures that the frequency band limiting causes a significant sharpening of the peak of the convolution function and reducing the width of the main lobe of the correlation function.

Note that, for larger values of ω_1, that the width of the main lobe of the correlation function becomes significantly less than that of the original star. This demonstrates a potential advantage of low frequency band rejection in improving angular accuracy determination. As a point of reference note that for $\omega_1 = 0$ (i.e., no frequency band limiting) that the correlation function has a width, as expected, of twice that of the star image. For $\omega_1 = 1$ its width is about 1½ that of the star image. For $\omega_1 = 5$ the width of the correlation function is about 1/4 that of the star image. Hence it is evident that spatial frequency band limiting does sharpen the correlation function and can potentially lead to improved tracking accuracy.

2.3.2 Correlation with a Multiple Starfield Pattern.- Let us consider next the nature of the multiple starfield image as far as recognition is concerned. Once again we will consider each star to be recorded on the input plane as a simple binary disk. Consider, initially two stars having the same diameter "a" and having the distance between their centers of D. Define the input image axes as x and y and the corresponding frequency plane axes as u and v. Assume that the y and v axes are aligned along the direction defined by line joining the two star centers.

The frequency plane representation will be (cf. p. 338, ref. 14):

$$f(u,v) = \frac{2\pi a J_1\left(a\sqrt{u^2+v^2}\right)}{\sqrt{u^2+v^2}}\left(e^{j\frac{D}{2}v} + e^{-j\frac{D}{2}v}\right)$$

This resembles the previously described response for a single star. However, the function is modified by the exponential function as shown. Since the function no longer has radial symmetry, the relatively simple Hankel transforms no longer applies.

The frequency plane response along the x (or u) direction remains the same as for the single star. The conclusions discussed above concerning the shape of the correlation function for the one star case also holds here in the x direction. Along any other axis, however, it is further modulated by interference fringes from the two stars. Along the y axis of the frequency plane the response will be

$$f(u,v) = 2a\,\frac{J_1(av)}{v}\cos\frac{D}{2}v$$

The absolute value of this function is shown in Figure 2-5 together with an image plane representation of the input image. It is evident that D will be many times greater than "a" (typically by 3 or 4 orders of magnitude).

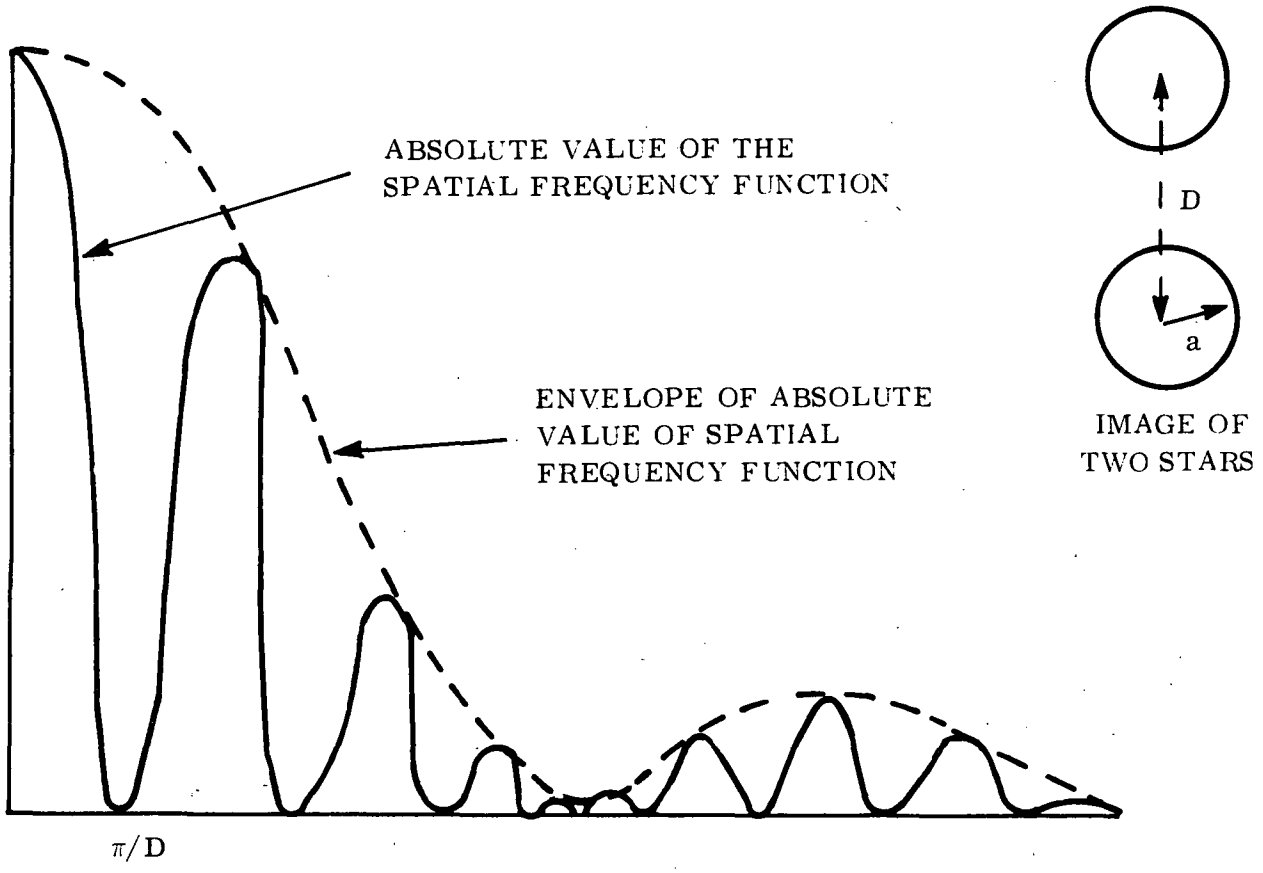

Figure 2-5. Frequency Plane Representation of Two Star Field
(Along Direction Between Stars)

Consequently we can anticipate that the term ($\cos \frac{D}{2}v$) will modify the basic $\frac{J_1(\omega)}{\omega}$ type of term, in the frequency plane, by a high frequency interference pattern. More than 2 stars will result in a multitude of cross-hatched modulation of the $\frac{J_1(\omega)}{\omega}$ response. The frequency and direction of these "cross-hatched modulations" is indicative, respectively, of the displacement and relative direction of each of the stars in the pattern. This has been observed to be the case in actual recorded spatial filters of starfields. It is the frequency and direction of these interference patterns which coincide with the stored pattern on the spatial filter (in the case of correlation with the starfield stored on the filter) or do not coincide (in the case of non-recognition). The frequency and orientation of the interference fringes must be maintained precisely from the standpoint of achieving a high recognition correlation of a specific starfield. This subject, in relation to spatial frequency filter registration requirements is discussed in Section 3.4.

From the standpoint of the effect of frequency band limiting on the autocorrelation response of multiple starfields, however, it is the envelope of the function (i.e., the $\frac{J_1(\omega)}{\omega}$ term) which will primarily determine the characteristics of the correlation function response. Consequently the shape of the band-limited correlation response as computed and as shown in Figures 2-3 and 2-4 are also descriptive of the response expected from an autocorrelation response of a multiple starfield and can be used as an input for predicting the accuracy performance of the multiple starfield tracking case.

This result conforms to an intuitive judgment that information which describes the relative location of stars in a multiple starfield should not have significant effect on the shape of the autocorrelation function (presuming, of course that no significant distortion of the input image or misregistration of the spatial filter exists). The shape of the autocorrelation function is determined primarily by the relatively high spatial frequency information in each star image. These comments apply, however, to the ideal autocorrelation case. As discussed in Section 3.5 any low frequency distortion in the image (stretching, pincushion, etc.) can result in partial or complete decorrelation of the starfield image.

2.3.3 Prediction of Tracking Accuracy.- The foregoing discussion leads to the conclusion that, for the idealized autocorrelation situation, Figures 2-3 and 2-4 provide a key to help predict the tracking accuracy possible with starfields. The results shown in this suggest that for values of ω_1 as high as say 5 or even 10, that the autocorrelation function center should be measureable to less than 1/10 the width of an individual star based on a single pulse center detection. By smoothing a number of such measurements (say 100) a further improvement of 10 might be expected.

Any realistic conclusions must, however, be made on the basis of some realistic assumptions of noise and image distortion. Although the above analysis can provide some considerable insight into the predicted performance, any complete appraisal will necessarily have to include estimates of noise

and distortion which will ultimately determine the optimum value of ω_1. This will necessarily be based on the specific characteristics of the optical-electrical readout device.

Based on a consideration of the above factors and the known performance of available trackers, it is expected conservatively that starfield tracking accuracy will be possible in the range of 1/20 to 1/10 the nominal diameter of a star image. For the parameters of the tracker considered here, this represents accuracies in the range of a $0.3(10^{-3})$ to 10^{-3} fraction of the optical field of view.

As discussed before the relaxation time constant of the optical-to-optical interface, or that of the imaging dynamics (whichever is the shorter), will determine the number of times the electro-optical tracker will be able to smooth the position of the correlation function and, hence, will also be very significant in determining tracking accuracy. Hence a navigation system operating with a medium such as photoplastic, the static correlation function can be smoothed over many seconds resulting in high navigation accuracy. However an attitude control determination system operating with a very fast relaxation time constant optical-to-optical interface will permit much shorter readout smoothing intervals and consequently expected reduced tracking accuracy. Thus there exists an evident trade-off between smoothing time and tracking accuracy.

3.0 INSTRUMENTATION INVESTIGATIONS

3.1 Investigation of Input Imaging Medium for Starfield Tracking.- Evaluation of alternative imaging media for a coherent optical starfield recognition and tracking system was the subject of the related predecessor contract (NAS 12-2148). About 30 different media or processes were considered in this evaluation. Criteria for the evaluation included sensitivity, resolution, diffraction efficiency, reusability, speed and simplicity of development and capability of being developed "in place".

The results of that contractural effort which was completed in late 1969 indicated that two types of imaging media had the most promise at that time for the present application: a photodeformable (i.e., an optically sensitive photoplastic) and a rapid process silver halide medium of the type characterized by Polaroid diapositive media. It is an intended function of the present contract to experimentally evaluate these two types of media. The results of this evaluation are discussed below.

Before discussing the details of this evaluation two points should be made:

- Recent developments in image intensifiers as well as the recent military declassification of a large class of image intensifiers can significantly affect the matter of image medium selection. Several advanced "real time" media which were previously considered unacceptable for reasons of low sensitivity may now look more attractive when used with an image intensifier.

- Some more advanced media have become potentially available since the completion of the above referenced survey. Among these are various types of optically addressable liquid crystal devices. This and other newer media will be considered further for the present application.

3.1.1 Method of Investigation.- The emphasis on the media evaluation has related to star images. This was justified when it became evident that material sensitivity was usually the single most critical characteristic of most of the candidate input media. Experiments were also made with landmark images and are discussed in Section 3.2. However, since the optical power density at the input image plane from a landmark is typically two or more orders of magnitude greater than that of a star, the sensitivity requirement for many applications is usually determined by the starfield problem presuming both landmarks and starfields are observed with the same telescope optics and with the same type of imaging medium.

Initial experimental investigations were made with laboratory simulated star images. However, in order to provide an even more realistic evaluation, further experimental evaluations were made with the 16 inch and 4 inch telescopes which are part of the facility at the General Electric Photo-Optical Observatory near Schenectady, New York. When appropriate compensations are estimated for atmospheric effects it is believed that this approach to evaluation would be more meaningful in terms of stellar magnitude and color temperature sensitivities of the media.

Specifically these experiments were made with photoplastic recording medium (PPR) and Polaroid diapositive medium.

Some comments should be made concerning the telescopes. As discussed in the final report to the preceding contract (NAS 12-2148), and further discussed in Section 2.3 of this report, the highest possible resolution (i.e., smallest possible point spread function) is not necessarily required or desired of the telescope optics for an ideal starfield correlator. Rather, importance is stressed on achieving a symmetric image for each star and a very low degree of distortion when viewing the overall starfield. As discussed, a matched design is desirable where the optical spread function of the optics, the imaging medium and, if used, of the image intensifier are nearly equal. As also discussed, the ideal point spread function also is a function of anticipated distortion in any one of these elements as well as a function of the image motion due to vehicular dynamics. To have an optical point spread function, for example, which is significantly smaller than the anticipated distortion of any element of the system could represent a counter-productive design factor.

With this in mind, it appeared desirable in our evaluation experiments, to make use of telescopes which provide a range of point spread functions. The use of the 16 inch and the 4 inch telescopes made this possible. The 16 inch telescope was adjusted so as to provide a minimum point spread function of about 0.07 mm. The 4 inch telescope was operated with an optical spread function of about 0.01 mm. In view of the expected range of possible point spread functions of the other key system elements, this was judged to represent, respectively, a maximum and a minimum value of the telescope optical spread function which should be considered.

3.1.2 Evaluation of Photoplastic Recording Material - A Summary of Results and Conclusions for a Starfield Tracker.- A photometric evaluation of this type of medium was made by viewing stars with the 16 inch and the 4 inch telescope. As a result of the interpretation of the results for this experimentation it was concluded that the optical energy density required for photoplastic recording material from blue-white stars was typically in the neighborhood of 10^{-4} watt-sec/cm^2. For red stars energy density requirements were evaluated as being about 10^{-5} watt-sec/cm^2.

Thus the photoplastic recording material as evaluated was judged to have nearly one order of magnitude less sensitivity for non-red stars than was predicted by the analysis of Contract NAS 12-2148. It is emphasized that this estimated sensitivity is not necessarily representative of the ultimate sensitivity of photo-sensitive deformables. It is believed, however, to be a realistic evaluation of photodeformables as they exist today.

An interpretation of the above result would, for example, indicate that a 5th magnitude blue-white star could be imaged with an 8 inch telescope with required exposures in the range of 100 seconds. Even the brightest blue-white stars in the sky would require an exposure of 1 sec or more with such a telescope.

Stars having their spectral response in the red spectrum, such as Betelgeuse and Antares, would require somewhat less energy density for the

photodeformable evaluated which has its peak sensitivity in the red spectral regime. However bright red stars are insufficiently numerous to depend on them alone for a realistic starfield tracker.

With regard to correlation signal to noise ratios, the photoplastic recording material used as a medium for storing input images has demonstrated response equivalent to that obtained with good silver halide input images (i.e., in the range of 100:1 to 400:1). Nevertheless, the overall conclusion is that photoplastic recording materials, as they exist today, have restricted applicability to the starfield tracking problem unless they are used with an image intensifier. The primary reason for this is the limited sensitivity, especially in the spectral band of most stars, of these materials which would result in a requirement for excessively large optics or excessively long exposure times.

This problem is believed to be shared with all other known non-silver media and, in the case of most other advanced media, to a more severe degree.

As will be pointed out in Section 3.3, however, the photoplastic media offer significant potential applicability to the starfield recognition problem when used with an image intensifier.

3.1.3 Evaluation of Photoplastic Recording Material (PPR) - Experimental Description.- A number of experiments were made with PPR at the Photo-Optical Observatory with both the 16 inch and the 4 inch telescope, as well as in the laboratory with simulated stars. Stars included among others, Arcturus, an orange-yellowish star having a +0.24 visual magnitude, and Vega, a blue-white star having a visual magnitude of +0.21.

The impulse response of PPR is a crater-like deformation, ideally symmetrical in shape. As such, the photometric impulse response is described primarily in terms of a diameter and depth of depression of the deformation. The response of these two parameters is a function of the intensity and diameter of the point spread function coming from the telescope as well as of the specific characteristics of the photodeformable (e.g., its resonant spatial frequency) and the mode and degree of its precharging and development.

In order to make an evaluation of the sensitivity of PPR it is necessary first to make some judgment of what constitutes a desired response in terms of depth and diameter (or spatial frequency response) of a phase storage medium. The relative amplitude of diffracted optical energy is a function of the relative phase optical shift. For a phase medium, the optical amplitude in a given diffraction "order" of a sinusoidal phase grating is proportional to the Bessel function of the first kind of that corresponding order where the argument of the Bessel function is the peak phase shift due to the deformation. In most coherent optical processors the diffracted energy of interest will be primarily in the first diffraction order. Based on an examination of the amplitude of the Bessel function as a function of the wavelength argument this would suggest that the maximum phase shift should not exceed about 1.0 to 1.5 radians if it is desired to avoid significant higher diffraction orders. Although this criterion is established for sinusoidal phase gratings it is usually a reasonable guide also for most other phase input images. (Note that the reasonable assumption is made here that the input imaging medium is a phase medium and that the spatial frequency filter medium is a

variable transmissivity medium which will not give rise to significant higher diffraction orders for a sinusoidal input.)

Based on the above considerations it is reasonable to limit the maximum deformation which results in a phase shift of about 1.5 radians.

Note that for most practical problems however that avoiding excessive phase shift is rarely a problem particularly for relatively thin deformable films (e.g., $<$ 10 micrometers) because of the limitations in sensitivity of the material. The more practical problem is deciding on the minimum phase shift which must be obtained for the weakest desirable signal. This is, to some extent, a function of the desired diffraction efficiency which in turn determines the required power of the on-board laser and the sensitivity of the electro-optical readout sensor. More practically, however it is determined by noise existing in the phase medium. More specifically it is determined by the magnitude of the noise which exists in the spatial frequency range of the desired signal. Based on correlation experiments made with a photoplastic input image it appears that minimum phase shift should be in the range of 0.05 to 0.1 radians. Such a phase shift should not only provide an acceptable signal to noise ratio, but it will provide realistic values of diffraction efficiency.

Phase shift can be related to deformation. For a transmissive phase medium:

$$\Delta \phi = \frac{2\pi}{\lambda} \quad (n-1)(b/2)$$

and for a reflective phase medium:

$$\Delta \phi = \frac{2\pi}{\lambda} \quad (b)$$

where b is the depth of deformation, $\Delta \phi$ is the phase shift, λ is the wavelength of illumination and n is the refractive index of the medium.

For PPR having a typical refractive index of about 1.6 and operating with the wavelength of a HeNe laser this becomes:

Transmission Medium: $\Delta \phi$ (rad) = b (microns) x 3.4

Reflective Medium: $\Delta \phi$ (rad) = b (microns) x 11.4

If, for the moment we consider a transmissive system, this indicates a minimum required signal deformation of about 0.02 to 0.04 microns.

Further investigation of noise sources is required to determine whether or not a reflective system can operate with significantly lower values of deformation.

At the present time we will assume, as a required sensitivity criterion, a conservative value of required deformation of a star image of 0.05 microns.

In order to evaluate the relationship between phase medium deformation and optical energy a rather large number of experiments were performed at the Photo-Optical Observatory with various stars. The following result is typical of those obtained for a blue-white star. This example is an exposure of the star Vega with the 4 inch telescope and is considered to be a good representation of the sensitivity of recording under favorable condition of exposure and development:

Stellar Magnitude	Calculated Power Available At Aperture (Neglecting Atmosphere) (watts)	Effective Power At Image Plane (watts)	Exposure (sec)	Energy Density At Image (watt-sec/cm^2)	Deformation (microns)
+0.14 (Blue-White)	10^{-10}	$0.2(10^{-10})$	60	$1.5(10^{-3})$	1.04

The effective power at the image plane is determined from the calculated available power at the aperture, suitably modified for estimated atmospheric attenuation and optics transmission at the time of the experiment.

Experiments have demonstrated excellent reciprocity of photoplastic recording material over exposure times ranging from hundreds of seconds to fractions of seconds. Based on this assumption of reciprocity, an energy density required to obtain a "minimum" deformation of 0.05 microns is computed from the above data to be about $7(10^{-5})$ watt-sec/cm^2.

In interpreting this data it should be recognized that there exists a rather poor spectral match between the blue-white star Vega and the spectral sensitivity of the photoplastic medium used. An improved sensitivity would be demonstrated from red stars such as Betelgeuse or Antares. However, such results would be less realistic in view of the predominance of blue and blue-white stars among the brightest stars of interest. In any event the results as shown for Vega above are believed to be somewhat conservative.

Based on this typical experiment as well as experiments with other exposures, other stars and other developing conditions the conservative conclusion is reached that a realistic energy density required for PPR when imaging blue-white stars is in the range of $0.5(10)^{-4}$ to 10^{-4} watt-sec/cm^2. This is about one order of magnitude less sensitive than that predicted by the results of Contract NAS 12-2148. Based on that analysis, particularly with regard to image motion, there appears to be a strong case for using an image intensifier in conjunction with PPR. Indeed without such an intensifier the photodeformables of this type do not presently appear practical for most coherent optical starfield tracking systems.

3.1.4 Evaluation of Polaroid Diapositive Material - A Summary of Results and Conclusions.- A photometric evaluation of this type medium was made by viewing stars with both of the telescopes previously discussed. As a result of the evaluation it was concluded that the optical energy density required was in the range of 10^{-8} to 10^{-7} watt-sec/cm^2. This was the range in the final report on Contract NAS 12-2148.

Starfield recognition experiments using Polaroid diapositive media as an input media have shown, in some cases, performance in terms of signal-to-(peak) noise ratio as high as 200:1. In other unpredictable cases, however, the existence of noise was judged to preclude adequate performance with starfield images (see discussion on noise below).

The sensitivity is judged as adequate for most applications of starfield recognition and tracking. For example, it would indicate that a 5th magnitude star could be imaged with an 8 inch telescope with exposures typically in the range of 10^{-2} to 10^{-1} seconds. Based on the analysis of factors such as image motion resulting from vehicle dynamics as presented in the final report to Contract NAS 12-2148 this is judged to be an acceptable sensitivity and exposure time for many vehicle applications. Other experiments have supported the position that, as expected, this material had adequate sensitivity and resolution for most practical landmark recognition and tracking experiments.

However in one other important aspect this material was judged to have disappointing and, probably for some applications, unacceptable performance. This relates to noise which appeared unpredictably in some of the images. The type of noise which was most disturbing was in the form of small "pinholes". These sometimes appeared in large numbers and sometimes had sizes and shapes having much the same characteristics as stars. Variations in the development were tried. However the noise problem persisted in so many cases to such an extent that this material was judged as having very low potential for holographic starfield recognition and tracking. Since it is very desirable to use the same type of medium for both landmarks and starfields its usefulness in landmark recognition and tracking is also questionable.

Therefore, based on these experiments it is recommended that this type of rapid process silver halide material no longer be considered as a prime candidate for the present application. The specific experiments and quantitative data resulting therefrom are described in some detail in Appendix B of this report.

This conclusion and recommendation is further supported by recent advances and declassification of certain image intensifiers. The availability of these intensifiers have made certain other advanced media, which may previously have been judged to have marginal sensitivity, to now appear more attractive. Also, unlike most rapid process silver halide techniques, some of the advanced media have advantages of reusability, and readily adaptable, rapid, "in-place" processing. The inability to avoid moving parts appears to be a major disadvantage to all known rapid process silver halide media.

3.2 Investigation of Input Imaging Media for Landmark Tracking.- Most of the emphasis in this section is placed on the applicability of photoplastic recording to landmark recognition and tracking. The reason for this is that much prior experimentation has been performed with conventional silver halide photos obtained in various space programs.

3.2.1 Evaluation of Photoplastic Recording Media for Landmark Tracking - Summary of Results.- Successful correlation experiments were performed using PPR as an imaging medium for recording landmarks under a wide range of conditions and parameters. These experiments are described in more detail in Section 3.2.2.

Based on an interpretation of the results of these experiments, a typical performance plot is presented in Figure 3-1. It shows the typical exposure required as a function of solar illumination angle when viewing a "good" landmark area under good atmospheric seeing conditions. As before, we define a good landmark as one having a significant amount of high contrast detail. Exposure requirements are shown for three values of lens speed. The results presented in the plot assume direct telescope imaging on the PPR without the use of an image intensifier.

The experimental results presented in Figure 3-1 are typical exposures required. Under poorer conditions of target quality, viewing conditions, etc., somewhat longer exposures could be expected. Under better conditions somewhat shorter exposures could be expected. Because there are many parameters relating to the operation of the PPR, there is reason to believe that some further optimization of these parameters could be performed leading to still shorter exposures.

In interpreting the results of Figure 3-1 it is necessary to consider the effect of image motion. Some typical results are shown in Figure 3-2. This is a plot of image smear in ground dimensions as a function of sun angle assuming the use of an f/2 lens. Since this plot does not take into consideration the effects of attitude rate errors, it would be typical of a vehicle having rather good attitude control such as one with Control Moment Gyros.

The effect of input image smear on the response of a correlation tracker is not a simple one. Image smear is equivalent to high spatial frequency loss in the input. It is well-known, however, that correlation tracking accuracy is not necessarily limited by the spatial frequency content of the input image. This is because the correlation operation tends to smooth redundant data resulting in a tracking accuracy greater than the input resolution. Tracking accuracy which is better than input resolution by one to two orders of magnitude can be expected. The exact performance is highly dependent on the amount and contrast ratio of the data existing in the scene as well as in the smoothing capabilities of the electro-optical read-out sensor.

An interpretation of the results shown in Figure 3-2 are encouraging from the standpoint of the usability of PPR under good viewing conditions. The limitations of applicability of PPR in terms of the degree of degradation of scene and viewing conditions have not been fully established. It is expected however that the use of an image intensifier may extend the usefulness of the system to lower light level conditions.

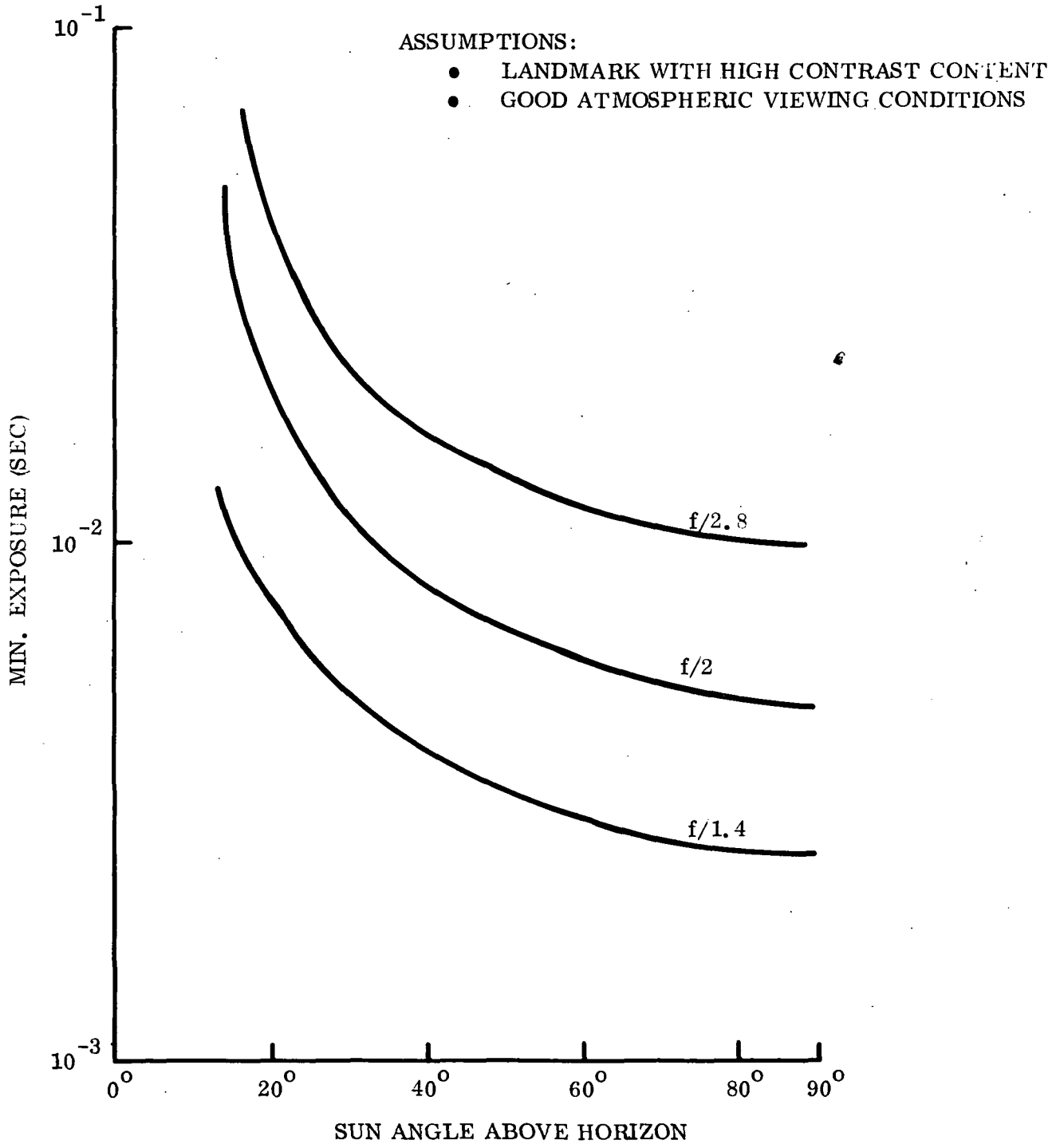

Figure 3-1. Typical Minimum Exposure Required for Imaging Landmarks on PPR as Determined by Experiments

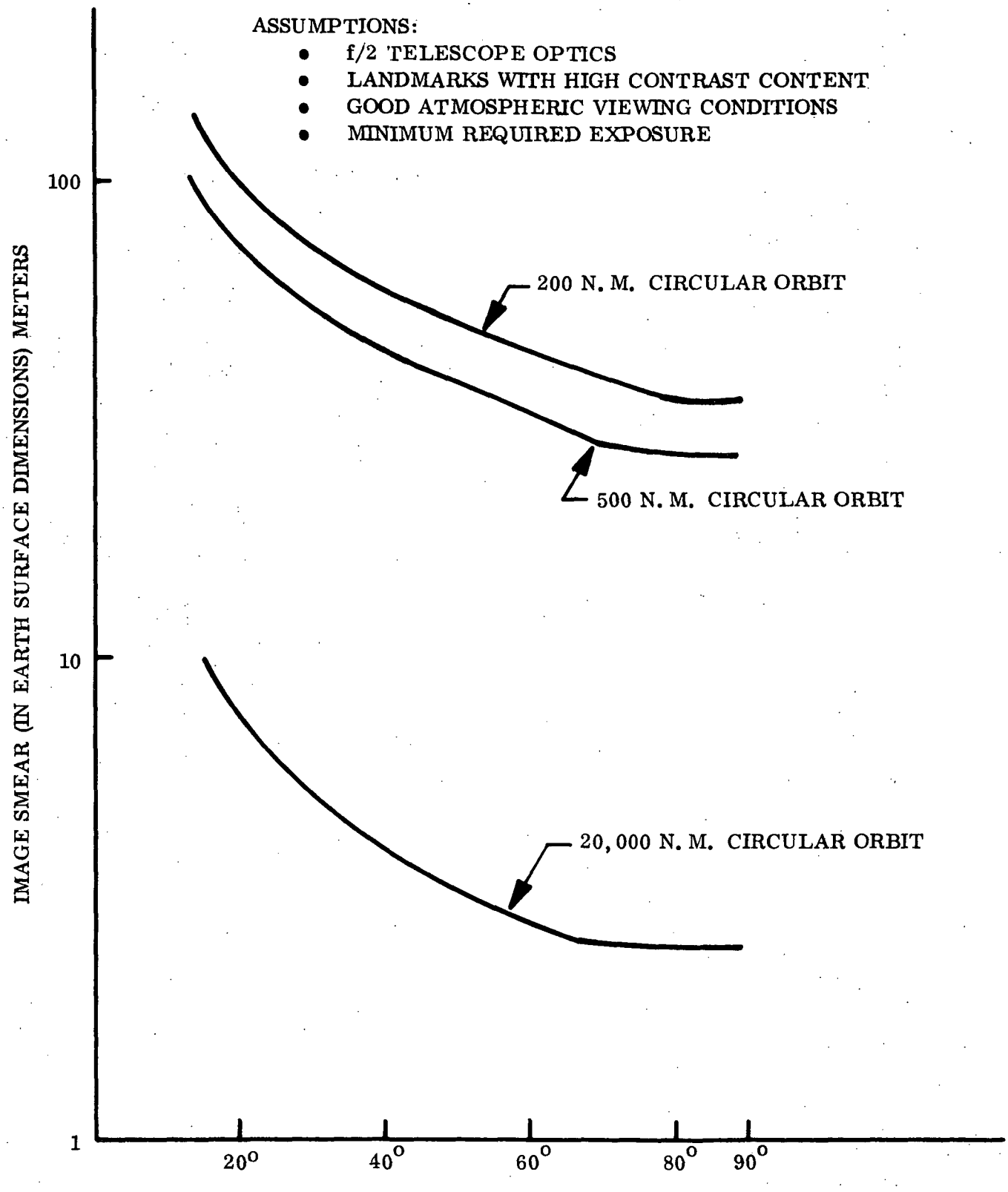

Figure 3-2. Image Smear Due to Orbit Dynamics Resulting from Imaging Landmarks on PPR

Section 3.2.2 discusses in somewhat more detail the experimental program which was pursued to evaluate PPR and a candidate imaging medium for landmark tracking.

3.2.2 Performance Evaluation of Photoplastic Recording Material as an Input Imaging Medium for Recording Landmarks - Description of Experiment.- Photoplastic recording material is a deformable material which is capable of storing an image as a phase effect. Like most phase media it is not responsive to uniform illumination or very low spatial frequencies. It has demonstrated reciprocity from fractions of a second to hundreds of seconds.

The diffraction response of a phase medium in a coherent system is a function of the phase shift produced by the image-modulated medium. For many practical applications the desired diffraction response is that which is described by the first diffraction order (i.e., that order whose amplitude is proportional to the 1st order Bessel function of the phase shift). If the medium phase modulation is limited to that value where the 1st order is predominant, then the diffraction response of a phase medium approximates very closely the diffraction response of an amplitude medium. This represents a desirable situation whenever it is appropriate to use a combination of a phase medium and an amplitude medium in the same coherent optical processor. Such a situation is attractive here where we are considering a phase medium for storing the input image and a silver halide film for storing the spatial filter. In such a case there may be a need to limit the maximum modulation of the phase image so as to avoid otherwise undesirable intermodulation products.

The peak 1st order intensity obtained by a phase medium occurs at a phase shift of 1.8 radians. As described in Section 3.1, for a transmission type of phase medium this will typically correspond to a deformation of about 0.6 microns when operating with a HeNe laser. For a phase medium used in a reflection mode this would correspond to a deformation of about 0.15 micrometers.

The deformation depth, signal spatial frequency and incident optical energy density are all interrelated and are also dependent on the rheological properties of the deformable medium and especially on the thickness of the deformable layer.

Here we will limit our discussion to experimental results obtained with one of the more promising types of photoplastic recording having a deformable film thickness of 7 micrometers.

In order to achieve a realistic spectral illumination, it was decided to conduct this experiment out of doors in natural sun-illuminated conditions. The scene which was used was a print of a photograph of the Arabian peninsula. This photograph taken from a Gemini spacecraft had been selected for previous simulated experiments because it was judged as being representative of a realistic navigation landmark area. It contains a wide range of data in terms of spatial frequency and contrast ratio content. For this test, a rigid copy set-up was made to hold a photograph of a landmark parallel to the film plane of the photoplastic recording camera. The copy set-up was oriented so that sunlight fell on the photograph nearly squarely. It could not be exactly square because the camera would have cast a shadow. The days chosen were

August 19 and 23, 1971 which were cloudless and the air very clear. All exposures were made within an hour of 1:00 P.M. DST which would be close to noon sun time.

The sunlight was measured by three different instruments, all of which agreed to within 10 percent. The value obtained on the Weston Standard Photometer is probably the most reliable and was 10^5 lumens/m^2, which is the nominal value for noon sunlight on an exceptionally clear day.

All of the images obtained here were taken with a lens setting of f/5.6. This appeared to provide the best image response for this particular lens. Had a higher quality lens been readily available for our photoplastic camera, a much faster setting could have been used. In this respect no reciprocity failure has ever been observed with photoplastic recording material for exposures ranging from fractions of seconds to hundreds of seconds. Hence data extrapolation to predict performance with faster lenses is valid.

In addition to exposure and lens speed there are two other primary parameters which influence the response of the photodeformable to an input image. They are the relative level of precharge of the medium and thermal energy applied to the development of the medium.

The effect of increasing the precharge level is to increase the stress on the medium and consequently the amount of deformation for a given exposure and hence an increase in the film sensitivity. In a practical case the charge level is increased until the effect of deformation noise (i.e., "frost") becomes excessive.

After exposure of the medium at various exposure times and settings of the other parameters, the depth of the deformation was measured. A usual instrument used for this measurement is the Nomarski microinterferometer. The only objection to its use is that it contains birefringent optics which produce two images. Under some conditions the overlap of these images and their interference fringes can result in confusing patterns. To be certain, the results were also checked on a Watson microinterferometer which works on a different principle and a Zeiss light-profile microscope which does not use interference in any way. All the results checked the Nomarski readings which are given below for PPR exposed at f/5.6.

MODULATION DEPTH OF PPR		
EXPOSURE SEC.	RELATIVE CHARGE	DEPTH IN MICROMETERS
10	60	.45
5	60	.50
2	60	.56
1	60	.56
.5	60	.48
.2	60	.32
.1	60	.24
.04	60	.08
1	70	.63
1	50	.48

The above results show that it is apparently not readily possible to obtain more than 0.63 micrometers of deformation on a film of this thickness (7 micrometers). This is believed to be due to a rheological property of this particular film and an inherent limitation. As has been described this is an advantage in that it prevents overmodulation. In order to obtain full deformation it was necessary to use a relative precharge of 70, but most of the images were made at a relative charge of 60. It was believed that the lower charge would have resulted in less noise. It is true that there was less noise when the film is viewed by reflected light but when tested in the recognition system there was no appreciable difference between exposures at relative precharge 50, 60 or 70. The noise seemed to vary more with the defects in the individual frame than with the charge and certainly did not correlate with the "frost" noise as seen by eye.

The effect of increasing charge is to increase the stress on the film and consequently the amount of deformation for a given exposure and hence to increase the film "speed". The three exposures at 1 second and different charge values indicate the effect of charge on deformation.

In retrospect it is possible to say that better results would have been obtained if all the exposures had been made at relative precharge 70 in which case the deformation would have been greater for less exposure.

Some mention should be made of the matter of overmodulation. Overmodulation, in excess of about 0.5 wavelength results in phase reversal which can produce an ambiguous image and unpredictable results. This problem previously was a concern when glass plates with photodeformable coatings 11-20 micrometers thick were used and it was then possible to obtain one wavelength of retardation or more. However, it is now known that maximum deformation is related to the thickness of the film and if this is kept at about 7 micrometers overmodulation will be impossible. In the present set of experiments where nearly one-hundred exposures were made, no combination of exposures, charge or development produced overmodulation.

Optical phase retardation is calculated from the modulation depth and the refractive index of the material which is polystyrene with an index of 1.585 at the sodium wavelength of 5893Å. Retardation for a transmissive medium is computed from the differential speed of light in the high index material and in air. A correction is made for the wavelength difference; the modulation depth is measured with an interferometer using sodium light and the retardation which would be produced by laser light at 6328Å is calculated.

A large number of experiments were performed with PPR in the manner described above. The results of one typical experiment will be presented as being indicative of the performance of PPR.

In this test a relatively large landmark area (i.e., one which is large relative to the telescope field of view) was used. The results obtained with one particular landmark made from this filter (designated as Filter #4832) were as follows:

PPR RESULTS WITH 4832 FILTER				
EXPOSURE	RELATIVE PRECHARGE	RETARDATION	RELATIVE SIGNAL	RELATIVE NOISE
1.0 sec.	70	.50 wave	100	2
1.0 sec.	60	.44 wave	110	3
.5 sec.	60	.37 wave	65	2
1.0 sec.	50	.37 wave	71	2
.2 sec.	60	.25 wave	40	1
.1 sec.	60	.18 wave	20	1
.04 sec.	60	.05 wave	10	.5

In this set of tests the signal level was much higher than in previous sets because the landmark area was larger. In this case even a 1 mw laser would be adequate to produce a fairly strong signal with the poorest transparency.

Conclusions from these experiments are:

1) With an aperture ratio of f/5.6 the optimum exposure in direct sunlight was 1 second. However exposures as short as 0.04 sec. give adequate response in terms of S/N ratio.

2) Most of the exposures were made at charge 60, though a few were made at 70 which resulted in greater film speed.

3) Useful exposures were obtained over the range 10 - 0.04 second.

4) If a charge value of 70 had been used then the exposure range would have been extended to less than 0.04 seconds. This would be equivalent to $5(10^{-3})$ sec. for an f/2 lens system.

5) With one filter (No. 4832), 0.04 seconds exposure was adequate even at a relative precharge 60.

6) In an optimum system (lenses the correct size for the transparency) a 1-2 mw laser would be adequate.

7) If they had been available first generation images should be expected to perform even better than the fourth generation images actually used.

3.2.3 Evaluation of Rapid Process Polaroid Media for Landmark Tracking.- Reference 15 describes the success of use of Polaroid material as both an input imaging medium and as a spatial filter medium. Similar experiments were conducted by GE with similar results. In general this medium can be successfully used in coherent optical correlation. However, the noise tends to be somewhat higher, probably due to non-uniformities in the material base and probably partly due to the incompletely removed "stabilized" silver salts which remain in this rapid process silver halide image.

Nevertheless signal to noise ratios as high as 20:1 were experienced when recognizing landmarks with this material. A further objective of these experiments has been to evaluate the speed at which the Polaroid material could be developed. It was found that development time could be reduced to about 1 sec. if the temperature were raised to about 110°F.

The general conclusion from the experiments is that this material can be used for an input imaging media. Optical sensitivity is generally not a severe restriction except under very adverse conditions.

However this material is not very attractive for this purpose due to the relatively higher noise introduced by it and especially due to the desire to avoid moving parts in the spacecraft. Any requirement for heating the film to shorten the development time would also be unattractive in a spacecraft.

Some of the details of this experimental evaluation is presented in Appendix C.

3.3 Application of Image Intensifiers to the Holographic Tracking Problem

3.3.1 Summary of Image Intensifier Characteristics.- Although not a specific part of the contract work statement, it became evident that a further investigation of the applicability of image intensifiers should be investigated as a means for reducing the size of the telescope optics and exposure time when viewing starfields and also landmarks under low light level conditions. This investigation was pursued by discussions with various suppliers of intensifiers. In addition a visit was made to the Army Night Vision Laboratory to discuss their work in image intensifiers.

A summary of typical characteristics of intensifiers which are potentially available is presented in Table 3-1. It should be noted that most of these characteristics were made available by suppliers and/or users and that maximum outputs and maximum gain ratings are primarily those applicable to long term continuous operation. There is reason to believe that, in some cases, these levels of gain and maximum output can be exceeded for intermittent mode operation as might be applicable to an autonomous navigation application.

As far as the starfield tracker is concerned, the sine qua non of an image intensifier is very low effective distortion. It is reasonably evident that an image intensifier will be counter-productive in imaging a starfield regardless of high gain, high resolution and low noise, if it has distortion which is so great that the individual stars of a starfield appear in the "wrong place". This makes the realistic presumption that there will be no a priori knowledge of how a given starfield may be located in the field of view of the telescope. The importance of system low distortion is of importance also for landmark trackers.

Ideally the distortion of the image intensifier should be sufficiently low throughout the usable field as to be negligible in relation to the resolution of the device.

TABLE 3-1

IMAGE INTENSIFIERS - TYPICAL CHARACTERISTICS

TYPE	LUMINOUS GAIN $\left(\frac{\text{ft.lambert}}{\text{ft.candle}}\right)$	RESOLUTION (lp/mm)	DISTORTION	MAX. OUTPUT BRIGHTNESS (ft.lamberts)	COMMENTS	SOURCE
1st Gen.-Single Stage-ES	30-40	55-80	4-6%	50-100		IT&T RCA Varo Varian and Others
1st Gen.-Three Stage-ES	40,000-100,000	25-30	15-20%	50-100		Ditto
1st Gen.-Three Stage-EM	100,000-200,000	30-40	1-4%	50-100	Typically Requires Large Magnet	Ditto
Proximity Focus		8-12				Bendix
2nd Gen.-Channel Plate Inverter Tube	25,000-50,000	20-30	2-4%	5-10 (30 W/O Brightness Control)	2-5 Volts for Gating	RCA Zenith-Rauland Varo Varian
2nd Gen.-Channel Plate Waver Tube	10,000-25,000+	20-30	0	5-10 (30 W/O Brightness Control)	3/4 In. Long 500 Volts for Gating	IT&T Litton Bendix
TSEM (Transmission Secondary Emission)	25,000	?	?		Research Type	GE RCA

There are about 5 potential approaches to achieving a low distortion high gain intensifier:

1) Use a multi-stage 1st generation intensifier with compensating optical correction built into the optical system. This is not favored because of the added complexities of the optical design and the variations in the tube distortion which are expected when operating at different voltage levels or when a tube is interchanged by another tube even of the same type.

2) Use the center portion of an "oversize" 1st generation tube. Thus, an 80 mm, 3 stage 1st generation tube might typically be expected to have a 20% pincushion distortion at the periphery of the tube. However maximum distortion of about 2% would be predicted if only the center 20 mm x 20 mm section of the tube were used. This approach is also not the most favored approach because of the excessive size of such a tube and because maximum distortion in the range of 2% is, at best, only marginally acceptable.

3) Specify a low distortion 1st generation multi-stage electrostatic tube for an image intensifier supplier. Such low distortion tubes have been proposed by at least two suppliers. A predicted 2 to 4% distortion, compared with a more usual 16% to 20% distortion for a 3 stage 1st generation tube has been proposed. This approach is not the most favored approach because the predicted residual distortion is still regarded as excessive and because, to our knowledge, such a tube has not yet known to have been proven in service.

4) The use of a 1st generation electro-magnetic tube. These tubes may, in some cases, have nearly acceptable low distortion but are rejected because of the excessive weight and size of such a device.

5) The application of a 2nd generation wafer type of channel plate image intensifier. Recent advances by at least one vendor has indicated the recent availability of a very low noise tube of this type in contrast to the somewhat noiser versions of this tube which were previously available.

A tentative preference is made for selection of the wafer type of intensifier primarily because of its inherently low distortion. Its very compact size also make it look very attractive. As presently used in military applications, the gain is limited to about 10,000 and the output brightness is limited to the range of about 1 to 5 ft. lamberts. The tube has been operated in a gatable mode by modifying the input voltage. Typically a 200 volt gating voltage is required.

By removing brightness control it is expected that luminous gain of 25 000 or more could be realized. Output brightness in the range of 20 to 30 ft. lamberts have been projected. Provided that a good spectral match can be made between the intensifier and the input imaging device, this is the range of output brightness which is required. This mode of operation may result in some increase in noise and perhaps some decrease in resolution and

tube life. Thus, while the wafer type of tube shows good promise, there is a clear need for further experimental evaluation with it before firm recommendation can be made for its incorporation in the system.

In the event that experiments should demonstrate that this type of intensifier is inadequate for the present application, a backup recommendation would be made to use a 3 stage 1st generation tube or an inverter type of 2nd generation tube with suitable optical correction of the distortion.

3.3.2 Experimental Evaluation with an Image Intensifier - Results and Recommendations.- A limited experimental evaluation was performed during the present contract to determine the potential of using an image intensifier to compensate for the sensitivity deficiencies of a "real time" input imaging medium which might otherwise have inadequate sensitivity.

These experiments were facilitated by the loan of a "3 stage 1st generation" image intensifier made available to GE by the U.S. Army Night Vision Laboratory of Fort Belvoir, Va. This particular intensifier had an optical gain, as measured by the NVL, of 47 000. From a gain point of view this device was expected to be more than adequate. From the outset of this investigation it was recognized, however, that this specific type of intensifier would not be adequate from a distortion point of view. Nevertheless the photometric evaluation has meaning in view of the recent availability of "distortion-less" intensifiers. The primary objectives of these investigations are to determine the effect of gain, noise and resolution limitation contributed by the intensifier.

Figure 3-3 shows a set-up for the evaluation of the intensifier together with a PPR camera in the laboratory. The details of these experiments are described in Appendix E.

In summary, the experiments showed an effective optical gain in the range of 200 to 400. By no means was the experimental set-up optimum. (For example, a relay lens was used which had estimated efficiency in the range of 3% to 4%.)

By implementing several improvements such as more efficient transfer lens and a better spectral match of the phosphor and medium, it is expected that this type of intensifier could result in usable gains in the range of 10^3 to 10^4. Elimination of the need for a relay lens would be especially attractive. This would then effectively be in the same sensitivity range as typical silver halide media and would indicate that advanced materials such as PPR would be applicable, from a photometric point of view, for the starfield tracker.

In these evaluations with the image intensifier it was observed that although the deformations on the photoplastic recording material were less sharp there was no noticeable increase in noise introduced by the intensifier. Further correlation experiments are needed to determine the effect of the non-sharpness of the images caused by the intensifier tubes.

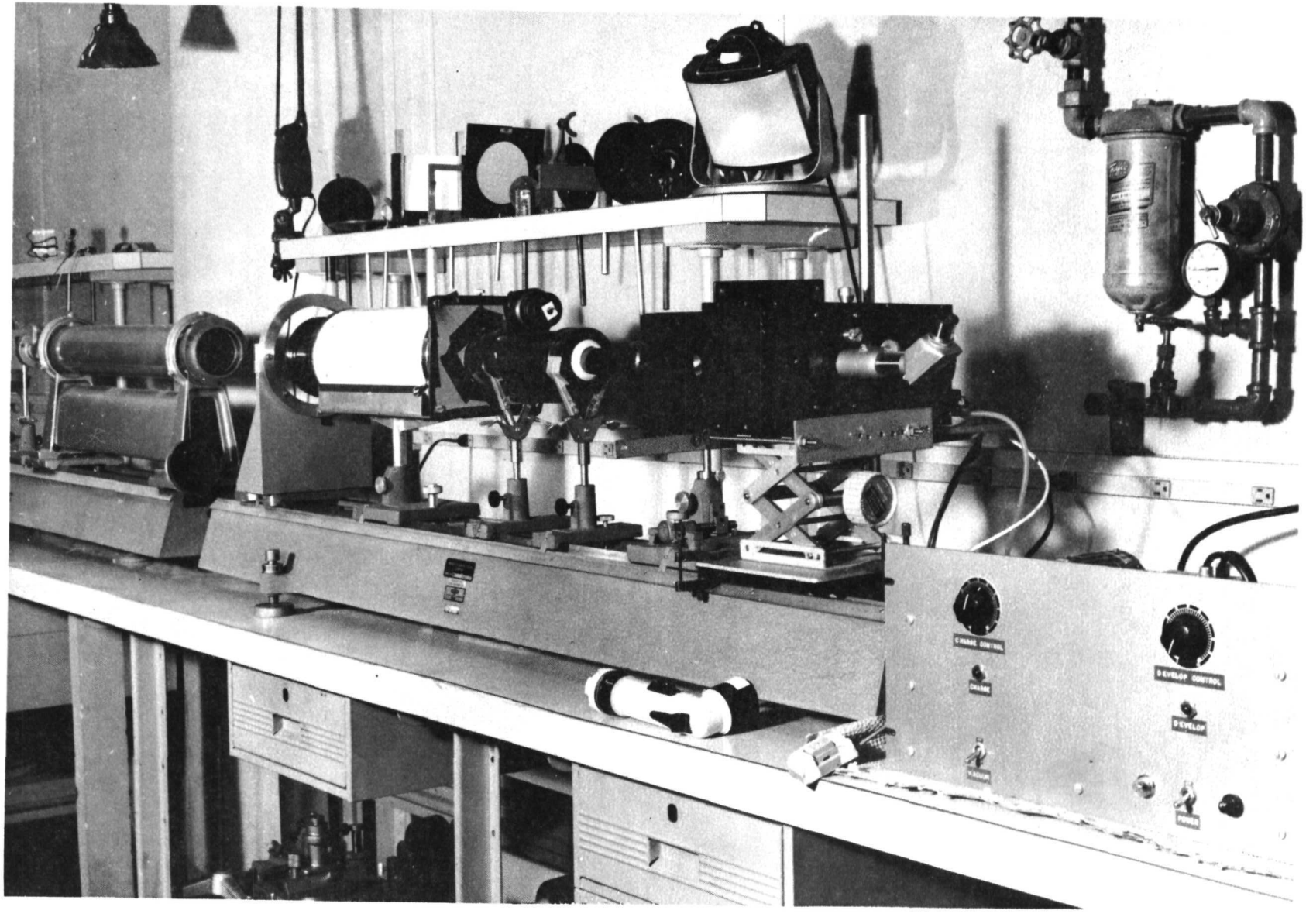

Figure 3-3. Laboratory Set-Up for Evaluation of Image Intensifier Operating with a Photoplastic Recording Camera and Simulated Star Field Images

3.4 Investigation of Electro-Optical Readout Techniques

3.4.1 Definition of the Problem.- The problem is to precisely determine the location of the correlation function (i.e., "correlation spot") in the "output" plane. The size and shape of the intensity of the correlation function as a function of image type and degradation of the image has been investigated by experiments. Furthermore an analysis of the idealized cross-correlation function has been made (Section 2.3). Based on the results of both the experiments and the analysis and on the scale factor for the planned system, the typical correlation function will have a diameter ranging from 10 to 50 micrometers as measured to the half power points.

For most experiments a HeNe laser has been used resulting in a spectral response of the correlation spot of 6328 Å. In selecting a readout technique however consideration should also be given to using light sources of other spectral responses including a GaAs laser having a wavelength of 9000 Å.

In most of the correlation experiments with degraded input images of landmarks the resulting degradation of the correlation function maintains considerable symmetry until such a point that the signal can no longer be detected in the field of noise. In general, if detection of correlation is still possible (e.g., with S/N ratios of 10:1 or more), then it has been found by numerous experiments that non-symmetries in the correlation function will contribute a position uncertainty which is typically less than 10^{-3} of the dimension of the output plane.

For the system scale factor selected, the 10 to 50 micron diameter correlation function will be located somewhere in an output plane having dimension of 25 cm x 25 cm. The problem of locating the correlation function in the output plane is very similar to that of locating a star image with an off-axis star tracker except for one important difference: the accuracy of the off-axis star tracker performance is usually limited by the dynamics of the vehicle and tracking system. In the case of the correlation tracker the detection of the correlation spot will have the dynamics of the optical-to-optical input device. In the case of a navigator using a non-self-erasing input device, such as PPR, the correlation spot then is stationary and its readout can be smoothed over long periods of time.

In the case of a self-erasing optical-to-optical interface device (e.g., NASA's optically excited liquid crystal device) the image storage time is much shorter and a somewhat lower accuracy readout might be expected for those cases where the vehicle attitude is experiencing rapid attitude changes.

3.4.2 Alternative Electro-Optical Readout Devices.- Several investigators have automated the operation of the readout of the correlation function. Image orthicons, vidicons and image dissectors have been used for this function. In some cases the sensor was used only for TV display of the output signal whereas in other cases a digital readout has been incorporated. No known end-to-end experimental effort has been made to detect the location of a correlation function to the accuracy desired for the present holographic tracker.

However off-axis star trackers have been developed, which in static tests have demonstrated high position determination accuracy throughout the field of the level desired for the present application. One such off-axis tracker was developed under NASA Contract No. NAS 2-1087 - "Optical Inertial Space Sextant for an Advanced Space Navigation System". This tracker was based on the use of a one-inch vidicon which incorporated a special reticle on the face of the tube for purpose of establishing linearity references for the tube. The tracker also incorporated interpolation and pulse center detection techniques of an advanced design to detect the center of the small star image. In tests, the optics imaged simulated static star images in the 20 to 50 micron diameter range on the face of the tube. These tests[1] demonstrated tracking accuracy in the x axis with uncertainties of 10^{-3} (1σ) of the field of view and in the y axis with uncertainties of $1.6(10^{-3})$ (1σ).

The purpose of the above discussion of this vidicon tracker is presented only to illustrate that tracking accuracies of "star-like" images have been demonstrated, for a static situation, in the range of 10^{-3} of the field.

Another approach to electro-optical readout is the application of an image dissector tube. Discussions were held with IT&T Corp. concerning the adaptation of a star tracker based on an IT&T Image Dissector Model F4011. Preliminary investigations indicate that this adaptation can result in position determination uncertainties that are less than 10^{-3} of the output plane. This would be an adaptation of a space qualified tracker currently produced by IT&T.

3.4.3 A More Advanced Approach - Parallel Electro-Optical Readout.- An alternative to the scanning devices discussed above is the use of parallel readout detector arrays. The most practical array application at this time appears to be that of linear arrays rather than rectangular arrays because of their greater availability.

In order to use a linear array it is necessary to either sweep the image plane past the array or to convert the correlation function to a linear function which will intersect the array. Mechanical sweeping is clearly unattractive for a space application.

If the correlation function could be transformed into a cruciform image (i.e., a cross which spans all or part of the output plane in two axes) then the readout of the correlation function could be accomplished by two linear arrays mounted orthogonal to each other.

There are at least two ways in which the correlation function can be transformed into such a cruciform image: by the application of a beam splitter and two orthogonally mounted cylindrical lenses (one for each split beam segment) or by use of a cruciform encoding spatial frequency filter. By an encoding filter here we refer to a spatial frequency filter which will be designed to directly produce the desired cruciform image instead of the more usual correlation function. Although this has not yet been done experimentally for starfields, it appears to be a practical approach. Such filters would be made by using a reference beam imaged in the form of the desired cruciform

---

(1) cf. Reference 16.

before interfering it with the candidate image. This represents an alternative to the usual approach of bringing the reference beam to a point focus before interfering it with the reference signal.

Although this parallel readout is conceptually attractive, some limitation will exist due to the reduction of signal to noise which will result in "spreading the energy over a line".

Some calculations can be made to estimate the extent to which this approach can be used. In laboratory experiments, simulated starfields have been recognized with signal-to-noise ratios typically as high as 200:1 to 500:1. Typically the parallel solid state readout will provide a usable output with a signal to noise ratio of 5:1. This means that each arm of the cruciform image could be designed to span a length equivalent to 20 to 50 resolution elements. Thus to obtain a 10^{-2} readout accuracy, some two to five array rows would be required in each axis. To obtain a 10^{-3} readout accuracy, some 20 to 50 array rows would be required. The number of arrays in each array row would depend on the number of resolution elements in each array.

Consider a specific case: A typical presently available linear array is one of the type PIN SA 50 produced by United Detector Technology Company. These arrays have 50 elements and are 0.4 inch long. If an output tracking accuracy of 10^{-3} of the field were desired in two axes then 20 arrays would be required for each array row.

Based on the previous discussion, assume that 20 array rows would be required in each axis. This is equivalent to a total of 800 arrays or 40 000 elements. Note that this is 1/25 the number of resolution elements which would be required had the cruciform approach not been used and a parallel readout were performed with a n x n square matrix array.

In a more modest approach, if a tracking accuracy of 10^{-2} of the field were required, then only 8 arrays or 400 elements would be required. This more modest goal would seem to be attractive for an initial evaluation of this advanced parallel readout approach.

3.5 Investigation of Other Key Components

3.5.1 Telescope Design.- In every component of the input imaging system it is essential that the distortion be low relative to the resolution. In the recording of starfield images it is important that the distortion in any usable part of the field be small relative to the dimensions of the point spread function resulting from the imaging of a star by the telescope. This necessity for a low distortion telescope becomes one of the primary specifications of the telescope design.

The selection of the upper limit of the optical field of view will be determined largely by the desired system accuracy. To a large extent, system accuracy will be determined by the performance of the electro-optical readout system. As pointed out in Section 3.4 typical readout accuracy may be in the range of a $2(10^{-3})$ (for an initial feasibility model) to a $0.5(10^{-3})$ (for an operational model) fraction of the field of view. As discussed in Section 2.1

accuracy goals ranging from 15 to 200 arc seconds may be expected depending on the type of spacecraft, the application (i.e., attitude reference or autonomous navigation) and whether the initial feasibility or the operational model is being considered. Based on these considerations a maximum field of view will be expected to range from about 4^{o} to 10^{o}.

A further analysis considering false alarm probabilities, stellar populations as a function of magnitude and the required number of stars in a given candidate field have led to the selection of a telescope field of view of 8^{o}.

The primary requirements then for the telescope are a field of view in the order of 8^{o}, a relatively fast system to compensate for the limited sensitivity of the imaging media and a level of distortion which is low compared to the resolution of the system. An analysis of the combination of these requirements leads to the selection of a Schmidt-Cassegrain telescope design as the most favored design. No other telescope design is known to provide the desired combination of low distortion, small angular field of view and high speed. This conclusion is supported by the work of many other investigators (cf., for example references 17 and 18). Linfoot, in reference 17 (p. 262) enters into some detail the optical correction factors needed to provide a distortion-free Schmidt design.

It remains to decide what clear aperture should be selected. It has been established in Section 2.1 that about a 5^{th} magnitude star is desired to be detected. A 20 cm clear aperture telescope will collect approximately 10^{-11} watts of power from a 5^{th} magnitude star. A high quality 20 cm clear aperture relatively fast telescope (i.e., in the range of f/1.6 to f/2) can be expected to have an optical spread function of about 10 microns (see reference 7). Considering the optical efficiency of the telescope elements this would lead to an optical power density on the input of an image intensifier of about 10^{-6} watts/cm^2. Based on a conservatively estimated effective intensifier gain of 10^2 to 10^3 this would result in a power density ranging from 10^{-4} to 10^{-2} watts/cm^2 on the input imaging medium. In consideration of the image motion problem and the associated maximum permissible exposure as well as the level of media sensitivities expected this is the level of optical energy density desired.

Hence we establish a telescope design as a Schmidt-Cassegrain having a clear aperture of 20 cm, a focal length of about 32 cm and a field of view over a 40 mm format of 8^{o} designed for minimum distortion.

This design of a telescope comes rather close to the design of several available commercial designs from various telescope manufacturers. It is expected that such a telescope would be suitable for an initial design. An operational model would however require greater refinement particularly with respect to dimensional stability over an operational temperature range and optical quality.

3.5.2 Image Rotation Sensitivity and Compensation.- It is well known that the matched spatial frequency filter operation will generally be sensitive to rotation about the optical axis. For many autonomous navigation or attitude reference applications the holographic tracker will be used in a

"vernier mode". In many of these cases initial rotation errors will be acceptably low so that no further rotation compensation will be required. In-house experiments have demonstrated landmark tracking correlation with acceptable signal to noise ratio performance with initial rotation errors, in some cases, as great as 20^{o}. For other applications rotation sensitivity may be a problem needing a solution.

Several approaches and combinations of approaches can be made to the problem of image rotation sensitivity of the correlation function. Among these approaches are:

- Design a spatial frequency filter to be relatively insensitive to rotation angle. This can be done in several ways such as using relatively small angular field landmark and starfield images. In the case of starfields this necessitates depending on fainter magnitude stars than would otherwise be required. Another approach is to use relatively large star images (e.g., defocused star images) when making the filter and/or when forming the candidate starfield input image.

- Take advantage of the rotation sensitivity as a rotation reference for controlling the vehicle attitude. An example here would be to make use of a known landmark viewed near the vehicle nadir to provide a yaw angle reference. In this approach a relatively large landmark is desired for which rotation angular sensitivities have been shown to be typically 0.1^{o} or less.

- Make use of vehicle rotation (this applies particularly to a spin stabilized spacecraft) to, in effect, provide a rotation search. In this way, by measuring both the time of correlation, as well as the usual two axes location of the correlation function, the three axes attitude of the spacecraft can be determined (i.e., one of which is varying as a function of time). This appears to be a very applicable approach for a spin stabilized spacecraft. It is only necessary that the time constants of the optical-to-optical interface device and of the electro-optical readout be fast relative to the vehicle spin rate.

- Make use of a large number of spatial filters for each landmark and starfield image to be stored, each one of which is made for a different rotation angle. In this way rotation search can be combined with pattern search by using multiple filters. This approach can make use of multiplexed and/or mechanically registered multiple filters as may be indicated by the application.

- Provide a means, in the vehicle, for rotating the candidate input image relative to the spatial frequency matched filter. In principle, this can be done by rotating either the input imaging device or the matched filter or an optical element located between these two. The first two are clearly unattractive whereas the third approach may be acceptable for some applications.

If such an image rotation is required on board the vehicle, one of the most attractive approaches is to make use of a motor driven derotation prism. Several types are available including the Dove, Pechan or K prisms. Although the Dove prism is the most common*, the Pechan or K prisms are preferred because of their greater off-axis capability and shorter lengths. The prism would be mounted in high precision bearing and would be aligned with high precision. Derotation prisms mounted in such high precision bearing are used in certain types of military periscopes.

A continuous driven prism rather than nulling servo drive is recommended. Rotation rates would be selected which are compatible with the time constants of the input imaging device and the electro-optical readout. Criteria are similar to that for the spin stabilized spacecraft. An angular pick-off is required to provide prism rotation attitude as a function of time.

These prisms can be obtained as both reflective and refractive types. The refractive devices are generally solid glass prisms whereas the reflective devices are generally hollow and are made with an assembly of optical flats assembled in such a way as to perform the desired prism function.

The reflective prisms are generally lighter and less expensive than the refractive prisms and have performance which is generally independent of wavelength.

With respect to stability and accuracy of performance some conflicting claims are made by various designers and manufacturers of prisms.

Based on a review and interpretation of available data supplied by several manufacturers as well as a survey of the technical literature, a conservative recommendation would favor a refractive Pechan prism. There are indications that these are operable over angular field of view ranges of 10^{o} or more with lateral and angular deviations which would be equivalent to $2(10^{-5})$ radians or less. This is an error which would not be observable within the expected resolution limits of the input image system.

The reflective prisms look very attractive but lack of extensive performance data suggests that further evaluation of their performance would be recommended.

3.5.3 Coherent Illumination Source.- Because of the small size of the star image as well as the relatively few stars in a typical starfield it will be the starfield correlation operation rather than the landmark correlation operation which will dictate the minimum allowable output power level of the laser. Typically 5 stars will exist in the starfield. Each star will typically have an aperture dimension which is 1/500 of the width of the input image media. If we assume that all of the output laser illumination is spread uniformly over the input imaging media, then the amount of light which transits the input media through the 5 star image is $5\left(\frac{\pi}{4}\right)\left(\frac{1}{500}\right)^2$ or about $2(10^{-5})$ of the laser power available.

---

*See Reference (19) which describes the characteristics of these prisms in some detail.

A conservative approximation based on experiments with such starfields can be made that, operating with a typical spatial frequency matched filter, 0.005 to 0.05 of the light which transits the star aperture will appear in the correlation function. Thus the overall "efficiency" of the input imaging medium when operating with starfield images is judged to range from 10^{-7} to 10^{-6}.

Let us compute laser energy required to operate with the solid state detector arrays as described in Section 3.4. In the arrangement as described there with the cruciform correlation function, the laser energy will typically be equally spread over about 50 elemental areas of the array. Each element of the PIN SA 50 array has an area of $3(10^{-8})$ meters^2. The total illuminated area will then be $1.50(10^{-6})$ m^2. The typical noise equivalent signal for a solid state detector of this type is 10^{-6} watt-sec/m^2. Hence the noise equivalent signal over the illuminated area would be $1.50(10^{-12})$ watt-sec. A conservative requirement would be to achieve a minimum readout signal to noise ratio of 10. Hence minimum required signal energy at the output plane is $1.5(10^{-11})$ watt-sec. We make the realistic assumption, for this type of detector, that it is operating in a power integrating mode. Hence exposure time can be traded off for laser power over rather wide limits.

Based on the previously discussed input medium efficiency of 10^{-7} to 10^{-6} we conclude that the laser energy required for each correlation operation would range from $1.5(10^{-5})$ to $1.5(10^{-4})$ watt seconds. In order to arrive at a conservative design requirement we will assume a typical energy requirement of 10^{-4} watt sec.

From the standpoint of a navigation system operating with a long relaxation time constant input medium, the power of the laser can be very low (e.g., some fraction of a milliwatt) because relatively long integrating time periods can be employed. For an attitude determination application utilizing a fast relaxation time constant input imaging medium a higher power laser would be required. For example if the imaging medium had a relaxation time constant of 1/30 sec, then, for an energy requirement of 10^{-4} watt sec, a laser having a power in the range of 3 milliwatts would be required.

For conditions of poorer spectral mismatch and/or higher attitude dynamics an even higher power laser may be required.

We conclude that for the type of electro-optical readout described a laser power of 0.1 mwatt or less would be adequate for a navigation system whereas a laser power of as much as 10 mwatts could be required for an attitude determination system.

A conservative recommendation is made to incorporate a space qualifiable HeNe laser having a power rating in the 1 to 5 mwatt range. For an initial feasibility model, a laser such as the 1 mwatt Hughes Model 3078H is appropriate.

The 5 mw space qualifiable laser developed under contract to NASA (reference 28 and 29) is a candidate for an operational model of the system. This contract had led to the proposed development of a space qualified laser of 5 mwatts with a total weight of 8 lbs and an input power requirement of 15 watts. The laser head is a 16 inch long cylinder having a 2.5 inch diameter.

A further alternative exists in the form of a Gallium Arsenide laser diode (cf. reference 20). The application of this very small low power device to optical data processing has been described by Dr. A. Hussain-Abidi in reference 10. The output of this device operating at room temperature is at a wavelength of 9000 Å. Some inconvenience may be expected in initial alignment of the system with non-visible radiation. Furthermore some further investigation may be required to determine the optimum electro-optical readout with this device.

At the present time all known GaAs lasers which provide coherent radiation do so in a pulsed mode (typically 100 μsec pulses at 50 pulse/sec rep rate). Some CW GaAs lasers have been operated experimentally at cryogenic temperatures. However the cryogenic complications are clearly unattractive for the present application. If and when GaAs lasers having high coherent CW outputs at room temperatures become available, they will be prime candidates for a source of illumination for the present application.

Based on the initial experiment of Dr. Hussain-Abidi of NASA (Goddard) there is reason for encouragement in the use of this device eventually as a practical low power compact source of laser illumination.

3.5.4 Alternative Read-In and Read-Out Modes of Input Imaging Medium.- The input imaging medium must operate in two modes: read-in and read-out. It is essential that either of these two functions not interfere with the other. In this discussion we will presume the necessity for using an image intensifier to compensate for the relatively low optical energy in relation to the sensitivity of the input imaging medium.

If the imaging medium cannot be placed directly against the output face of the intensifier, then a relay (or transfer) lens will be required. If we eliminate all designs which would involve moving the input medium relative to the intensifier then, for transmissive media, a relay lens is required. For those input media which can be operated in a reflective mode (e.g., certain types of photodeformables) then the medium can be mounted directly on the intensifier output face and a relay lens will not be required.

Several general ways for accomplishing the read-in and read-out function are possible including those discussed in Table 3-2.

Figures 3-4 and 3-5 respectively show sketches of two different ways for accommodating the read-in and read-out function in a single interface device. Note the likely requirement for all cases, except the reflective readout case shown in Figure 3-5, of a relay lens when operating with an image intensifier. The requirement for relay lens is not an insignificant disadvantage, particularly from the point of view of optical energy loss.

An evaluation of relay lens operating with an intensifier has been made which indicate these typical idealized transfer efficiencies:

TABLE 3-2

A COMPARISON OF THREE ALTERNATIVE MODES OF OPERATION OF OPTICAL-TO-OPTICAL INTERFACE DEVICES

TYPICAL GENERIC TYPE OF SEPARATING READ-IN - READ-OUT FUNCTIONS OF OPTICAL-TO-OPTICAL INTERFACE DEVICE	TYPICAL CHARACTERISTICS	TYPICAL SUCH DEVICES WHICH MAY OPERATE THIS WAY
(a) A Spectrally Separated System Simultaneous non-coherent read-in and coherent read-out by optical spectral bands sufficiently separated as to interfere with each others function.	Read-in and read-out tends to be simultaneous with the maximum permissible scene dynamics determined by device relaxation time constant.	Optically Excited Liquid Crystal Device Optically sensitive photo-deformable oil film.
(b) A Time Increment Separated System Operate in a very rapid sequence two step mode: A read-in mode followed by a read-out mode. This would likely involve rapid alternate electronic shuttering of an intensifier and the laser.	This approach tends to be somewhat more cyclic. It lends itself well for use with an optical-to-optical interface device which are not automatically self-erasing and for applications where variations in read-out (i.e., processing) times may be desired.	Many devices including most transmission types of photo-deformables.

TABLE 3-2 - Concluded

A COMPARISON OF THREE ALTERNATIVE MODES OF OPERATION OF OPTICAL-TO-OPTICAL INTERFACE DEVICES

TYPICAL GENERIC TYPE OF SEPARATING READ-IN - READ-OUT FUNCTIONS OF OPTICAL-TO-OPTICAL INTERFACE DEVICE	TYPICAL CHARACTERISTICS	TYPICAL SUCH DEVICES WHICH MAY OPERATE THIS WAY
(c) A system separated by read-in and read-out on opposite sides of a non-transparent optical-to-optical interface device.	Requires reflective read-out. Permits simultaneous non-coherent read-in and read-out. Does not require a transfer lens (between intensifier and optical-to-optical interface device). Reflective optical-to-optical interface sometimes have critical "flatness" problems.	Reflectively coated photo-deformables.

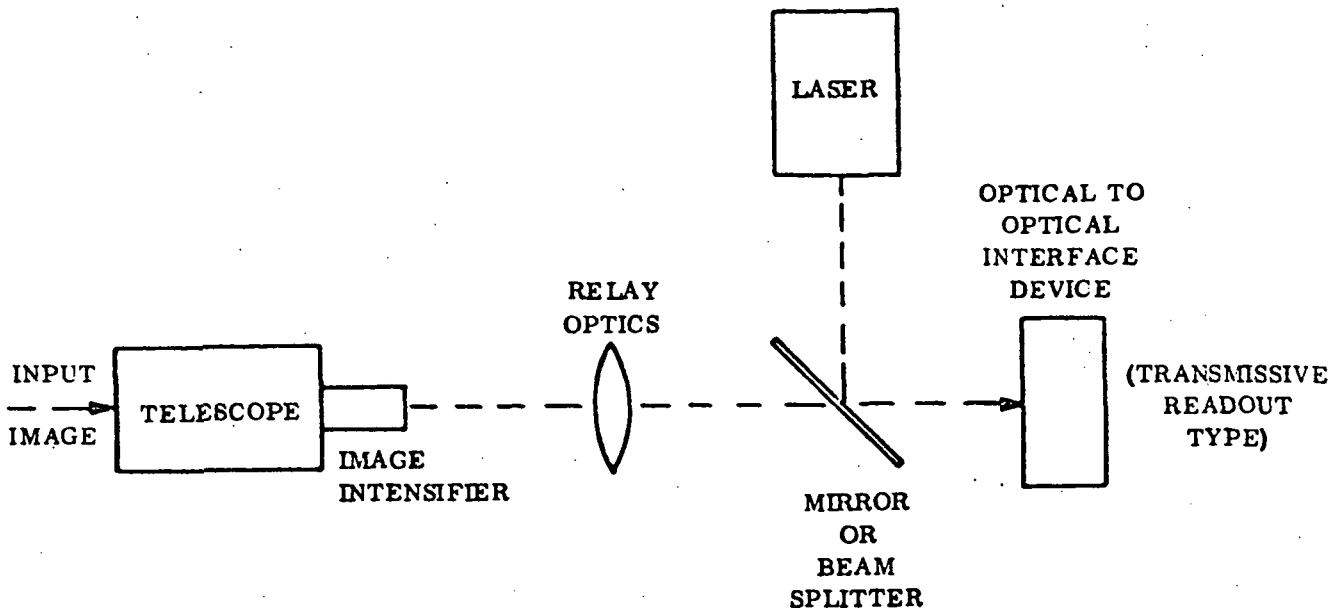

FIGURE 3-4 - NONCOHERENT READ-IN AND COHERENT READ-OUT ACCOMPLISHED ON SAME SIDE OF OPTICAL-TO-OPTICAL INTERFACE DEVICE (SPECTRAL SHARED TYPE A OR TIME SHARED TYPE B)

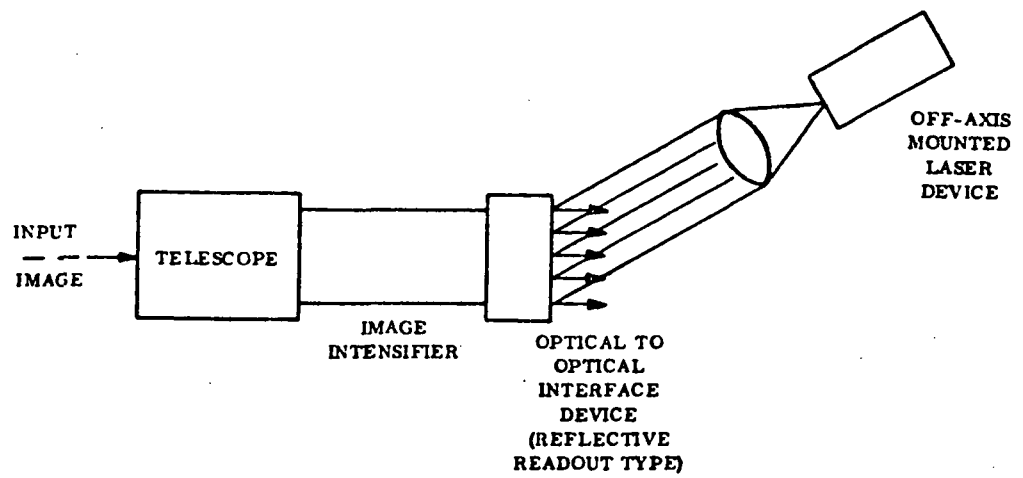

FIGURE 3-5 - NONCOHERENT READ-IN AND COHERENT READ-OUT ACCOMPLISHED ON OPPOSITE SIDES OF OPTICAL-TO-OPTICAL INTERFACE (TYPE C)

f/#	Transfer Efficiency
0.7	29%
1.0	13%
1.3	7%
1.6	5%

These numbers assume that each point on the intensifier phosphor radiates with equal intensity over a hemisphere and that the transmissivity of the lens is 100%.

Since a relay lens much faster than about f/1.3 does not appear attractive from an aberration point of view, a practical relay lens will have a maximum efficiency in the neighborhood of 5 to 7%.

The above advantage of the reflective medium approach has to be weighed against a very practical problem of mounting the reflective media. It has been shown in several in-house experiments that "flatness" of the image medium is far more critical for reflective media than for transmissive media. In some experiments it was found that it was very difficult to hold the reflective medium sufficiently flat even though several techniques were tried (e.g., various versions of vacuum plate holders). In most cases bowing of the deformable film was excessive. Several other holding techniques were suggested which have not yet been evaluated.

A further possible problem of the reflective readout approach is possible adverse electric field interaction between the intensifier and the photodeformable such as photoplastic. It is expected that this problem may be minimized, however, by operating the intensifier with its output plane at ground potential. This has not yet been proven however.

Because of the advantages of avoiding a relay lens, further experimental investigations of a reflective photodeformable are recommended. In the absence of any favorable results of such an evaluation a relay lens, however, operating with a transmissive medium is recommended.

3.5.5 Storage and Retrieval of Matched Spatial Frequency Filters.- For both the autonomous navigation problem and the attitude reference problem there exists a problem of storage and retrieval of matched spatial frequency filters. The number of required spatial frequency filters will be application-oriented. However for a number of typical missions, the number of matched spatial frequency filters required will typically be:

. For Autonomous Navigation

20 to 200 landmark filters
10 to 50 starfield filters

. For Attitude Reference

10 to 100 starfield filters

For most applications* it is expected that these filters will be made in an Earth-based laboratory environment and will be recorded on a high resolution, high stability recording medium. A typical medium would be Kodak 649F spectroscopic film.

At least three techniques are potentially available for storage, selection and retrieval of match spatial filters on board the spacecraft:

- Use of mechanical motion techniques to store and retrieve spatial frequency filters each one of which is stored on a separate frame.
- Use of some type of "multiplexing" for multiple storage of spatial frequency filters on a single frame.
- Use of advanced optically addressable 2D or 3D holographic storage medium.

Each one of these will be discussed below. It is worthwhile to note that the system which combines two of these techniques is also possible. For example, multi-complexed spatial frequency filters each of which is stored in a mechanical retrieval system would provide an exceedingly large number of spatial frequency filters.

Mechanical Storage and Retrieval of Spatial Filters.- In this approach each matched filter is stored on a separate frame in the form of a slide or a frame of a film loop. Filter selection and/or search is performed by selectively moving the desired frame into precision registration in the spatial frequency filter plane.

From the viewpoint of making the spatial filters this is very attractive since there need be no concern with operational cross-coupling of multiplexed filters. Furthermore it represents a technique which has been proven in the laboratory**.

However there are also several disadvantages, the principle of which is the concern for long life reliability in a space mission. A further ultimate concern may relate to speed of response of the selection and retrieval mechanism.

In general two approaches to mechanical storage and retrieval can be considered. These two approaches are compared in Table 3-3.

---

*With the exception of the so-called "Unknown" landmark tracking mode of autonomous navigation.

**Reference 9, for example, cites the successful use of a pin registration movie camera mechanism to perform this function.

TABLE 3-3

A COMPARISON OF TWO MECHANICAL SPATIAL FREQUENCY FILTER STORAGE AND RETRIEVAL TECHNIQUES

TECHNIQUES	EXPECTED REGISTRATION UNCERTAINTY	TYPICAL RETRIEVAL SPEEDS	COMMENTS
Pin Registered Film Loop	$5(10^{-4})$ cm	1 - 5 secs	Registration uncertainties may increase slightly after many hundreds of uses due to wear of film.
Individual Slides	10^{-3} cm	1 - 10 secs	Registration is poorer than in case of film loop typically by a factor of 5 to 10. However no degradation with wear is expected.

Spatial Filter Multiplexing Techniques.- The concept of multiplexing spatial frequency filters is very attractive primarily because it provides a means of either completely avoiding or, at least, minimizing the need for using moving parts for storage, selection and retrieval of spatial frequency filters.

In principle, the ability to multiplex spatial frequency filters is limited only by the space bandwidth product of the storage medium and the ingenuity for encoding the multiplexed filters.

Starfields are ideal candidates for spatial frequency multiplexing. This is because unneeded redundant data in the image can be readily eliminated. This can be done by eliminating unnecessary stars in a scene when making a spatial filter by suitable amplitude thresholding. The number of stars required for making a spatial filter is that which will insure acceptably low false alarms and also an acceptable signal level in the event that part of the starfield is truncated by the field of view of the telescope.

Although many multiplexing schemes could be considered, the approach of Gorstein and Hallock (reference 8) is thought to be most appropriate. These investigators have used a dual reference beam concept in making the spatial filters. One reference beam remains fixed in the filter making device whereas the other beam is allowed to have a new relative "shear angle" when exposing each starfield. As a consequence of this type of filter multiplexing, the correlation operation, upon realizing a recognition will yield two "correlation points" in the output plane. One correlation point will appear in the output plane having an X-Y location which indicates, in the usual sense, the vector direction to the starfield relative to the telescope optics. The second correlation point will indicate the specific starfield out of the ensemble of multiplexed starfields which is being recognized. The readout of its location will be read out and the position will indicate the starfield recognized.

The above described technique can be regarded as a type of encoding filter in which the reference beam (here actually a 2 lobe reference beam) is reproduced upon a successful correlation experiment. A somewhat different approach to making multiplexed filters is described in reference 13. This approach involves making the filter with a single exposure and using a separate reference beam for each starfield so transformed. Upon recognition, the location of the single "correlation spot" provides both starfield identification and vector direction information.

Spatial Frequency Matched Filter Registration Accuracy Requirements.- The accuracy with which the spatial frequency matched filter must be registered and its relationship to system performance is a strong function of the nature of the signal to be detected and the noise existing in the system. More specifically it depends heavily on the space bandwidth product of the signal.

Before considering specific examples, some insight may be gained by recalling what happens to an image when it is transformed to the spatial frequency domain. Consider a binary circular image of some finite radius (i.e., an aperture function). When this image is transformed to the Fourier domain the function has the familiar $J_1(x)/x$ Airy function response. The smaller the "aperture" in the spatial domain, then the larger is the "diameter" of the Airy function and vice versa. The single dimensional Gaussian function

demonstrates this "inverse" relationship even more clearly. The Fourier transform of a Gaussian function is known also to be a Gaussian function. The standard deviation of these two functions will be inversely related.

Consider also the extreme case of a "delta" function and a two-dimensional uniform distribution function. These are known to be related to each other by a Fourier transformation.

From the above discussion we arrive at an intuitive concept of an inverse relationship in the dimension of information existing in two domains which are related by Fourier transformations. Hence we can expect that an input image which has information over a wide extent will have a relatively critical sensitivity to registration of a matched filter in the Fourier transform domain.

In considering registration sensitivity, the matter of system scale factor must also be taken into account where we here define scale factor as the units of displacement in the spatial frequency domain per units of spatial frequency in the spatial domain*. The scale factor is:

$$\frac{\lambda F}{2\pi} \quad \frac{\text{units displacement}}{\text{spatial resolution/unit displacement}}$$

where λ is the wavelength of the coherent illumination and F is the focal length of the transform lens.

Consider next some specific quantitative examples.

a) Making Matched Spatial Frequency Filters of Starfield Images.- In the extreme case (not necessarily of practical significance) the simplest starfield will consist of a single star. If we assume the star is adequately described by a binary disk aperture then the Fourier transform of its intensity will be described by $J_1(x)/x$. This is shown, in a center cross section view, by the envelope of Figure 3-6. This figure shows the relative intensity of the signal not only as a function of spatial frequency as existing in the spatial domain but also as a function of lateral displacement in the spatial frequency domain. (Recall that it is this displacement in the spatial frequency domain with which we are primarily concerned when we address the problem of registration of spatial frequency images.)

   In a spatial frequency matched filter experiment with a single star image the $J_1(x)/x$ function of the coherent aerial image should be superimposed precisely on that of the stored reference filter. The tolerable lateral departure of the spatial frequency filter would be a function of the diameter of the star in the spatial domain. Clearly for a very small star image (i.e., in the limit approaching a delta function) there is no registration problem at all.

---

*Note that, for the present discussion, we do not have to be much concerned which is the spatial domain and which is the spatial frequency domain. It suffices to say that two domains exist which are related by a Fourier transformation.

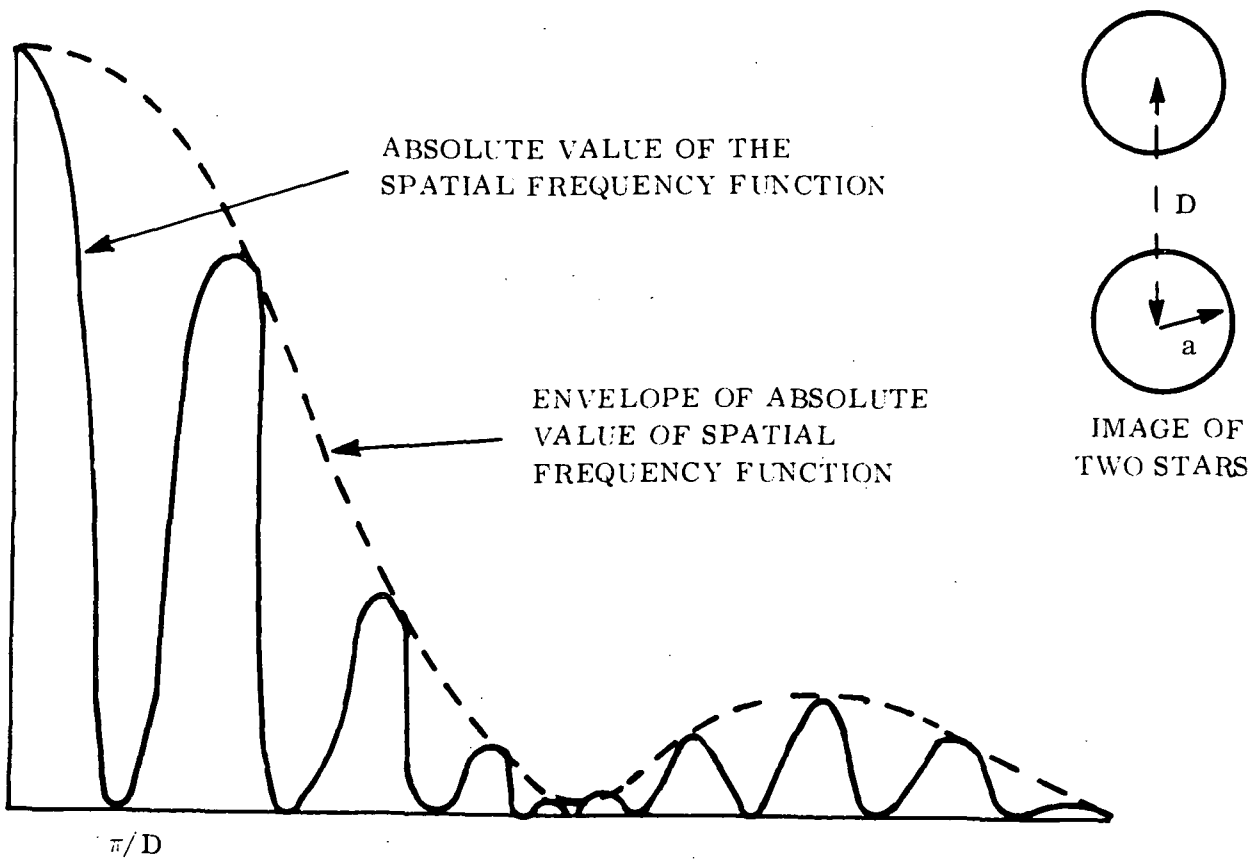

Figure 3-6. Frequency Plane Representation of Two Star Field (Along Direction Between Stars)

Consider next the more practical problem of two stars in the starfield. Figure 3-6 shows that the Fourier transform is a relatively high spatial frequency interference fringe pattern, the amplitude of which is contained within the $J_1(x)/x$ envelope. The "size" of each star determines the "size" of the envelope (in the inverse way as discussed above). The relative displacement of the two stars determine the higher spatial frequency interference fringe pattern. A criterion for practical registration for this starfield comes clearly in view. The registration error should be small relative to the displacement (in the Fourier domain) of these interference fringes*.

Note, for example, that the first interference fringe occurs at a spatial radian frequency of π/D where D is the displacement of the stars in the spatial domain. Applying the coherent scale factor discussed above this corresponds to a displacement in the Fourier domain of:

$$\frac{\lambda F}{2\ D}$$

Evidently the misregistration of the filter should not exceed some fraction of the fringe distances. Typically it should not exceed it by a factor in the range of 0.2 in order to avoid excessive degradation. Specifically a misregistration by a factor of 0.2 will result in a decrease in correlation energy of 20%.

Based on this assumption and an assumption of $\lambda \approx 0.6$ micrometers we conclude that misregistration should not exceed:

$$6(10^{-2})\ \frac{F}{D}\ \text{micrometers}$$

As we will see in Section 4 a convenient value of F will typically be about 50 cm. The maximum value of D will depend upon the image format size (which we will assume to be 4.0 cm) and some expected fraction of the format size over which a given starfield might extend (which we will assume to be 0.25). Based on these assumptions we conclude that the misregistration of the spatial filter shall not exceed $\approx$ 5 micrometers. As was discussed in Section 2.3 this is the anticipated registration capability of mechanical approaches which are typically available. Furthermore this matched spatial frequency registration sensitivity is typical of that which have been measured experimentally.

---

*These interference fringes formed by multiple star images must not be confused with the much higher carrier spatial frequency existing in the spatial frequency filter as a means of storing both phase and amplitude in the spatial frequency filter.

An analysis of starfields containing more than two stars can proceed in a similar fashion. It is evident that by having a larger number of stars in the starfield and consequently relatively larger displacements between them that the registration sensitivity will be further reduced. Furthermore if it were necessary to do so, filter registration sensitivity could be further reduced by selecting even larger values of the parametric ratio F/D. As discussed in Section 4, F could be realistically increased to values as high as 100 cm and the maximum value of D could be even further reduced.

From the above analysis we conclude that for realistic starfield recognition, spatial filter misregistration ranging from 2.5 to 10 or even more micrometers can be tolerated.

We will consider next the matter of spatial filter registration for landmarks.

b) Landmark Images.- The analysis of filter registration relative to landmarks will be based on the approach of VanderLught (reference 21). In that approach the author predicts the effect of performance response as a function of sensitivity of spatial filter registration. In doing this the author assumes somewhat of a worst case situation where a relatively "long" input signal in the input plane is assumed. Specifically an input signal of the type $|S(u)|^2 = 1 \quad 0 \leq u \leq L$ is assumed. He then proceeds to predict performance based on the parametric ratio $\left(\frac{F}{L}\right)$ where F is the Fourier transform lens focal length. The similarity of this ratio to the ratio $\left(\frac{F}{D}\right)$ as discussed above for starfields is evident.

Based on an assumption of uniform noise the author's analysis predicts a tolerable misregistration ranging from about 5 micrometers for a very low value of $\left(\frac{F}{L}\right)$ and a misregistration of 20 to 50 micrometers for a value of $\left(\frac{F}{L}\right)$ of 200. The ratio $\left(\frac{F}{L}\right)$ can be thought of as being indicative of the relative spatial frequency content of a landmark image. For a "typical" good landmark there will be considerable high frequency detail. Each detail can be considered as having an $\left(\frac{F}{L}\right)$ parametric ratio associated with it. For example a river may be in the image plane typically having a width (its "L") of 0.1 or 0.2 cm. If the system has a Fourier lens of 50 to 100 cm this would correspond to a parametric ratio $\left(\frac{F}{L}\right)$ in the range of 250 to 1000. For this image a spatial filter misregistration of 50 to 100 micrometers could be tolerated.

The author points out that for certain types of non-uniform noise the spatial filter registration could be somewhat more critical than for the case of uniform noise. (It should also be pointed out, however, that based on still other noise model assumptions that spatial filter registration may be even less critical than that for uniform noise).

Because of the randomness involved it becomes difficult to find a model for predicting the performance of landmark correlation and sensitivity to registration of spatial filters. However it is evident from the cited analysis that landmarks having significant high frequency detail will have relatively less critical spatial frequency registration requirements. Landmarks having only low frequency data (e.g., relatively low relief landscapes) will have more critical filter registration problems and, furthermore will also be less favorably considered because of the relatively poor correlation function which can be anticipated.

In summary landmarks having high frequency detail should be selected for best performance.

Experimental results at General Electric have indicated that, for a wide range of input image, misregistration of spatial filters of 10 to 20 or more micrometers could typically be tolerated.

This appears to be consistent with results of other investigators. Reference 9, for example, reports on the use of movie camera pin registration techniques for selecting and registering spatial filters. Furthermore this was performed successfully in a search operation at conventional motion picture rates. The device used is known to have registration uncertainty in the range of 5 to 10 micrometers. This seems to be consistent with the analysis and the known experimental results.

4.0 OVERALL CONCEPTUAL BASELINE DESIGN OF THE "HOLOGRAPHIC TRACKER"

4.1 General.- Based on the overall analysis and experimental effort discussed in the foregoing sections some conclusions can be summarized in such a manner as to provide the basis for a baseline conceptual design. Note that the conceptual design is intended to prove the feasibility of the automated system. A design of an operational system may have somewhat different characteristics depending on the purpose of the application.

The baseline design will be a compact configuration achieved through the manner of optical folding which appears most appropriate. This will provide not only a relatively small size but will insure the desired high structural rigidity.

The key components of the conceptual design, based on the foregoing investigation will be:

- A 1 mwatt HeNe laser.
- A 20 cm Schmidt-Cassegrain telescope having an 8^{o} field of view when operating with a 40 mm image format.
- A 40 mm wafer type of image intensifier.
- An 80/20 beamsplitter to illuminate the input imagery medium.
- An input imaging module containing a near real-time optical-to-optical interface.(Section 4.2).
- Functional and folding optical elements of the image processor (Section 4.3).
- An electro-optical readout (Section 4.4).
- An input image rotating prism (an optional feature).

A conceptual layout of an overall system is provided in Section 4.5.

4.2 Input Imaging Medium.- Because there exists more than one candidate for the input imaging medium a recommendation is made to incorporate in the conceptual design the capability for operating with alternative image storage devices on an interchangeable module basis. This is attractive in view of the recent advances in non-conventional imaging media and also because of differing needs for different applications.

A prime candidate would be some version of an optically excited liquid crystal device. This is a self-erasing device capable of non-interfering simultaneous read-in and read-out. Relaxation time is not variable and is believed to be about 10^{-1} sec at the present time. Continued successful evaluation of this type of device would further encourage the use of this device.

Another promising candidate is GE's photoplastic recording material (PPR). Since this is a device which requires a separate erasing function it would be attractive where a long or variable correlation time were desired. A preliminary investigation indicates that the presently moving charging and heating head can be replaced with a grid of fixed charging and heating wires, thus avoiding the requirement for this moving element.

It is recommended that the system be designed so as to accept these input imaging devices as well as other newer devices presently under development.

4.3 Comparison of Reflective vs Refractive Optics in the Design of the Coherent System.- Until recently most coherent optical data processing has been performed on an optical bench using transform lenses as the primary Fourier transform optical elements. When designing a compact flight qualifiable device optical folding of the system with reflective elements becomes very attractive.

A recent report (reference 10) has described the application of paraboloidal mirror segments to obtain the Fourier transform function and at the same time provide folding of the system. The author of the reference has presented an analysis predicting that a lower degree of aberration would be expected from the use of these functional mirrors as compared to spherical lenses. The author of the referenced report has also demonstrated good performance of such a system in the laboratory.

Since there is no known experimental evaluation of a functional mirror system versus a functional lens sytem evaluated under the same conditions it is difficult to make a performance comparison. It would seem that it may be just as difficult to make perfect mirrors as to make perfect lenses. Lenses can, for example, also incorporate aspheric surfaces such that aberrations can be made less than anything which is measurable.

Although the functional mirror system looks attractive, there may be greater problem of light scattering from the mirror surface than from the lens surface. Previous measurements indicate the effect of light scattering from a mirror surface may be as much as 10 times that of a lens. In general scattered light close to the optical axis of a coherent system can result in reduction in correlation performance in terms of S/N by a factor as great as 10. Such scattering might come from dust or imperfections in the surface. This is an area that needs more investigation. The question to be asked is: Under ideal dust free clean conditions, and in view of the usually greater light scattering sensitivity of reflective surfaces, how does the S/N performance of a functional lens system compare to that of a functional mirror system when evaluated under the same conditions? The answer to this question is critical in view of the desire to maintain acceptable S/N performance under degraded viewing conditions. A further question yet to be answered relates to the relative costs of functional lenses and functional mirrors having equivalent performance.

The most attractive feature of the paraboloid mirror segment approach is its self-folding characteristic. Because of this and because of the thus far

encouraging experimental results of the author of the referenced report, the paraboloid mirror segment approach will be tentatively recommended for the base line system of the conceptual model.

4.4 Overall Scale Factor Considerations.- The scale factor of the system will be determined by the performance goals and the available sizes of key components.

For the initial feasibility model tracking accuracy goals of 1 min. of arc (3σ) have been established (see Section 2.1). Furthermore an 8^{o} field of view for the telescope has been established (Section 3.5). Thus the ratio of tracking accuracy to field of view of about $2(10^{-3})$ is established. A conservative approach for a conceptual design would lead to the selection of an input imaging system which has a total resolution in the neighborhood of $\left[2(10^{-3})\right]^{-1}$ line pairs in two axes. This is conservative since, as pointed out, the band limited spatial frequency process, when operating on a starfield, for example, can lead to a tracking accuracy which is significantly greater than the resolution of the input imaging system of a single star. This is a consequence of the smoothing function of the correlation function and its readout as well as of the peaking function of the band limited filter.

The application of a 40 mm image intensifier would be consistent with this conservative approach. The wafer tube can provide some 20 to 30 lp/mm resolution or a total of about 800 to 1200 line pairs along a diameter.

Standard sizes of most intensifiers are in the 18 mm, 25 mm, 40 mm, and 80 mm diameter sizes. The 18 mm and 25 mm size is judged as being too small and the 80 mm size as being excessively large. Furthermore the intensifier having a useful diameter of 40 mm would be consistent with the near 35 mm size format of the photoplastic recording and the optically excited liquid crystal device.

Based on the above a 40 mm active input image area is selected. The input device itself as well as the spatial filter are selected in a 40 mm format.

It remains then to select the parameters of Fourier transform optics. Recall that the scale factor relating displacement in the spatial frequency plane to spatial frequency in the input image is proportional to λF where F is the focal length of the Fourier transform optics. In order to achieve a relatively high scale factor a relatively high f/# system should be used. In typical practical systems the f/# will range from the extremes f/40 to f/11. A compromise must be made between a relatively short system and a system which produces a convenient scale factor. As discussed previously (Section 2.3), a scale factor of about 10^{-3} cm/rad/cm is convenient. For a HeNe laser this is achieved with transform optics having about 60 cm focal length. The optical element (i.e., lens or mirror) will have to be somewhat larger than the 40 mm circular format of the image. As a minimum the transform optics must have an incremental radius great enough to capture the highest spatial frequency signal existing near the periphery of the image. For the scale factor selected (10^{-3}) cm^2 and for an assumed peak input resolution of about 30 lp/mm this

corresponds to an increment of 1.8 cm. Thus the minimum aperture of the functional optics should as a minimum be 40 mm + 18 mm or about 6 cm.

As a realistic compromise between physical length and scale factor transform optical elements having focal lengths of 66 cm operating over the 6 cm center of a 7 cm diameter element is proposed.

For the conceptual design a further conservative recommendation is to use an image dissector type of electro-optical readout based on the use of a one inch image dissector. Thus the active readout area of the readout system is consistent with the overall scaling of the optical processor.

Although the image dissector is tentatively recommended, the ultimate goal is to use a solid state detector array.

Based on the scale factor as discussed and the components selection previously discussed a conceptual layout of the overall system can be established.

4.5 A Conceptual Layout of an Overall System.- A layout sketch of one conceptual design is shown in Figure 4-1. It incorporates all of the components described in Section 4.1.

It incorporates off-axis paraboloidal section mirrors resulting in a triangular shape compact design. Since an application of current interest is that of starfield tracking for a spinning vehicle, no rotation compensation device is incorporated.

The overall device would fit in a volume 132 cm x 48 cm x 24 cm and would be expected to weigh about 30 lbs. The estimated operating power would be 15 to 30 watts.

It should be evident that many variations of layout and physical packaging are possible so as to be compatible with a given spacecraft and mission. The layout of Figure 4-1 is but one representative example of a compact design.

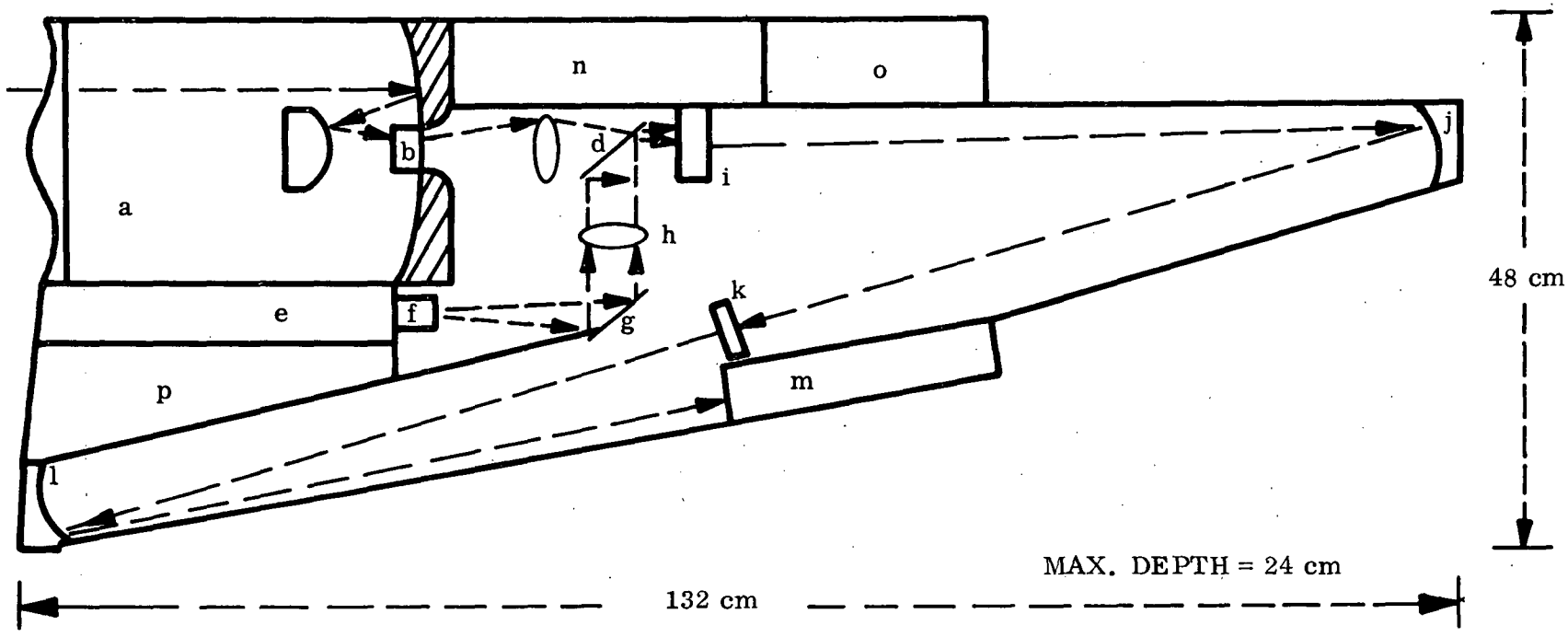

(a) SCHMIDT-CASSEGRAIN TELESCOPE
(b) WAFER TYPE IMAGE INTENSIFIER
(c) TRANSFER LENS
(d) 80:20 BEAM SPLITTER
(e) HE-NE LASER
(f) PINHOLE AND MICROSCOPIC OBJECTIVE
(g) BEAM DEFLECTION MIRROR
(h) COLLIMATING LENS
(i) OPTICAL-TO-OPTICAL INTERFACE
(j) 1ST FOURIER TRANSFORM MIRROR
(k) MULTIPLEXED MATCHED SPATIAL FILTER
(l) 2ND FOURIER TRANSFORM MIRROR
(m) IMAGE DISSECTOR READOUT
(n) IMAGE DISSECTOR ELECTRONICS
(o) POWER SUPPLY FOR OPTICAL-TO-OPTICAL INTERFACE DEVICE
(p) LASER POWER SUPPLY

Figure 4-1. A Conceptual Layout of a Holographic Tracker

5.0 CONCLUSIONS AND RECOMMENDATIONS

5.1 Conclusions.- The "holographic tracker" concept appears to be a practical approach to providing sensed data for a spacecraft attitude reference and/or an autonomous space navigation system.

As previously indicated the performance believed achievable is compatible with realistic space mission requirements. Its demands on the spacecraft in terms of size, weight and power are compatible with realistic space missions.

5.2 Recommendations.- The primary recommendation of this investigation is that the program be pursued through phases of detailed design and fabrication and laboratory tests of a "holographic" tracker.

Following these phases an extensive evaluation of the device in a physical simulator is recommended.

In addition to the pursuit of the above recommended effort, further supportive technology effort is also recommended in these specific areas:

- Further experimental evaluation of some of the more advanced (including various channel plate types) image intensifiers together with advanced real time input media (including PPR, optically excited liquid crystal devices and others).

- Development of cruciform encoding spatial frequency filter or cylindrical lenses together with solid state linear array detectors to permit more compact "parallel" readout of the correlation function (as discussed in Section 3.4).

- Experimental evaluation of laser diodes in a pattern correlation operation in order to lead to a more compact lower power source of coherent illumination.

- Further experiments with multiplexed spatial filters of starfields in order to establish the practical limits on the number of reference patterns which can be thusly stored.

- Further evaluation of reflective readout imaging material such as reflective type of photoplastic recording so as to ultimately avoid a requirement for a relay lens when operating with an image intensifier. Primary problem of reflective readout media is that of holding the media sufficiently flat.

APPENDICES

Appendix A - The Application of Spatial Filter Techniques to Precision Autonomous Space Navigation.- This appendix describes an autonomous space navigation system which uses optical spatial filter techniques for automatically recognizing and tracking both known planetary surface features and starfields. The primary navigation constraints utilized are the vector directions to known landmarks measured relative to a stellar reference frame. The technique is applicable to navigation of a wide range of both manned and unmanned spacecraft. It provides high precision navigation especially when in planetary or lunar orbit and also during terminal guidance.

The unique part of the system relates to the spatial filter method by which the landmarks and the stellar reference directions are recognized and tracked.

Specific features and advantages of the navigation system are:

a) It has greater potential for navigation accuracy than other known autonomous techniques. It can provide primary unsmoothed measured navigation constraints with uncertainties under 30 meters even in the presence of a high degree of natural obscuration, such as clouds.

b) Recognition by this system eliminates the critical registration problem; a pitfall of conventional "map-matching" techniques.

c) It is completely self-contained and passive and can be adapted to either fully automatic or manually-assisted operation.

d) It can provide recognition and tracking data in either digital or analog form with equal precision for both planetary landmarks as well as starfields (which can be as low as $\pm$ 10 sec of arc).

e) Laboratory tests on several features of the process have shown signal-to-noise ratios as high as 400:1 for starfields and 250:1 for lunar and planetary features. In most cases the target area can be as much as 90% obscured and still allow realiable tracking.

f) The use of a light-sensitive fast response imaging medium permits real-time navigation. (Typical processing time delay is 50 milliseconds.)

Navigational Concept.- A brief review of some navigational concepts may be helpful. If the angle between a known star reference direction and a landmark having known planetocentric coordinates is measured on board a spacecraft, the spacecraft is known to be located somewhere on a conical locus having the landmark at its vertex. Simultaneous measurement of the angles between two star references and a landmark would correspond to the locus of two intersecting cones or two radial intersecting lines. In practical navigation it is simpler to take measurements between star references and landmarks at successive known times to provide all necessary data.

The data from a continuing sequence of landmark tracking is processed by recursive statistical techniques, such as a Kalman filter, to provide updated estimates of the vehicle's present and future position and velocity state. This approach makes the usually realistic assumption that the vehicle's state estimate can be adequately described in terms of a linearized departure from a nominal vehicle ephemeris. Since the general statistical approach is similar to that described for other space navigation systems, this report covers the techniques for automatically obtaining constraints by means of spatial filters.

In the present system obtaining the vector direction of a landmark relative to a stellar frame involves automatic recognition and tracking of both planetary landmarks as well as stellar reference fields by spatial filter techniques. Since it is desirable to use the same equipment for both functions, a short period reference is used for determining the orientation of the recognition and tracking system while it is performing, in sequence, these functions of landmark and starfield tracking. This relative angular measurement can be most effectively implemented by means of an intermediate short-period inertial reference.

Usually the computer would have initial approximate state data (based on prior measurements or launch data) which is to be updated. This data should be adequate to permit recognition filter selection. It will be the function of the optical recognition system to identify the landmark and to provide a recognition signal indicating the location of the landmark in the camera's field-of-view. The direction of the telescopic camera optical axis will, in turn, be obtained by the short period inertial references mounted on a common frame with the telescopic camera.

Recognition and Tracking by Spatial Filtering.- Mathematically, a spatial filter is a two-dimensional Fourier Transformation of a conventional optical image into the new optical information domain of spatial frequencies. The physical mechanism by which this is accomplished is the phenomenon of diffraction, and the spatial filters used in this work are a special type of recorded diffraction spectra.

In practice, the starting point is a photographic transparency of the desired information or landmark. By placing this in an appropriate optical system the diffraction image or frequency transformation is obtained and can be photographically recorded. This recording is the spatial filter. It is also possible to produce a diffraction spectrum of the filter and return to the original image. This process of "reconstruction" is possible because the Fourier Transform of a Transform is the original subject. Thus both the physical apparatus as well as the mathematical description for obtaining transformations back and forth between the two optical image domains are seen: the conventional image domain and the domain of spatial frequencies. Ideally, all the information of a given scene can be described in either domain.

Those more familiar with electrical or time-varying signals are aware of the advantages of matched filtering to separate and/or recognize signals in a background of noise. In the optical analogy, the two-dimensional optical signals are converted to frequencies by the diffraction system and passed through the two-dimensional spatial filter. The correct frequencies pass almost

unattenuated while other frequencies are largely suppressed. The transmitted frequencies are then reconstructed to form a normal image which becomes the signal. The leakage of other frequencies reconstruct to produce a "noise" background.

One advantage of this frequency transformation is that an object can be recognized anywhere in the field of view with no requirement for image overlaying or registration. Further, the technique can be mechanized to accommodate rotational misalignment and varying image sizes encountered at different ranges. The spatial filter also provides very exact position information for the landmark in the field of view which is needed for a precision navigation system.

In all these transformation, recognition and tracking operations it is necessary to operate with a transparency of the image. This transparency can be either the conventional photograph with opacity variations which produce amplitude modulation of the light, or a surface deformation material which produces phase modulation of the light. Recently developed surface real time materials can permit real time operation of the system.

Figure A-1 shows the basic optical layout of a recognition and tracking system. There are three optical "domains":

a) A conventional image domain where the input transparency is located.

b) A frequency domain where the appropriate spatial frequency filter is placed.

c) A second conventional image domain in the output plane where the recognition image appears. Due to the special way the spatial filter was made, the recognition image in every case is a round spot of light rather than an image of the object.

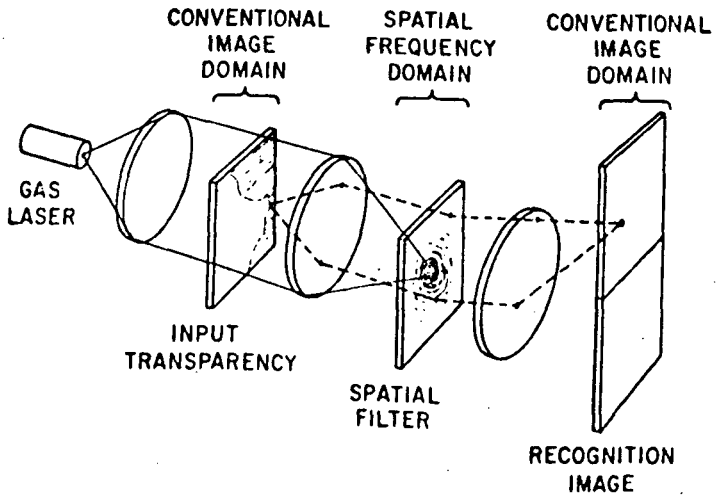

FIGURE A-1

An essential feature of the system is that the position of the image in the frequency domain is independent of the x-y location of the object in the input plane making it possible for an object to be recognized anywhere in the field. On the other hand, the recognition image is conjugate to the object and its position in the field can be used to determine the location of the landmark.

Making the Spatial Filter.- Consider the means for making a spatial filter for an object to be recognized and tracked. The best method is the "two-beam" process,[1] diagrammed in Figure A-2, which used a second or reference beam of coherent light to introduce interference fringes, these fringes act as grating-like elements in the filter causing the recognition image to appear as a star-like spot of light off the axis of the optical system.

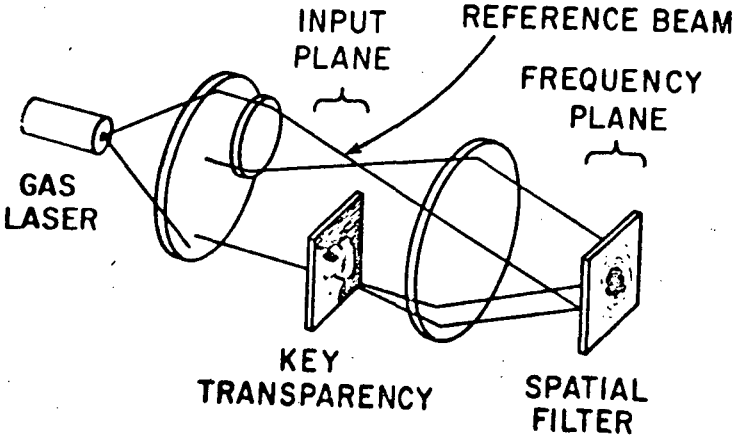

FIGURE A-2

Experimental Results of Earth Landmark Recognition and Tracking.- A number of features of the proposed system have been tested in the laboratory. Landmark tracking experiments were conducted using photographs obtained from GEMINI GT-4 and GT-5 flights. The experiments were made with transparencies derived from prints obtained from the United States National Aeronautics and Space Administration and in particular those showing areas of Arabia, the Nile Valley and Lower California.

---

(1) A. VanderLught, "Signal Detection by Complex Spatial Filtering", IEEE Transactions on Information Theory, April 1964, p. 139.

Selection Landmark.- Figure A-3, a portion of the high contrast coast line at the end of the Arabian peninsula photograph from which typical results were obtained was the first and most obvious choice of landmark from which a spatial filter was made. During recognition experiments this gave very good results although equally good results were obtained by using either much smaller or larger areas as those outlined. To obtain good recognition, it was also found practical to choose a small valley area circled in Figure A-3, or a fairly inconspicuous desert area.

These tests, conducted on several different photographs including some of poorer quality, showed that a conspicuous landmark is not necessary. Any land area containing distinctive detail is satisfactory.

Artificial Generation of Landmark Image.- Tests showed it also possible to use drawings or maps of landmarks as a basis for making spatial filters to recognize areas in these photographs. In general, the signal-to-noise ratios obtained were lower than when a portion of a photograph was used. This was due to inaccurate drawings and omission of details.

Effect of Obscuration on Recognition.- According to present estimates, the Earth mass is covered by clouds 70 percent of the time. It was difficult to obtain additional high altitude photographs of these areas with different amounts of cloud cover and the situation was simulated by adding cotton wool "clouds" to the photographs. It was found that up to 90 percent of the area of the landmark could be covered by clouds without interfering with the recognition of the landmark. It was confirmed by tests that if a portion of the landmark appears at the edge of the field-of-view, the landmark will be recognized.

Effect of Obscuration on Tracking.- Several tests were made to determine if partial obscuration of the landmark by clouds or other cover would deviate the "aiming point" or cause a loss of tracking accuracy. In every case the uncertainty was under one part in 1000 of the field-of-view. This corresponds to uncertainties of less than 11 seconds of arc for a three degree field-of-view camera system.

Effect of Rotational Misalignment.- A series of tests were conducted to determine the error tolerance permissible in the rotation of the filter in relation to the landmark. Some results are shown in Figure A-4. They can be summarized by stating that if the landmark area is small the tolerance can be large, up to 20 degrees, and if the landmark area is very large the tolerance is small and can approach one minute of arc, if desired. This variable sensitivity can be an asset. Mechanical means have been developed to rotate the filter and peak the output signal to allow additional navigational data to be obtained from vehicle orientation.

Effect of Size Mismatch.- The spatial filter must be made for a landmark at some particular size. If the size as seen by the camera on board the spacecraft is different due to change in altitude or slant range, recognition may not be obtained. A series of tests were made to determine the error tolerance and the results were very similar to the rotational tolerance. Size differences up to 15 percent were acceptable for small landmarks, while for very large landmark areas the tolerance can become less than one percent.

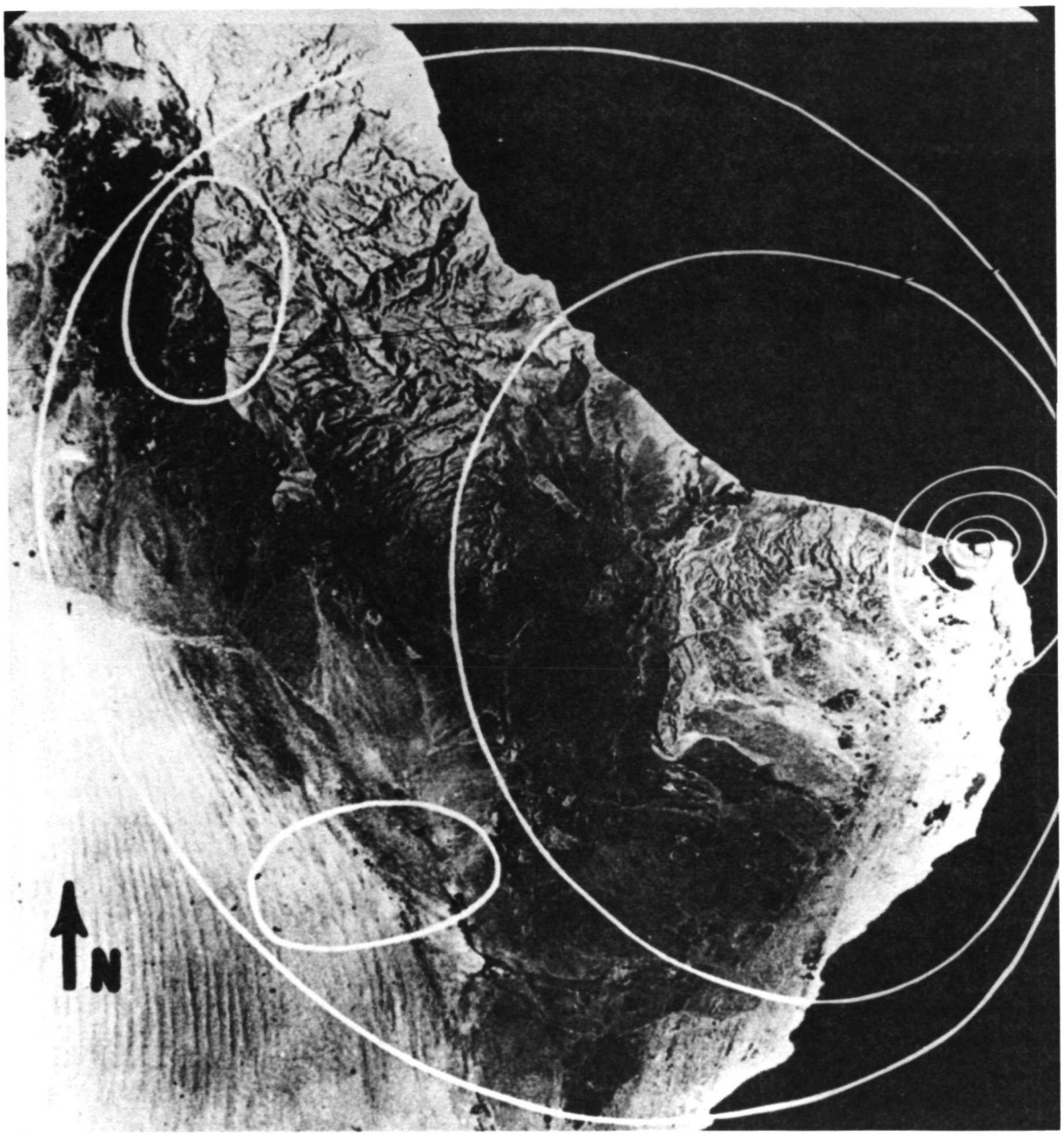

Figure A-3. Arabian Peninsular Showing Various Landmark Areas

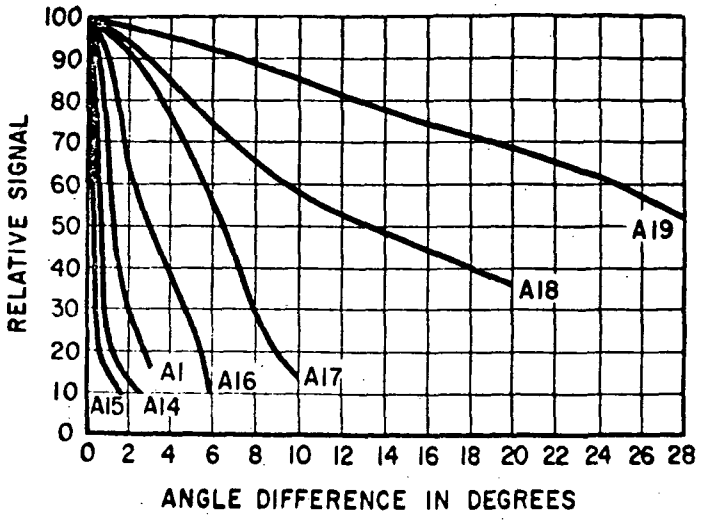

FIGURE A-4 - SIGNAL vs ROTATION ERROR

Mechanical means have also been developed for varying the effective size of the image that will cover size variations up to ten times. This sensitivity could also be used to calculate additional navigational data such as altitude or slant range.

Lunar Landmark Tracking.- This discussion relates to several possible missions necessitating realistic future requirements for high precision self-contained navigation when near the moon. One of the major questions related to automatic lunar "landmark" tracking is: Can one devise a spatial filter which will provide recognition and tracking over a wide range of solar illumination angles?

Experiments were conducted using a series of photos of the same area of the moon shown under different solar angles. One area was Mare Vaporium adjacent to the Sea of Tranquility and was obtained from lunar Atlas Photos(1). Four photo areas are shown in Figure A-5. The specific "landmark" selected surrounding Crater Manilius is shown encircled.

In each photo the lighting is different and it may be assumed that the libration and nutation are also slightly different showing the same area in a somewhat different perspective. It is evident from the photos that the various solar angles significantly effect the observed landmark geometry. Nevertheless, the ability to devise a single spatial filter to recognize the landmark in every case with a signal-to-noise ratio of 30:1 or greater has be been experimentally verified.

(1) Photographic Lunar Atlas, University of Chicago Press, Edited by G.P. Kuiper.

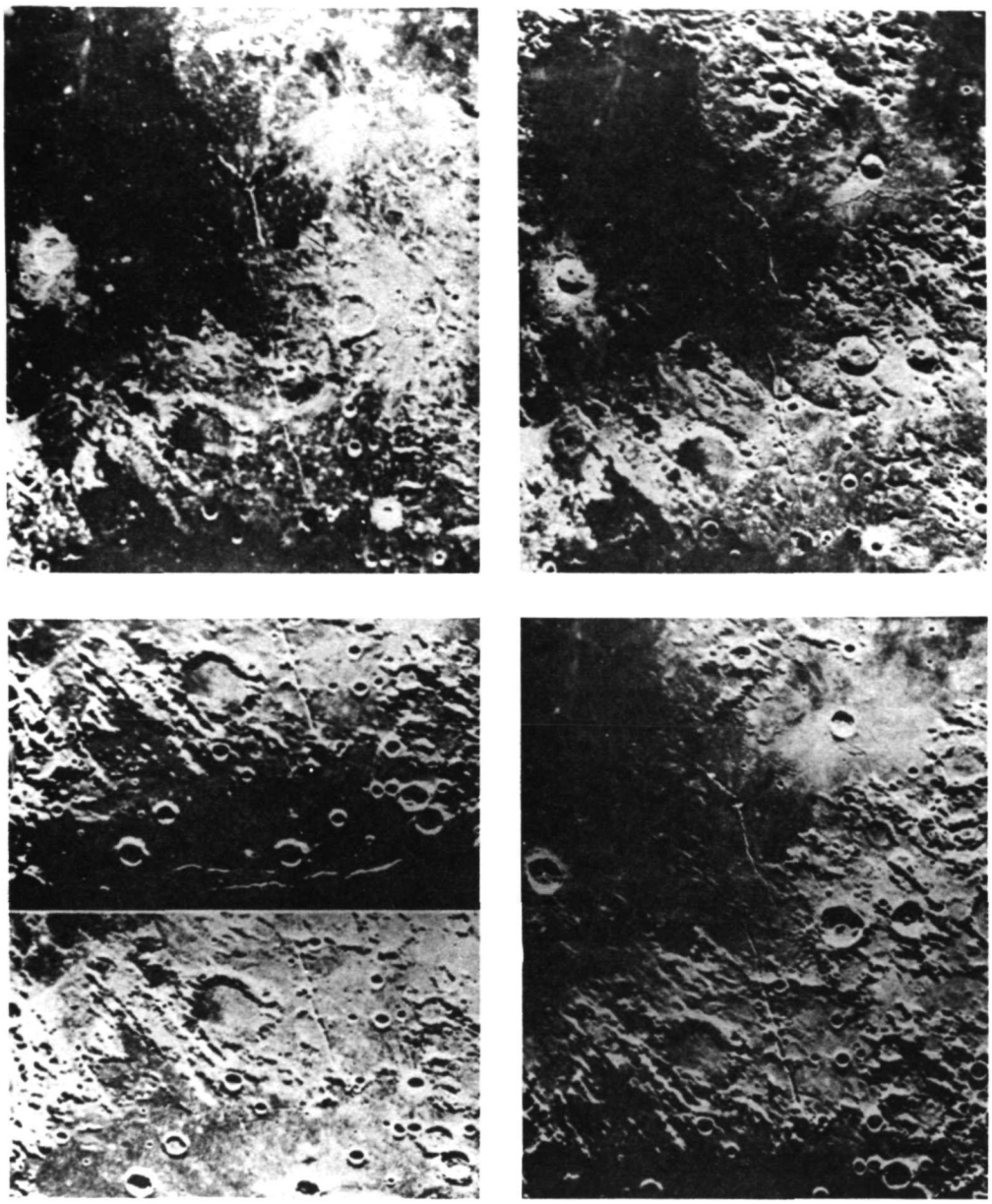

Figure A-5. Five Photographs of the Same Area of the Moon at Different Times in the Lunar Day

Obtaining Stellar References.- Experiments have also demonstrated starfield recognition and tracking. In these experiments starfield "recognition areas" were extracted from images of larger starfields. These "recognition areas" were then converted to spatial filters for use in the recognition and tracking operation. Good results were obtained regardless of whether the starfield was thinly or richly populated; whether it contained bright stars or no bright stars and in the presence of diffuse nebulosity. Several recognition areas were chosen near the North Celestial Pole, in thinly populated regions of Ursa Major and in densely populated regions of Auriga containing the galactic equator. Spatial filters were made from areas containing as many as 236 stars or as few as seven stars. These experiments were conducted with both silver photographic transparencies of the starfields and photodeformable transparencies with equivalent results. Typical signal-to-noise ratios were 400:1 which indicate very good performance.

As in the case of landmarks, the sensitivity to relative rotation of the starfield and the filter can be varied by choosing an appropriate size recognition area, and the tolerance can be as large as several degrees or as small as a minute of arc. The system can be mechanized to take advantage of this sensitivity and obtain complete three-axis reference signals from one starfield.

Because the inertial reference is used only as a short-period reference, gyros need not be of high performance in terms of drift characteristics. The spatial filter technique can be used to monitor and update a gyro inertial frame which serves as the real-time attitude reference. The gyro can be established without the need for a conventional inertial platform by using high angular freedom gyros, the bases of which are attached to the optical system.

Aspect Angle Compensation.- The spatial filter for any landmark can be made only for one aspect angle, ideally from the local zenith. If the landmark is viewed from a greatly different angle it will appear foreshortened in one direction and sometimes may not be recognized. The sensitivity to aspect angle is a function of the size of the landmark area, and for typical areas, we have measured tolerances in aspect angle up to 20 degrees from zenith. Still larger variations in aspect angle can be accommodated if optical compensation is used. This can take the form of an anamorphic lens or the same effect can be produced by tilting the object transparency normal to the optical axis. Compensation for aspect angles up to 45 degrees has been obtained and presumably larger angles could be accommodated.

Signals for mechanizing any of these compensations, rotation, size or aspect need not be obtained from any independent navigation of a priori ephemeris system response itself. In view of the fast response of the electro-optical readout, these compensation operations can be performed in a very short time.

Total System Error.- Since experiments have demonstrated that uncertainties in location of the recognition image, due to various obscuration effects, were under 1 part in 1000, vidicon readout resolution (with a demonstrated point readout resolution of one part in 1000) can be expected to be the primary (exclusive of mapping errors) source of uncertainty in obtaining an

unsmoothed navigation constraint. Unsmoothed single measurement constraint uncertainties are in the range of 20 to 40 feet for low altitude satellites. Uncertainties are reduced if a longer focal length telescope system is selected.

Appendix B - Star Exposure Experiments with Rapid Process Silver Halide Material

General.- As discussed in the final report for NASA Contract (NAS 12-2148) certain types of rapid process silver halide material were judged as having possible potential as an input image medium. Because of the relative simplicity of processing, Polaroid diapositive film (Types 46L and 146L) were judged to typify approaches which merited further consideration.

Although this type of medium is normally developed by moving it through rollers, a modification whereby the rollers would pass over the film resulting in the desired "in place" development was conceived. Further GE experiments have also demonstrated the practicality of using relatively high temperatures to develop this type of film at very high speed. Specifically development in periods as short as 1 second was demonstrated.

The initial judgement concerning the suitability of this media for the present application, however, was subject to further experimental evaluation. The results of this experimental evaluation is discussed here.

Two types of Polaroid diapositive were evaluated:

Type 46L (Normal Contrast), ASA 800
Type 146L (High Contrast), ASA 200

In these experiments several stars were imaged. We will report here on experiments with the star Arcturus which were judged to be among the most meaningful. Arcturus has a visual magnitude of +0.24 and an orange to yellow color.

Experiments with 16 Inch Telescope.- Figure B-1 shows plots of the image diameter of Arcturus as formed on Polaroid diapositive Types 46L and 146L, with the 16 inch telescope under atmospheric conditions which were judged fair to good. As discussed previously the basic resolution of the telescope was adjusted to provide a minimum point spread function of about 0.07 mm. Hence star image size greater than this can be attributed to blooming in the photo and, as such, a measure of sensitivity.

The faster 46L film is shown to require about 1/4 the exposure of the slower 146L film. This is the ratio as expected.

In addition to an abscissa scale showing exposure time there is also another scale showing the energy density scale assuming the following estimated conditions:

. Telescope Point Spread Function	:	0.07 mm
. Atmospheric Attenuation Factor	:	0.4
. Optical Transmittance of Telescope	:	0.6
. Spectral Mismatch	:	0.8

The total input optical power to the telescope, neglecting atmospheric effects, is computed to be approximately $2(10^{-9})$ watts. Based on the above attenuation factors the useful collected optical power from Arcturus at the

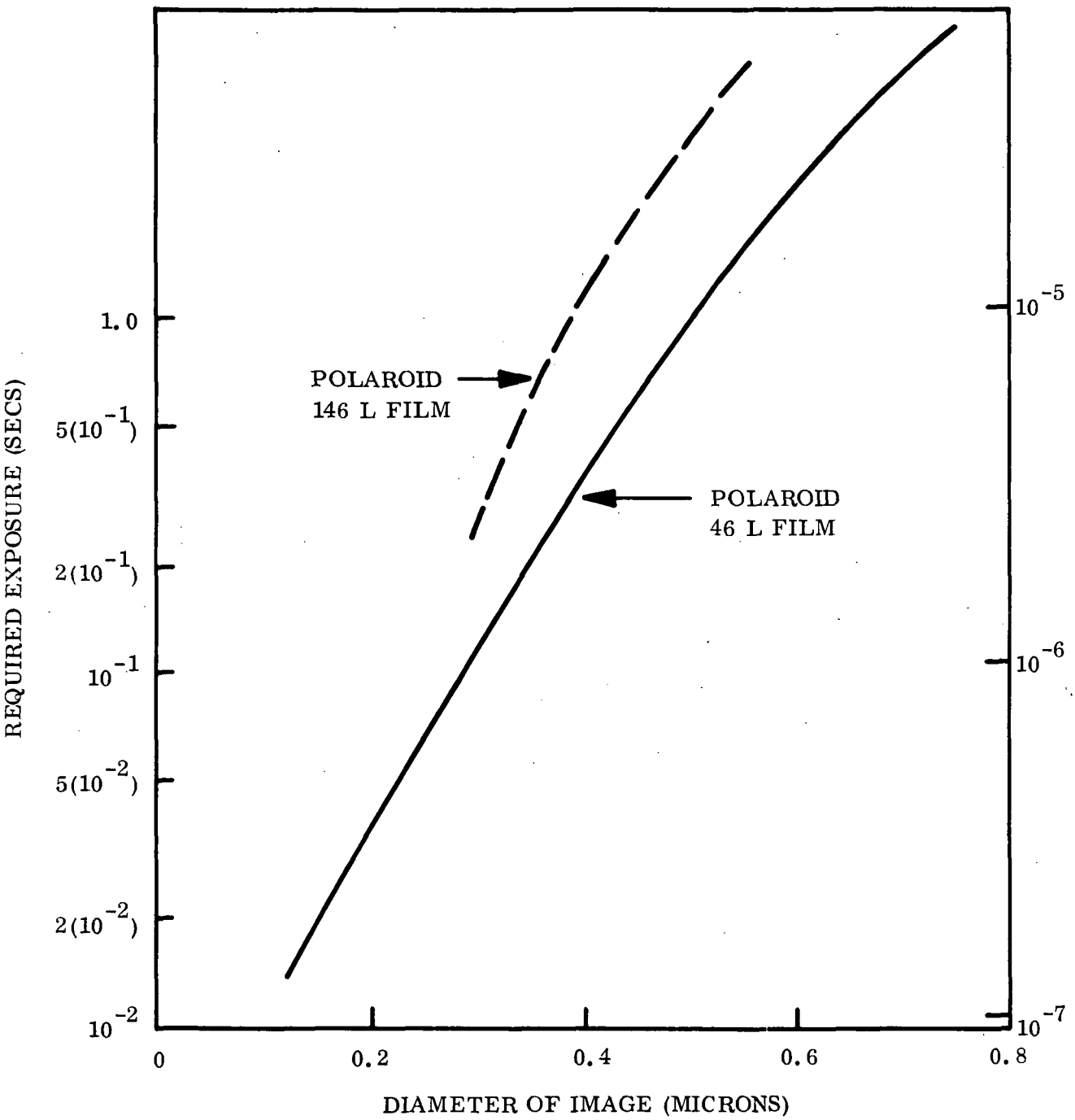

Figure B-1. Required Exposure and Energy Density to Obtain Star Image of a Given Diameter on Polaroid Diapositive Film

image plane of the telescope is computed as approximately $4(10^{-10})$ watts. Based on the above diameter of the telescope point spread function this corresponds to an optical power density of 10^{-5} watts/cm^2. With this as a basis it is possible to put an energy density scale on Figure B-1 which is proportional to exposure time.

If we assume that we wish the medium spread function to be about the same as the telescope optical spread function (0.07 mm in this case) then an examination of Figure B-1 would indicate an energy density requirement of about $5(10^{-8})$ watts sec/cm^2 for the 46L material and about $2(10^{-7})$ watts sec/cm^2 for the 146L material.

This compares with 10^{-8} and $4(10^{-8})$ watts sec/cm^2 as predicted for 46L and 146L respectively and as reported in the final report to NAS 12-2148.

In order to obtain a broader basis for this photometric evaluation it appeared appropriate to experiment with more stars in addition to Arcturus. Next we will report on an evaluation with some very faint stars.

In order to obtain an evaluation of Polaroid with fainter stars the evaluation continued with images of Epsilon Lyrae. This is a well-known double double high in the sky at 10:30: RA, 18 hr. 41 m, Dec. N 39 deg. 35". It is composed of a southern pair known as epsilon 1 consisting of a 4.6 and a 6.3 M star separated by 3 seconds and a northern pair known as epsilon 2 consisting of a 5.2 and a 4.9 M star separated by 2.6 seconds. The separation of 1 and 2 is 207 seconds.

The 46L tranparencies show 1 and 2 to be 7.8 mm apart, therefore the scale of all the photographs taken through the 16 inch telescope is verified as 1 mm = 26 seconds. The field of view through the shutter measures about 28 mm demonstrating that the total field of view is 12 minutes of arc. In none of these photographs obtained with the 16 inch telescope were the components of epsilon 1 or epsilon 2 resolved, although the images are non-round.

Halfway between 1 and 2 and off to one side is a 9.5 M star and directly then between is a 12.5 M star. Our photometric evaluation here will be based on images of these stars.

The diameter of the recorded star image which were obtained on two different nights in 1971 are as follows:

EPISON LYRAE ON 46L FILM

EXPOSURE	STAR	DIA. STAR IMAGE JUNE 10	DIA. STAR IMAGE JUNE 21
30 sec	E1	.49 mm	.43 mm
	E2	.45 mm	.39 mm
	M 9.5 Star	.30 mm	
	M 12.5 Star	.067 mm	
5 sec	E1	.34 mm	
	E2	.31 mm	
	M 9.5 Star	.072 mm	

The 30 sec exposure and the 5 sec exposure were judged to be about the minimum exposures for the M 12.5 and the M 9.5 star respectively.

Based on our previously discussed parameters the usable power and power density in the image plane of the M 9.5 and M 12.5 stars are estimated as follows:

STAR	POWER AT TELESCOPE APERTURE NEGLECTING ATMOSPHERE	USABLE OPTICAL POWER AT IMAGE PLANE	OPTICAL POWER DENSITY
M 9.5 Star	$3(10^{-13})$ watts	$0.6(10^{-13})$ watts	$1.5(10^{-9})$ watts/cm^2
M 12.5 Star	$2(10^{-14})$ watts	$0.4(10^{-14})$ watts	10^{-10} watts/cm^2

Based on the exposure data and the previously discussed point spread function criteria it is concluded that about a 30 sec exposure was required for the M 12.5 star and a 5 sec exposure for the M 9.5 star. This would correspond to energy density requirements as follows:

STAR	OPTICAL ENERGY REQUIRED
M 9.5	$8(10^{-9})$ watts sec/cm^2
M 12.5	$3(10^{-9})$ watts sec/cm^2

Therefore based on the detection of much dimmer stars than Arcturus we still converge on an estimated energy requirement for the 46L material in the range of $5(10^{-9})$ to $5(10^{-8})$ watts sec/cm^2 for the 46L material and about 4 times that for the 146L material. This appears to be in reasonably good agreement with the expected value of the energy required.

Experiments with 4 Inch Telescope.- As discussed in Section 3.1 the 4 inch telescope was in adjustment so as to provide an optical point spread function of about 0.01 mm. It appeared appropriate to evaluate the Polaride medium with this smaller point spread function so as to determine whether or not this smaller input point spread function would have any effect on the sensitivity or noise characteristics of the film.

These experiments were performed on the night of August 12 under unusually good seeing conditions. Experiments were made with a large number of stars centered around Alpha Cygnus, Gamma Cygnus and Beta Serpentis. Stars imaged on the medium in these experiments included stars as faint as 9th magnitude.

An estimation of the key typical parameters of the experiment with the 4 inch telescope is as follows:

- Telescope Point Spread Function : 0.01 mm
- Atmospheric Attenuation Factor : 0.4 mm
- Optical Transmission of Telescope: 0.6 mm
- Spectral Mismatch : 0.8 mm

Table B-1 summarizes results of the experiments with 46L film with respect to exposure, energy and energy density required to image a star of a given magnitude.

TABLE B-1

MIN. EXPOSURE TIME, ENERGY, ENERGY DENSITY REQUIRED TO IMAGE STAR OF LIMITING MAGNITUDE

LIMITING STELLAR MAGNITUDE	MINIMUM EXPOSURE (sec)	EFFECTIVE OPTICAL POWER AT APERTURE (NEGLECTING ATMOSPHERE) (watts)	ENERGY AT APERTURE (NEGLECTING ATMOSPHERE) (watts sec/cm^2)
9	300	$3(10^{-14})$	$9(10^{-12})$
8.4	120	$5(10^{-14})$	$6(10^{-12})$
8	60	$9(10^{-14})$	$5(10^{-12})$
7	25	$2(10^{-13})$	$5(10^{-12})$
6	10	$7(10^{-13})$	$7(10^{-12})$
5.4	7	(10^{-12})	$7(10^{-12})$
5	4	$2(10^{-12})$	$8(10^{-12})$
4	1.6	$5(10^{-12})$	$8(10^{-12})$
3	.6	$1.1(10^{-11})$	$7(10^{-12})$
2	.2	$3(10^{-11})$	$6(10^{-12})$
1	.08	$8(10^{-11})$	$6(10^{-12})$

Based on a telescope optical spread function of 0.01 mm the data in Table B-1 indicates a required energy density at the star image in the neighborhood of 10^{-7} watts sec/cm^2. Although this suggests a sensitivity somewhat lower than that obtained with the 16 inch telescope, it still indicates a sensitivity within a usable range even for starfields without an image intensifier.

The noise problem continued to persist and continues to suggest considerable doubt as to the utility of this material for starfield recognition and tracking.

Consideration of Noise.- In most of the experiments with the Polaroid diapositive media discussed above a disturbing type of noise appeared in a degree greater than was anticipated. This noise was in the form of "pinholes" which, in appearance were not greatly dissimilar to the images of stars themselves. Typically these noise pinholes had diameters in the range of 0.1 to 0.5 mm and appeared in density distributions typically comparable to that of a typical realistic starfield.

In analyzing the star images themselves it was frequently difficult to distinguish the stars from the pinholes. Positive identification of stars could sometimes be accomplished only with the aid of a star atlas. Variations in the development (i.e., temperature and, as suggested by the film manufacturer, speed of pulling medium through the rollers) were tried. However none of these techniques seemed to improve the noise situation.

A possible solution might be to overexpose the stars so that even the faintest desired star would be significantly larger than the largest noise pinhole. This would suggest a required energy density in the range of 10^{-6} watt sec/cm^2 or more. However the better approach seems to be to look for more suitable material operating with an image intensifier.

Appendix C - Landmark Experiments with Rapid Process Silver Halide Material.- These experiments were performed to evaluate the performance of Polaroid 146L and 46L diapositive material as an input imaging medium for a landmark tracker. The results of this work is summarized in Section 3.2.

The initial tests were made to determine to what extent added heat could increase the development speed of the material.

A print of Arabia, four generations from the original, one of the GEMINI photographs was used. This was copied using a Polaroid camera. Exposures were first made on 46L film to compare results. The copies on 46L (low contrast film) showed better gray tones, but the reproduction of detail on 146L (high contrast film) was remarkably good.

All of the exposures on 146L film were made at f/8 at 1/125 second. The properly developed transparency left little to be desired in general appearance. When the development at room temperature (75 degrees F) was reduced to 5 seconds the transparency still looked good but had less density in the black areas.

When the development was reduced to 3 seconds minor tearing of the image appeared and at 2 seconds the tearing was severe, a considerable portion of the image was lost. This tearing results in a series of parallel wrinkles in the emulsion which in coherent light produce strong diffraction resulting in noise in the readout.

In the next series of tests the platen in back of the film and the roller that spreads the developer were both heated with an infrared lamp to about 120 degrees. The film was in contact with the platen during exposure and pulled under the roller during development. The temperature of the film was not known, but was somewhere between room temperature (75 degrees) and 115 degrees.

Using this system to heat the film, good transparencies were made with development times of 3 and 2 seconds. Some of these show tearing, others do not, and in general the density is higher than transparencies developed at room temperature for the same length of time.

It took several tried to reduce the development time to 1 or 1½ seconds and the resulting transparency was very low contrast, the image a pale brown color and while there is no obvious tearing of the emulsion, when it is examined in coherent light one can be seen across the image. Probably the reason this is not easily seen is the very low contrast of the image.

Results.- The above set of transparencies were compared to a spatial frequency filter for the "Mountain scene", No. 2390 and the signal and noise measured.

One input transparency with 46L low contrast film as the input imaging media gave the following result:

Signal	Noise
100 (full sensitivity)	3

(Full sensitivity means maximum sensitivity of the meter and all subsequent values are on a comparable basis.)

The following results were obtained with 146L (high contrast film):

EXPOSURE	DEVELOPMENT TEMP. °F	SIGNAL	NOISE
15 sec.	75 deg.	320 (See Note)	16
5 sec.	75 deg.	110	15
2 sec.	75 deg.	- (See Note)	50
3 sec.	110 deg. No. 1	80	7
3 sec.	110 deg. No. 2	210	23
3 sec.	110 deg. No. 2 (Masked)	210	5 (See Note)
3 sec.	110 deg. No. 3	147	25
2 sec.	110 deg. No. 1	230	7
2 sec.	110 deg. No. 2	115 (See Note)	7
1 sec.	110 deg.	-	50

Notes on Above.- The 15 second development 146L transparency gave a stronger signal than the 46L transparency. This is probably due to the fact that the latter was more dense and transmitted less light. The 146L transparency is probably close to the ideal density.

The transparency developed 2 seconds at 75 degrees showed considerable tearing and ripples in the emulsion which acted as gratings and scattered light. The correlation image could not be found.

The 3 second development No. 1 had two flaws which were not serious.

The 3 second development No. 2 had two short tears which produced considerable noise. These tears were in one corner and could be masked. This did not change the signal, but did reduce the noise from 23 to 5 scale divisions.

The 3 second development No. 3 had four small tears due to separation of the emulsion. These produced a high noise signal. Due to their location they could not be masked to reduce the noise.

The 2 second development No. 1 was a low contrast image, but produced a good signal.

The 2 second development No. 2 was much denser than No. 1 and produced a weaker signal.

The 1 second development produced a correlation image that was too weak to measure. The transparency was very low contrast and noisy due to a tear across the center.

Comparison with Microflat Plate.- In order to obtain a comparative reference some experiments were made with microflat plates as an input image media. A very good transparency on 649 emulsion gave the following result:

Signal	Noise
420	10

The chief difference that could be seen was that the diffraction pattern of the microflat plate was nearly perfect and undistorted, while the diffraction patterns of all the Polaroid film transparencies were wavy and broadened due to thickness variations in the film.

It should be noted that this effect was not seen in the case of stars because in the star transparencies most of the picture was opaque and the star images were extremely small. Therefore the likelihood of a thickness error occurring in one of these tiny images was extremely small. In the present case of a landmark the images extend over a large area and thickness variations are seen. The stars are thus seen to be a rather special case and resulted in a signal and a signal-to-noise ratio practically the same as the microflat plates. In the landmark experiments the thickness variations result in a spreading of the diffraction image so that all of its light did not fall on the proper area of the filter and the signal was less.

Except for the consistently lower signal values and the occasional high noise values due to tearing of the emulsion the results on 146L film are approximately the same as the glass plates. The correlation images were always sharp and free of satellites and the noise background uniform and normal.

The size of the image on the transparency was 50 x 52 mm. If the experiment had been done with smaller images the effects of thickness variations in the film would have been less.

Polaroid P/N Film.- One transparency was made on Type 55 P/N film. The chief difference between this image and 146L is that the image is a negative instead of a positive and the transparent areas are gray instead of clear. For this latter reason and the general low contrast of the image the signal is less than with 146L film.

Signal	Noise
37	1.5

Appendix D - Description of Experimental Evaluation of Image Intensifier Operating with PPR Imaging Medium.- The experimental set-up was previously shown in Figure 3-3. The image intensifier used was a 3-stage Generation I intensifier made available by the Night Vision Labs of the U.S. Army. Measured luminous gain of this device was 47 000.

The experiments were performed using a set of five simulated star images of various magnitudes. The nature of the test was to make a relative comparison of the PPR response with and without the intensifier.

In order to get the best image quality from a set-up as complex as the one used, it would be necessary to make a careful alignment of all the elements; collimator, telescope lens, image intensifier, relay lens and camera. The elements should be square to the axis and co-linear. Also the focusing of the object on the intensifier and the focusing of the second image on the film should be done with great care and the results checked by making a series of exposures with slight changes in these distances. None of these refinements were exhaustively tested and it is possible that our results in terms of resolution are less than optimum.

Relay Lens Used.- The available relay lens was a Perkin-Elmer 5½ inch focal length, f/2 lens made for 1:1 conjugates. The total distance from the input image at the rear of the intensifier to the output image on the film was 15 inches. With a shorter focal length lens this could have been reduced to 8 inches or less. The white light transmission of the lens used was 73 percent. The image quality over a 1 inch field was in excess of 100 line pairs/mm at the last time the lens was tested. All relay lenses are specials since there is little demand for them and this one owned by GE cost $3000. If we assume that the phosphor screen on the intensifier radiates light at uniform intensity over a hemisphere, then the phosphor light is spread over 180 spherical degrees. An f/2.0 lens has a collection angle of 28 spherical degrees. The flux collected is therefore calculated as 2.98 percent of the total, based on uniform radiation. In practice it turns out that depending on the face plate construction, phosphor backing and other considerations, estimates on the basis of Lambertian distribution may be low by a factor as much as 2.

Combining the 2.98 percent flux collection and the 73 percent transmission results in an efficiency value for ten relay lens of 2.17 percent with the further consideration that non-Lambertian distribution may raise this as high as about 4 percent.

It is possible to buy more efficient relay lenses, though the increase in efficiency is paid for in bulk and weight which increases faster than the efficiency. An f/1.0 system is about as fast as can be made with lenses and the increased number and thickness of the glass elements results in less transmission of light then the geometrical aperture ratio would indicate. Very fast relay systems are made of a pair of Schmidt telescopes face to face with added field flattening lenses. Such a system can have an aperture ratio of .60 or better, but it has considerable losses due to mirror reflections and central obscuration. The actual efficiency of the best relay system is believed to be about 10 percent, based on Lambertian distribution, though this may be closer to 20 percent in practice.

Test of Relay Lens.- The relay lens was not believed to be an important contributor to loss of resolution in the test set-up. However it undoubtedly contributed to some loss of contrast, all lenses do.

To make this test the resolution chart was photographed directly through the Boller and Chivens telescope on PPR, it was photographed through the telescope plus the relay lens and through the entire set-up of telescope, image intensifier and relay lens.

TEST OF RELAY LENS

EXPOSURE (Sec)	CONDITIONS	RESOLUTION 1 pr/mm on PPR
21	Telescope Only	44+
19	Telescope and Relay	44
8	Telescope, Relay and Intensifier	19

Discussion of Test of Relay Lens.- These values seem reasonable. The finest set of bars on the chart were at 44 line pairs per mm. It is impossible to accurately predict the effects of a combination of lens and film resolution without very detailed information about both of them. The simplest approximation is:

$$\frac{1}{\text{Resolution Film}} + \frac{1}{\text{Resolution Lens}} = \frac{1}{\text{Resolution of Combination}}$$

The resolution of the telescope lens is about 100 lp/mm. This is based on the fact that a 5 micrometer star image is the smallest that was obtained. This represents a "line". A line pair would then measure 10 micrometers and the resolution would be 100 lp/mm.

The resolution of 7 micrometers thick PPR when tested with the "deep" images is about 200 lp/mm. Therefore, on the basis of the approximate equation given above the resolution of the combination should be 67 lp/mm.

The loss in resolution caused by adding the relay lens was very small, but the loss caused by the intensifier was considerable. As mentioned earlier, this could be due partly to faulty alignment or focus.

There is also considerable difference in the appearance of the images of a bar chart with and without the intensifier. The lines on the original chart are exactly equal in width to the spaces. The PPR images made without the intensifier show this relation maintained down to all but the smallest set of bars. The images made with the intensifier all show the luminous images wider than they should be at the expense of the spaces.

This image spread is equal to about 30 micrometers added to the width of each bar. If this is a correct interpretation of the effect, then bars wider than 30 micrometers should be resolved. For bars 30 micrometers in width or less the irradiance will completely fill in the space and resolution will be lost. A bar having a width of 30 micrometers is equal to 16.6 lp/mm which is close to the measured resolution of 19.

If this condition holds for star images they will all be about 30 micrometers larger with the intensifier than without.

Measurement of Diameter and Depth of Star Image Deformation.- Nine PPR exposures were made of a set of "large" simulated stars using the intensifier. The diameter and depths of the deformations obtained on the PPR are tabulated below.

The development and charge conditions were constant in all exposures.

DEPTH AND DIAMETERS (MICROMETERS) OF SIMULATED STAR IMAGES ON PPR WITH IMAGE INTENSIFIER

EXPOSURE (Sec)	STAR NO.							
	1		2		3		4	
	Depth	Dia.	Depth	Dia.	Depth	Dia.	Depth	Dia.
15	.48	159	.36	120	.36	90	.24	51
7	.45	132	.45	96	.36	84	.18	48
4	.36	105	.27	81	.18	-	.09	-

The chief difference between these images and those obtained without the image intensifier is that these images are larger and the slopes on the sides are less steep. In the case of star images made without the intensifier the diameter to depth ratio was as high as 20:1 and seldom less than 50:1. In the above tests with the intensifier the ratio varied from 150:1 to 300:1.

Comparative Exposure Gain Using Intensifier.- This measurement was made using the artificial star projector with its lamp operating at 80 volts and included tests 8 and 9. This intensity was too great for the image intensifier which was attached to the back of the telescope. The light was attenuated by neutral density filters to a suitable level and exposures made. After the test the filters were checked in white light and red light for transmission and were found correct to at least .1 density. Exposures were then made with the intensifier and its relay lens removed using the same lamp voltage, but no filters. The same exposure time was used in each case. It is not possible to say that the images with and without the intensifier are exactly the same because of the difference in diameter and slope angle of the depressions produced in the two cases, but they appear equivalent.

COMPARISON OF IMAGES - STARS

Without Intensifier: Filter none, Time 15 seconds. Four stars well defined, depth .6 - .3 micrometers

With Intensifer : Filter den. 3.0, Time 15 seconds. Three stars well defined, depth .42 - .2 micrometers.

Filter den. 2.5, Time 15 seconds. Four stars well defined, depth .6 - .2 micrometers.

Of the above two exposures, the best agreement is with the second in which a filter with a density of 2.5 was used. This filter results in a light attenuation of 320 times so that the comparative gain of the intensifier in this application is 320 times.

A further set of tests was made with the resolution chart instead of the artificial star plate and a voltage of 110 volts.

COMPARISON OF IMAGES - BAR CHART

Without Intensifier: Filter none. Time 5 seconds. Depth coarse bars .63. Fine bars .40.

Filter den. .5. Time 5 seconds. Depth coarse bars .54. Fine bars .36.

Filter den. .7. Time 5 seconds. Depth coarse bars .63. Fine bars .18.

With Intensifier : Filter den. 3.0. Time 5 seconds. Depth coarse bar .43. Fine bars .18.

The best match in this case is between 3.0 density for the intensifier and .7 density without. This is a difference of 200 times, or an exposure gain of 200 times.

Estimation of Gain-Second Method.- A second set of tests were made using the bar chart and a light level which appeared to saturate the intensifier. Exposures were made with light absorbing filters behind the image intensifier. The lamp voltage and exposure time were constant.

SECOND METHOD

EXPOSURE NO.	FILTER	DEPTH COARSE BARS	DEPTH FINE BARS
15	None	.36	.18
16	1.0	.54	.24
17	1.6	.18	-

Exposure No. 15 is clearly overexposed and No. 17 is underexposed. The variation between the first and last is 40 times (density 1.6).

Probable Effect of Weak Slopes.- In the tests described the chief difference between the images with and without the intensifier was that the intensifier appears to diffuse the image and results in PPR modulation with a somewhat weaker slope angle. This difference may have an effect similar to unsharpness in an amplitude image. In amplitude images sharp edges result in many orders of diffraction and a high total of integrated diffracted light. Diffuse edges result in fewer orders of diffraction and a low total diffracted light. Diffuse images therefore produce weaker correlation images and are difficult to detect. It seems possible that the weaker slopes of the intensified images may have an analogous effect in the phase image, though no tests of this have been made.

REFERENCES

(1) Holeman, J.M. and Welch, J.D., "Recognition and Tracking of Star Fields by Spatial Filter Techniques", GE Report 66-C-258, Sept. 1966.

(2) Welch, J.D. and Holeman, J.M., "Investigation of Autonomous Space Navigation Concepts Utilizing Spatial Filter Techniques", GE Report 66-C-191.

(3) Welch, J.D. and Holeman, J.M., "Autonomous Space Navigation Concepts Utilizing Spatial Filter Techniques, Phase II", GE Report 66-C-199.

(4) Holeman, J.M. and Welch, J.D., "Autonomous Navigation for Lunar Orbital and Terminal Missions Utilizing Spatial Filter Techniques", GE Report 66C-249.

(5) Holeman, J.M. and Welch, J.D., "The Application of Spatial Filter Techniques to Precision Autonomous Space Navigation", Presented at 17th International Astronautical Federation Meeting, Madrid, October 1966.

(6) U.S. Patent No. 3 636 330 - John M. Holeman and Joseph D. Welch, - "Autonomous Space Navigation Utilizing Holographic Recognition".

(7) Welch, J.D., "Image Media Investigation for Holographic Starfield Mapper", (Final Report for NASA Contract NAS 12-2148), Jan. 1970.

(8) Gorstein, M., Hallock, J. et al, "Two Approaches to Star Mapping Problem for Space Vehicle Attitude Determination", Applied Optics, March 1970.

(9) Thomasson, J.T., "Creating Holographic Filters for Autonomatic Recognition Systems", SPIE Pattern Recognition Studies, June 1969.

(10) Husain-Abidi, A.S., "On-Board Spacecraft Optical Data Processing", NASA X711-71-259, June 1971.

(11) Margerum, J.D., Nimoy, J., Wong, S.Y., "Reversible Ultraviolet Imaging with Liquid Crystals", Applied Physics Letters, Vol. 17, No. 2, 15 July 1970.

(12) Thomas, C.E. and Hall, W.D., "Film Study for a Starfield Correlator, Final Report for Contract NAS 12-2212 (by KMS Technology Center).

(13) Valge, J., "Characteristics of Star Mapper Sensors, Catalogs and Computers", R.S. Draper Laboratory Report R 696.

(14) Papoulis, A., "System and Transforms with Applications in Optics", McGraw-Hill, 1968.

(15) Stroke, G., "An Introduction to Coherent Optics and Holography", Academic Press, 1966.

(16) Foley, W. et al, "Optical-Inertial Space Sextant for an Advanced Space Navigation System", Phase A, Final Report, Contract #NAS2-1087.

(17) Linfoot, E.H., "Recent Advances in Optics", Oxford Press, 1955.

(18) Willey, R., "Comparison of Cassegrain Systems", Sky and Telescope, April 1962.

(19) Elliott and Dickson, Laboratory Instruments, Chemical Publishing Co., 1960.

(20) Femly, R.A., "An Expanding Role for the GaAs Laser", Optical Spectra, Dec. 1971.

(21) VanderLugt, A., "The Effects of Small Displacements of Spatial Filters", Applied Optics, July 1967, Vol. 6, No. 7, pp 1221-1225.

(22) Alward, J.L., "Spatial Frequency Filtering", Willow Run Lab Report 2389-87-T, Dec. 1965.

(23) Harman, W.H., "Optical Viewers for Continuous-Tone Images Recorded on Thermoplastic Film", MIT Electronics System Lab Report, ESL-TM-338, Jan. 1968.

(24) Shulman, A., "Optical Data Processing, John Wiley, 1970.

(25) Jenson, N., "Optical and Photographic Reconnaissance Systems", John Wiley, 1968.

(26) A Diffraction Limited Schmidt-Cassegrain Telescope, Sky and Telescope, April 1966.

(27) "A Schmidt-Cassegrain Optical System with a Flat Field", Sky and Telescope, May and June 1965.

(28) Larson, R.K., "Experiments in Spatial Coherent Optical Filtering", NASA X711-71-792, June 1972.

(29) Quasius, G. and McCanless, F., "Star Trackers and System Design", Spartan Books, 1966.

(30) Bridges, W., "Design of a Space Qualified Laser, Phase I", NASA Contractor Report, CR 1663, Oct. 1970.

(31) Kolb, W., "Research Directed Toward Perfecting a Design for a Space Qualified HeNe Laser", NASA Contractor Report CR 1664, Sept. 1970.